MICROEMULSION SYSTEMS AND MICELLAR CATALYSIS

A THESIS

SUBMITTED TO THE

UNIVERSITY OF POONA

FOR THE DEGREE OF

DOCTOR OF PHILOSOPHY (CHEMISTRY)

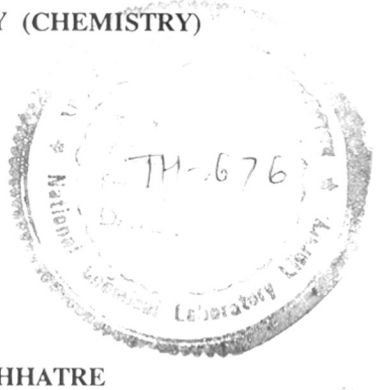

BY

AJAY SADASHIV CHHATRE

M.Sc. (Chemistry)

CHEMICAL ENGINEERING DIVISION

NATIONAL CHEMICAL LABORATORY

PUNE - 411 008

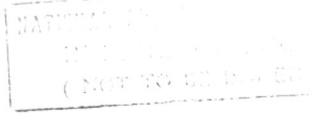

AUGUST 1992

DEDICATED TO MY PARENTS

AND TEACHERS

Form - A

Certified that the work incorporated in the thesis **"Microemulsion Systems and Micellar Catalysis"** submitted by Ajay Sadashiv Chhatre was carried out by the candidate under my supervision. Such material as has been obtained from other sources has been duly acknowledged in the thesis

Dr. B. D. Kulkarni

Research Guide

वैज्ञानिक/Scientist
राष्ट्रीय रासायनिक प्रयोगशाला
National Chemical Laboratory
पुणे/PUNE-411 008.

ACKNOWLEDGEMENTS

I am extremely grateful to my research advisor Dr. B. D. Kulkarni for guiding me in the research work presented in the thesis. It would not have been possible to bring out this thesis but for his inspiring guidance and constant encouragement.

A special mention of thanks goes to Dr. S. S. Katti for all the help extended. It is indeed a pleasure to acknowledge the support received from all his group members.

My heartfelt thanks are due to Dr. S. S. Bhagwat, UDCT, Bombay, for his helpful suggestions during the initial stages of the research work. I would also like to express my deep sense of appreciation to Dr. S. R. Inamdar for having inspired me throughout this research work. Special mention goes to Mr. Jayanta K. Bandyopadhyay for his cheerful help. Thanks are also due to Dr. Mrs. Rajani Prasad, Dr. Parkash Badola, Dr. Mrs. Archana Sharma and Mr. Murlidhar Nair for their timely cooperation. It is a pleasure to thank Dr. V. Ravi Kumar, Dr. S. S. Tambe, Dr. V. K. Jayaraman, Dr. N. K. Yadav and Dr. S. K. Kamat for their courtesy and helpful advice.

I take this opportunity to express my gratitude to Mr. Bhujang and Mr. Joglekar for their kind assistance in drafting the figures.

I am greatly indebted to Dr. L. K. Doraiswamy, former Director, and Dr. R. A. Mashelkar, present Director of this Laboratory, for providing me all the facilities for doing research. It is indeed a great delight to thank the University Grants Commission for the award of a Fellowship during the tenure of this work.

Last but not the least, I would like to express my gratitude to my family members for their patient cooperation.

(Ajay S. Chhatre)

ABSTRACT

Last decade witnessed renewed interest in research on supramolecular assemblies in solutions, such as micelles and microemulsions, due to their extensive applications in industry. The applications include catalysis, detergency, biotechnology, and enhanced oil recovery. Microemulsions are multicomponent fluids that are characterized by equilibrium globular domain or network-like structures on length-scales of around 1000°A. In microemulsions the oil and aqueous phases, tend to form domains with the third component, surfactant, at the interfaces between them. Most systems with domain structures coarsen while approaching an equilibrium state of complete phase separation. It is the spontaneous solubilization of oil in water or water in oil via the surfactant that distinguishes microemulsions from emulsions or macroemulsions. The system is self-organizing and determines its microstructure by minimizing its free energy. The organization of the globules in solution is important in determining the phase behavior and transport properties of the system.

Microemulsions can be obtained by titration of an ordinary emulsion having milky appearance to clarity by addition of a medium-chain alcohol, such as pentanol or hexanol. When oil, water and surfactant are blended together and allowed to equilibrate, two or more phases may appear, and in most of the cases almost the entire inventory of surfactant will reside in one of the phases, together with various proportions of oil and water. The phase behavior of interest involves at least three components and often more. The phase behavior of three components can be represented by using a ternary phase diagram. These diagrams provide a global perspective of phase behavior that is difficult to capture so transparently in any other way. Further, the phase boundaries of systems containing more than three components can also be usefully shown in ternary diagrams. The study of such a phase behavior of three or more components is of prime importance since this is useful in optimizing relative quantities of the components to be used in case

of a micellar catalyzed chemical reaction. Such a study is also helpful in various applications such as tertiary oil recovery by microemulsion flooding, separation processes, hydrometallurgy and electrorefining.

Owing to their solubilization property, microemulsions serve as better media for various heterogeneous reactions. The microemulsion droplets offer the possibility of transport of substances through a medium where they are not soluble or very poorly soluble. It is for this reason that microemulsions have been exploited with a view to achieve considerable enhancement in rates of heterogeneous reactions. While on one hand these serve as better media for reactions, on the other hand, the surfactants themselves being amphiphilic in character, tend to orient the reacting molecules at the interface. This leads to another advantage of using microemulsions for achieving better enantio-selectivity in reactions. This property of microemulsions however has not been adequately studied so far. In the present work, experimental data on various industrially important reactions carried out under microemulsion conditions have been reported. The distinctive features of microemulsions, *viz*. rate enhancement and selectivity have also been demonstrated in some reactions. In order to optimize the relative quantities of reactants, a complete phase behavior of microemulsion systems incorporating the appropriate components have also been studied in details.

Chapter 1 gives a brief introduction to micellar and microemulsion systems. The phenomenon of solubilization in the micelles has been described. A method for obtaining the phase diagrams has been discussed. The various uses of microemulsions such as effective medium for interfacial reactions and interfacial synthesis have also been enunciated.

Chapter 2 describes the general characteristics and phase behavior of various microemulsion systems studied. The method for delineating various domains in a ternary and pseudo-ternary system has been described. The effect of change in

system parameters such as concentration of the components, temperature, etc. on the phase behavior has also been explained. Simple methods for measuring the interfacial tension have also been discussed.

The chapter also considers, by way of example, a simple reaction of amino acid esterification. The esters of various amino acids, which are important from pharmaceutical viewpoint, are prepared conventionally by reacting the amino acids with alcohol under highly acidic conditions. The acid requirement is usually large and in view of the heterogeneous nature of the system, the rates are negligibly small. Also, isolation of the ester from the reaction medium requires neutralization of the excess acid, which means that equally large quantities of alkali have to be used. A novel microemulsion system has been prepared to carry out the esterification of DL-phenyl glycine using only catalytic amounts of sulfuric acid. The reasons for the observed rate improvements have also been highlighted.

The reaction between nicotine obtained from a kerosene extract of macerated tobacco waste, and sulfuric acid is a mass transfer controlled reaction. A suitably prepared microemulsion system which been used to carry out the reaction has been studied in Chapter 3. A complete phase behavior of the system at various temperatures have been reported for various microemulsion systems incorporating sulfuric acid, kerosene, and different mixtures of surfactants and cosurfactants. A simple indigenously built stirred cell reactor has been used for contacting kerosene containing nicotine and a microemulsion of kerosene in sulfuric acid. A simple kinetic model has been proposed to describe the enhancement in the overall rate of reaction.

Chapter 4 presents results for the same reaction carried out in a single drop column reactor, indigenously built for the purpose. Nicotine contained in kerosene drops, which are released from the bottom of the reactor, reacts with the stagnant

sulfuric acid at the drop surface. It has been shown that besides internal circulation in the drop, the interfacial film rigidity is also one of the factors which decides the mass transfer and hence the overall flux across the interface.

Chapter 5 illustrates yet another application of the microemulsion medium for conducting the important unit process of nitration. By way of example we consider nitration of phenol. Phenol nitrated by conventional means yields a mixture of ortho- and para-nitrophenol. The reaction is highly exothermic, and if the temperature is not controlled, a resinous product is formed. It is demonstrated here that the important unit process of nitration can be carried out using dilute nitric acid under microemulsion medium. The usefulness of such a microemulsion system in obtaining selectively ortho-nitrated product is also demonstrated.

CONTENTS

List of Tables

List of Figures

CHAPTER 1

AN INTRODUCTION TO MICELLAR SYSTEMS AND MICROEMULSIONS

1.1 Prologue

The phenomena of aggregation of molecules of a certain type when dissolved in water to form particles of colloidal dimensions is well known. The molecules which can form such aggregates are characterized by presence of two different regions in their chemical structure. One of them is a hydrocarbon chain which is hydrophobic in nature, and the other is an ionized group which is hydrophilic in nature. The existence of these two moieties in a single molecule has been termed as *amphipathy* by Hartley [1]. It is this nature of the molecule, which it is responsible for properties like micellization, surface activity, and solubilization.

Surfactants are surface active agents and show a tendency to get adsorbed at interfaces. They have been classified as anionic, cationic, nonionic, and even catanionic, depending upon the nature of its above said hydrophilic moiety and the corresponding counter-ion. Typical examples of surfactants are, sodium dodecyl sulfate, cetyl trimethyl ammonium bromide, Isooctyl phenoxy polyethoxy ethanol, etc. The process of micellization is very well studied. These studies indicate that at very low concentrations, the ionic surfactants behave like any other strong electrolyte in aqueous solutions. On increasing their concentration, a stage is reached when micelles begin to form; the concentration at this point is referred to as the critical micelle concentration (CMC). More accurate experimental work shows that this is not a single sharp concentration, but rather a narrow range after which the solution is composed mainly of spherical micelles. However on further increasing the concentration of the surfactant, the micellar structure may break-down to form various other structures like cylindrical micelles, hexagonal cellular arrays and liquid crystalline structures.

The reasons for micellization, as proposed by Hartley, are diverse. One of the main reasons is the strong adhesion between water molecules, which tend the hydrocarbon chains to be squeezed out from close contact between them. Other

reasons include overall decrease in free energy due to loss of hydrocarbon/ water interfacial energy (interfacial tension), and changes in the hydration of hydrophilic groups on addition of the surfactant to water. Owing to their hydrocarbon-like interior, these micelles can solubilize large amounts of organic compounds into the micellar solution. The difference between a micellar solution and a micro-emulsion has been a point of controversy since their advent [2]. However one point of difference is that microemulsions include an extra component, the co-surfactant, which may be a medium chain alcohol for example. The co-surfactant is responsible for reducing the interfacial tension to near zero leading to a spontaneous emulsification of the two phases. It is generally expected that in a micellar solution or a microemulsion the micelles are in equilibrium with each other. The average residence time of a monomer in the micelle is of the order of nano- to micro-seconds. The micellar phase is therefore more appropriately referred to as a pseudo-phase [3].

1.2 Solubilization

As stated earlier, one of the most important properties of micellar solutions and microemulsions is their ability to solubilize substantial amount of organic compounds. The process of solubilization is defined as formation of a thermodynamically stable isotropic solution of a substance which is normally insoluble in a given solvent, by using a micellar solution of an amphiphilic compound in the solvent. This property of micelles has been used in several applications such as reaction between mutually insoluble reactants, control of drug activity, and detergency. In order to optimize the relative quantities of the components used, it becomes necessary to study the solubilization properties of micellar systems if they are to be effectively used in industrial applications such as heterogeneous reactions.

1.3 Phase diagrams and microemulsion characterization

The data obtained from solubilization studies of a micellar system or microemulsion are represented by ternary phase diagrams wherein the phase behavior of systems incorporating three components can be best described at a given temperature. A triangular diagram is used in order to represent a three-component system in a plane. The composition at any particular point inside the triangle is represented by the ratios of altitudes drawn from that point to the sides of the triangle. The three vertices of the triangle represent each of the pure components. In case of a microemulsion, which includes a fourth component (co-surfactant), the phase behavior can be represented on a triangular diagram by keeping the ratio of any two components fixed. Usually since the interfacial behavior of the surfactant and co-surfactant is alike, the surfactant:co-surfactant ratio is kept fixed in the construction of phase diagrams [4]. The reason in doing so is that a quaternary phase diagram can be reduced to a simple pseudo-ternary diagram, which becomes easier to interpret. These diagrams are helpful in various ways, like knowing the extent of solubilization, presence of multiphases etc., corresponding to any particular composition chosen. Given a particular composition and the phase diagram, the phase behavior can be determined easily. The types of phase behavior may be any of the following (*fig.* 1). Starting from a molecular dispersion of the surfactant in water, an oil-in-water type of micellar solution is obtained by increasing the surfactant concentration. This type of solution is denoted as type S_1 emulsion in *fig.* 1, and is isotropic in nature. On further increasing the surfactant concentration one may obtain either of the three types of phases shown in the figure. The micellar structure may breakdown leading to an oil-in-water type of cylindrical micellar structure (M_1), or a bicontinuous and fluctuating structure which is isotropic in nature (*Type* III), or a rigid gel-like structure, commonly known as liquid crystals (G phase). In some cases an excess organic phase in equilibrium with a micellar solution of the form S_1, is also denoted

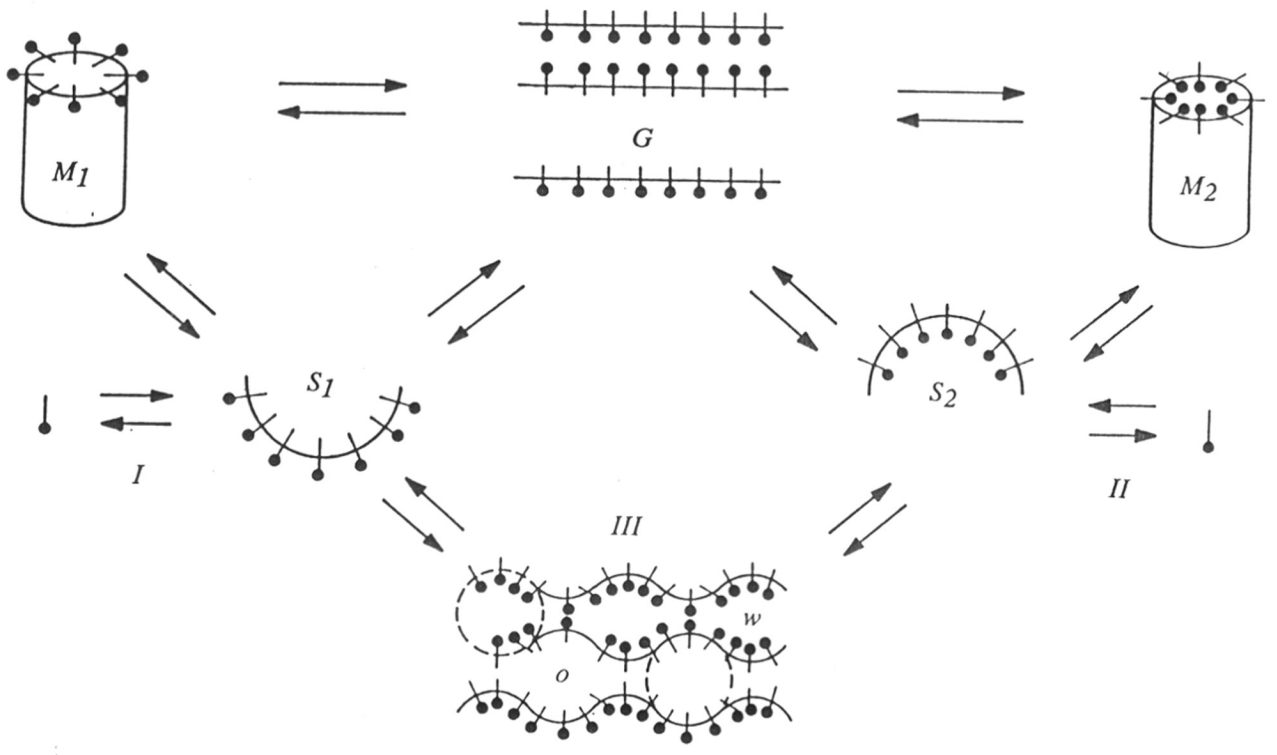

Fig. 1 **Types of phases occuring in a micellar system (adapted from reference 5):** M_1 :- *o/w* cylindrical micelles; M_2 :- *w/o* cylindrical micelles; *G* :- rigid structure (gels, liquid crystals, etc.); S_1 :- isotropic *o/w* spherical micelles; S_2 :- isotropic *w/o* spherical micelles; *type I* :- excess organic phase + S_1 two phase system; *type II* :- excess aqueous phase + S_2 two phase system; *type III* :- bicontinuous and fluctuating isotropic three phase system; *o* :- oil; *w* :- water.

as *type* I. Similarly, starting from a molecular dispersion of the surfactant in oil, a water-in-oil type of micellar isotropic solution is obtained (*type* S_2). With increasing surfactant concentration, one may obtain either of the three types of phases namely M_2, *Type* III, or G phase as depicted in the figure. In some cases when an excess aqueous phase is in equilibrium with a micellar solution of the form S_2, the phase behavior is denoted as *type* II. The micelles should not however be regarded as entities having any well-defined geometrical shapes [5]. Thus both S1 and S2 forms represent solutions containing aggregates which are dynamic entities uniformly distributed and rapidly exchanging molecules with the surrounding. The significance and importance of these types of phases lie in their applications. Also the transitions taking place between these phases on changing one or more physical parameters are of importance from application point-of-view. For example, a *type* III (or simply a middle phase) microemulsion which is obtained on changing the salinity of the aqueous phase or the temperature, is useful in applications such as tertiary oil recovery [6]. Since the micellar entities exchange matter between themselves on a time scale of milliseconds [7], reactants solubilized in these phases have better chances to react with each other. Thus a micellar solution or a microemulsion can serve as a better medium for reactions. Moreover, microemulsions being optically isotropic, are suitable for photochemical studies [8]. Microemulsions have been characterized by ultra-low interfacial tensions of the order 0.1 dynes/cm. The measurement of such low interfacial tensions despite being interesting has been difficult since instrumental methods currently available (for example ring tensiometer, Du Nuoy tensiometer) have not been very accurate. Also these methods make use of metals such as platinum. Other techniques such as spinning drop and pendant drop methods seem reasonable in comparison. In the work reported here, an indigenously devised apparatus for the pendant drop

method has been used to measure interfacial tensions. An apparatus for interfacial tension measurements by capillary method has also been devised for comparing the results.

1.4 Reactions in microemulsion media

Reactions in microemulsion media has been an interesting topic of research for some time. For example, reactions such as formation of ultra-fine colloidal particles of silver halide from aqueous solutions of silver nitrate and salt solution of the halide have been studied earlier [9]. These studies indicate that in a micro-emulsion the domain provided for such a reaction is very small, which in turn controls the crystal growth of colloidal particles. This helps in formation of monodispersed ultra-fine particles of the silver halide, which may be of interest in photographic films. Recently this technique has also been used in formation of theoretical-density microhomogeneous superconductor materials [10]. More recent studies in micellar reactions indicate that microemulsion systems besides improving the reactivity of organic reactants, also help in improving various physico-chemical processes such as selectivity, solubilization, and extraction [11-15]. It has been shown that any changes in the rate of reactions carried out under microemulsion conditions is due to partitioning of the reacting molecules at the interface [14-17]. The interfacial sub-volume of the reaction mixture is the site where reactants come together, react and the product formed may partition into either of the phases depending upon its partition coefficient into the respective phases. In the work reported in this thesis, several industrially important processes have been considered, and attempts have been made to study how rate enhancements can be achieved in such processes. For example, in the case of nitration process, it has been shown that microemulsions besides enhancing the rate of reaction can also help in the control of the rise in temperature, and improve selectivity. Important processes such esterification of amino acids (which conventionally require large amounts of mineral acid) have also been carried out using a

microemulsion medium. It has been shown that under such conditions, only catalytic amount of acid is required to obtain the same percentage yield. Complete or partial phase diagrams highlighting the phase behavior of microemulsion systems used in these reactions have also been reported at appropriate places.

1.5 References

1 Hartley, *Aqueous Solutions of Paraffin Chain Salts*, Hermann et Cie, Paris, (1936)

2 T. P. Hoar and J. H. Schulman, *Nature*, **152**, 102 (1943)

3 Romsted L. S. in *Surfactants in solution* (Edited by Mittal K. L. and Lindman B.) Vol. II pp. 1015-1068. Plenum Press, New York. (1984)

4 Shinoda K., and Kunieda H., *J. Coll. Interface Science.* **42**, 381, (1973)

5 Winsor P. A. *Chem. Rev.*, **68**, 1 (1968)

6 D. O. Shah and R. S. Schechter in *Improved Oil Recovery by Surfactant and Polymer Flooding*, Academic Press, New York, (1977)

7 P. D. I. Fletcher, B. H. Robinson, F. Bermejo-Berrera and D. G. Oakenfull in *Microemulsions*, (I. P. Robb ed.), Plenum Press, New York, pp. 221 (1982)

8 S. S. Atik and J. K. Thomas, *J. Phys. Chem.* **85**, 3921, (1981)

9 M. J. Hou and D. O. Shah, in a paper presented at the *60th National Symposium of Colloid and Surface Science*, Atlanta, Ga., June 15-18, (1986)

10 Ayyub P., Maitra A. N. and Shah D. O., *Physica C*, **168**, 571-79, (1990)

11 F. M. Menger and A. R. Elrington, *J. Am. Chem. Soc.* **113**, 9621, (1991)

12 M. Adachi, M. Harada, A. Shioi, and Y. Sato, *J. Phys. Chem.* **95**, 7925, (1991)

13 M. L. Moya, C. Izquierdo, and J. Casado, *J. Phys. Chem.*, **95**, 6001, (1991)

14 R. Schomacker, K. Stickdorn and W. Knoche, *J. Chem. Soc. Farad. Trans.*, **87(6)**, 847, (1991)

15 V. R. Hanke, W. Knoche, and E. Dutkiewicz, *J. Chem. Soc. Farad. Trans.*, **83(9)**, 2847, (1987)

16 I. V. Berezin, I. Martinek and A. K. Yatsimirskii, *Dokl. Akad. Nauk SSSR*, **194**, 840, (1970)

17 L. S. Romsted, in *Micellization, Solubilization and Microemulsions*, ed. K. L. Mittal, Plenum Press, New York, (1977)

CHAPTER 2

PHASE BEHAVIOR AND GENERAL CHARACTERISTICS OF MICROEMULSION SYSTEMS

2.1 Introduction

The phenomena of spontaneous formation of microemulsions has been known since long. They have been prepared by adequately mixing water, oil, and a suitable amphiphilic compound, called as surfactant, along with a cosurfactant in proper proportions. These systems are found to be multi-component liquids, having very low apparent viscosity and long term stability [1]. A notable feature of these types of fluids has been the ultra-low interfacial tensions observed between the solubilized oil and aqueous phases. One of the useful and significant feature of microemulsion media has been their optical transparency. It has been found that the micro-structures of these types of fluids are composed of micro-globules having diameters not greater than about 1000°A. Hence the interfacial areas are much larger than those obtained in a macroemulsion. It is for this reason that microemulsions have been used as a better medium for interfacial synthesis and chemical reactions [2-6]. Due to the ultra-low interfacial tensions exhibited by microemulsions, they have been also used as efficient fluid systems in novel applications such as surfactant flooding in tertiary oil recovery. In this case, the phase behavior of microemulsion systems has been one of the major factors determining the displacement efficiency of surfactant flood. Other applications include drug delivery systems, blood substitutes and organ preservation fluids [7-9].

For a given kind of water/ amphiphile (s)/ hydrocarbon system, the larger the microemulsion domain (the range of compositions corresponding to the existence of microemulsion medium), the higher the diversity of the microemulsion structure. This fact has been important, particularly in deciding the optimum path of reaction [10], or in designing speciality products and multi-component fluids, to be used in industrial processes. For example, the efficiency of a microemulsion-type fluid as a vehicle for some specific chemical or biochemical compound may be greatly optimized by formulating it in such a way, that its local structure helps to enhance the solubilization of the said compound. It has been therefore important

to know the effects of changes in parameters such as the pH of the medium, the concentration of the components, the temperature, salinity etc., on the phase behavior of the system, since the performance of these fluids greatly depends on these parameters.

The realms-of-existence of microemulsion domain can be delineated for most of the systems by studying their phase behavior. In the work presented in this chapter, various ternary and pseudo-ternary systems, and the effects of change in system parameters, like temperature and composition, on their phase behavior have been studied. Organic solvents such as benzene, toluene, p-xylene and kerosene have been important solvents extensively used in the industry. It has been of interest then to study the emulsification process of these solvents. This type of study is important and can help us in a suitable formulation of microemulsion in applications such as tertiary oil recovery, and in deciding a medium for chemical reactions in order to either enhance their rates or control the selectivity. In the present work these solvents have been used as "oil" components of the microemulsion system.

Characterization of micellar systems has been an interesting field in colloid and interface science. This requires sophisticated instruments such as light scattering, pulse radiolysis, laser photolysis, etc. As stated earlier, microemulsion systems are characterized by ultra-low interfacial tensions and the instrumentation required for such measurements would be quite sophisticated. Many such instruments like Du Nouy tensiometer, ring tensiometer, etc. are available currently. These methods despite being accurate, involve the use of precious materials like platinum for example. It would be of interest if one can devise a simpler method in order to measure such low interfacial tensions to required accuracy. In the present work, a simple apparatus has been devised for measuring the interfacial tension between various phases in a micellar or a microemulsion system by pendant drop and capillary method

As mentioned earlier, micellar media can be used for organic reactions. A simple esterification reaction of the amino acid, DL-phenyl glycine has been carried out under micellar conditions, using only catalytic amounts of sulfuric acid and making use of an ion exchange resin of catalytic grade.

2.2 Materials

Sodium dodecyl sulfate (SDS), Isooctyl phenoxy polyethoxy ethanol (TX-100), Sodium salt of di-isooctyl sulfo succinate (AOT) and Cetyl trimethyl ammonium bromide (CTAB) have been obtained from Aldrich chemicals and used as received. Sodium dodecyl benzene sulfonate (SDBS) has been obtained from SD chemicals and used as received. 1-Pentanol (AR grade) has been a Fluka guaranteed material. The solvents benzene, toluene, p-xylene and n-heptane have been obtained from SD chemicals. Kerosene has been obtained from local markets and used without further purification. The approximate composition of the kerosene used (volume %) has been given in Table 2.1. Water used in the experiments has been doubly distilled, and deionized. Concentrated Sulfuric acid obtained from SD chemicals, has been diluted to the required dilutions. The exact concentrations of the acid were determined by titration with standard sodium hydroxide solutions of appropriate strengths. Methyl alcohol and DL-phenyl glycine have been obtained from Sigma Chemicals. An ion exchange resin, Indion CXC-125 has been procured from Indian Ions.

Table 2.1 Composition of kerosene (volume%)

a) Aromatics	1. Mononuclear (single ring aromatic hydrocarbons)	15%
	2. Dinuclear (double ring aromatic hydrocarbons)	6%
b) Naphthenic rings	1. Monocyclic (single ring aliphatic hydrocarbons)	26%
	2. Dicyclic (double ring aliphatic hydrocarbons)	9%
c) Paraffins	1. Normal (straight chain aliphatic hydrocarbons)	25%
	2. Branched (aliphatic hydrocarbons with side chains)	19%

2.3 Phase behavior studies

In all the experiments for phase behavior studies, a mixture of surfactant, and 1-pentanol has been used in a fixed proportion by weight. Various microemulsion systems studied have been tabulated (Table 2.2). The boundaries of the microemulsion domain have been determined by progressive "dynamic" titration of mixture of two pseudo-components, viz. surfactant + cosurfactant, and the oil versus the aqueous component. These boundaries have been then confirmed by titrating mixtures of surfactant + cosurfactant, and the aqueous phase, versus the oil. The end points have been noted for a clear to turbid or a turbid to clear type of change in the appearance of the mixture. Usually, the titration paths followed in the triangular diagrams have been as shown in *fig.* 2.1. Only in some cases, when the phase boundaries used to be almost parallel to these paths, the titrations have been followed along paths shown in *figs.* 2.2 and 2.3, with the arrow heads pointing towards a "macroscopically homogeneous" composition. The concentrations of the titrant added, at which different transitions occurred, have been derived from precise weight measurements. All the titrations have been performed at a fixed temperature accurate to within 0.5°C. In some cases, it became necessary to carry "static" titration experiments. For this purpose, samples, whose overall composition was close to the transition composition (determined by the "dynamic" titration) were prepared and stored in a temperature controlled bath for at least a week. The phase behavior of these samples has been checked at regular intervals, until no change in the physical condition has been observed. It has been estimated that on an average, the relative uncertainty on the components' mass fraction corresponding to transition point has been less than 1 %. Finally points corresponding a set of particular transition have been plotted on a triangular diagram, and joined by a smooth curve, to get a boundary demarcating two distinct regions on the diagram. This curve has been a representative curve for that particular phase transition.

Table 2.2 Microemulsions Studied

No.	Temperature	System studied
1	25°C	SDS + 1-pentanol (1:2.23 by wt)/ water/ benzene
2	25°C	SDS + 1-pentanol (1:2.23 by wt)/ water/ toluene
3	25°C	SDS + 1-pentanol (1:2.23 by wt)/ water/ p-xylene
4	25°C	TX-100 + 1-pentanol (1:1 by wt)/ (2.5 mol/lit) H_2SO_4/ toluene
5	30°C	CTAB + 1-pentanol (1:1 by wt)/ water/ kerosene
6	30°C	CTAB + 1-pentanol (1:1 by wt)/ (0.13 mol/lit) H_2SO_4/ kerosene
7	30°C	CTAB + 1-pentanol (1:1 by wt)/ (0.26 mol/lit) H_2SO_4/ kerosene
8	30°C	CTAB + 1-pentanol (1:1 by wt)/ (0.365 mol/lit) H_2SO_4/ kerosene
9	30°C	CTAB + 1-pentanol (1:1 by wt)/ (0.55 mol/lit) H_2SO_4/ kerosene
10	30°C	CTAB + 1-pentanol/ (1.05 mol/lit) H_2SO_4/ kerosene
11	30°C	SDS + 1-pentanol (1:1 by wt)/ water/ kerosene
12	30°C	SDS + 1-pentanol (1:1 by wt)/ (0.05 mol/lit) H_2SO_4/ kerosene
13	30°C	TX-100 + 1-pentanol (1:1 by wt)/ water/ kerosene

Table 2.2 Microemulsions Studied (contd.)

No.	Temperature	System studied
14	30°C	TX-100 + 1-pentanol (1:1 by wt)/ (0.5 mol/lit) H_2SO_4/ kerosene
15	30°C	TX-100 + 1-pentanol (1:1 by wt)/ (2.5 mol/lit) H_2SO_4/ kerosene
16	40°C	TX-100 + 1-pentanol (1:1 by wt)/ (2.5 mol/lit) H_2SO_4/ kerosene
17	40°C	CTAB + 1-pentanol (1:1 by wt)/ (0.55 mol/lit) H_2SO_4/ kerosene
18	50°C	CTAB + 1-pentanol (1:1 by wt)/ (0.55 mol/lit) H_2SO_4/ kerosene
19	60°C	CTAB + 1-pentanol (1:1 by wt)/ (0.55 mol/lit) H_2SO_4/ kerosene

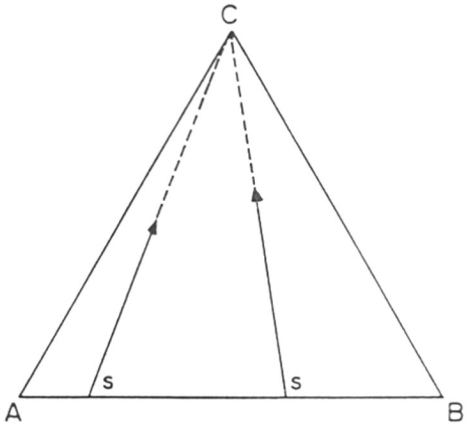

Fig.2.1

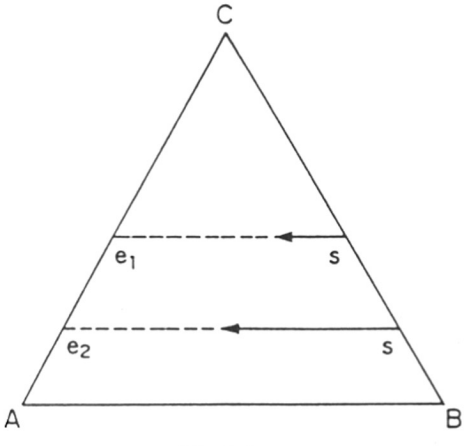

Fig.2.2

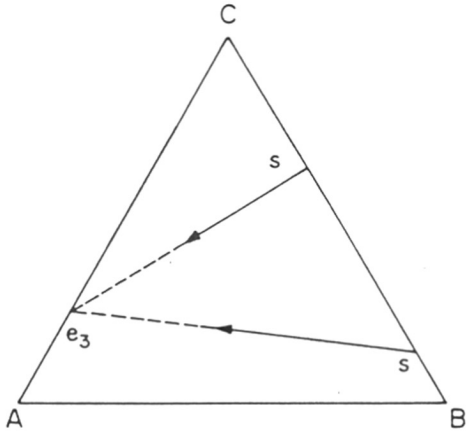

Fig.2.3

Fig. Titration paths followed in the experiments for determination of phase behavior of microemulsion systems: *A,B,C* :- various components used; *s* :- starting composition for the titration; e_1, e_2, e_3 :- macroscopically homogeneous compositions.

2.4 Interfacial tension studies

2.4.1 Theoretical derivations for pendant drop method

Theoretical derivations for determining the interfacial tension between two immiscible liquids by the pendant drop method are available in the literature. The profile of any liquid drop of given volume hanging from a smooth horizontal circular syringe is a function of the tube radius, the interfacial tension between the liquid and the surrounding medium, the difference in densities of the two liquids, and the gravitational acceleration. The drop detaches when its theoretical maximum weight is attained. Consider the pendant drop as shown in *fig.* 2.4. If d_e is the maximum equatorial diameter of the pendant drop and d_S is the diameter of the drop at a distance d_e from its apex (*fig.* 2.4) and defining the ratio of d_e and d_S as $S = (d_e / d_s)$ then the equation for interfacial tension has been given as,

$$\gamma_{ao} = \Delta\rho g \left(\frac{d_e^2}{H} \right) \qquad (1)$$

where $\Delta\rho$ is the density difference, g is acceleration due to gravity, and an empirical correlation between H and S has been given as[11]

$$\left(\frac{1}{H} \right) = 0.31270 \quad S^{2.6444} \qquad (2)$$

2.4.2 Interfacial tension measurements (pendant drop)

The apparatus for measuring of interfacial tension has been shown in *fig* 2.5. It consists of a microscope (magnification > 200) equipped with a horizontal and vertical micrometer screw gauge. A rectangular glass cell with thermostat contains the lighter liquid, and a syringe with thermostat jacket and needle contains the heavier liquid. Both liquids between which the interfacial tension was to be determined have been thermostated at the required temperature. Various needles

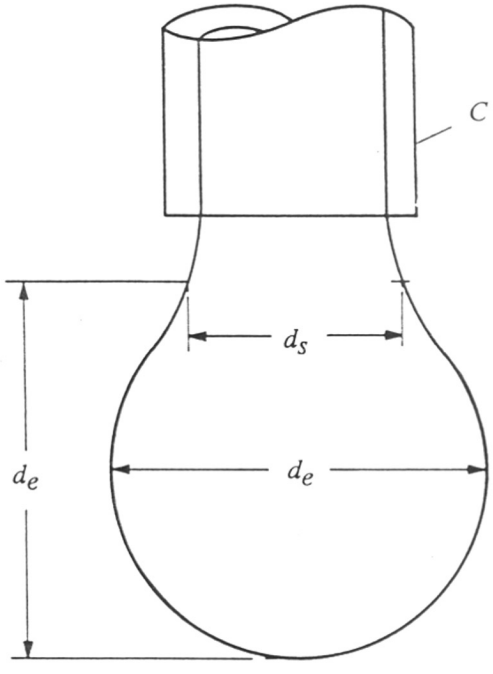

Fig. 2.4 **Profile of a pendant drop:** C :- capillary; d_e :- maximum equatorial diameter of the drop; d_s :- diameter of the drop at distance d_e from the apex.

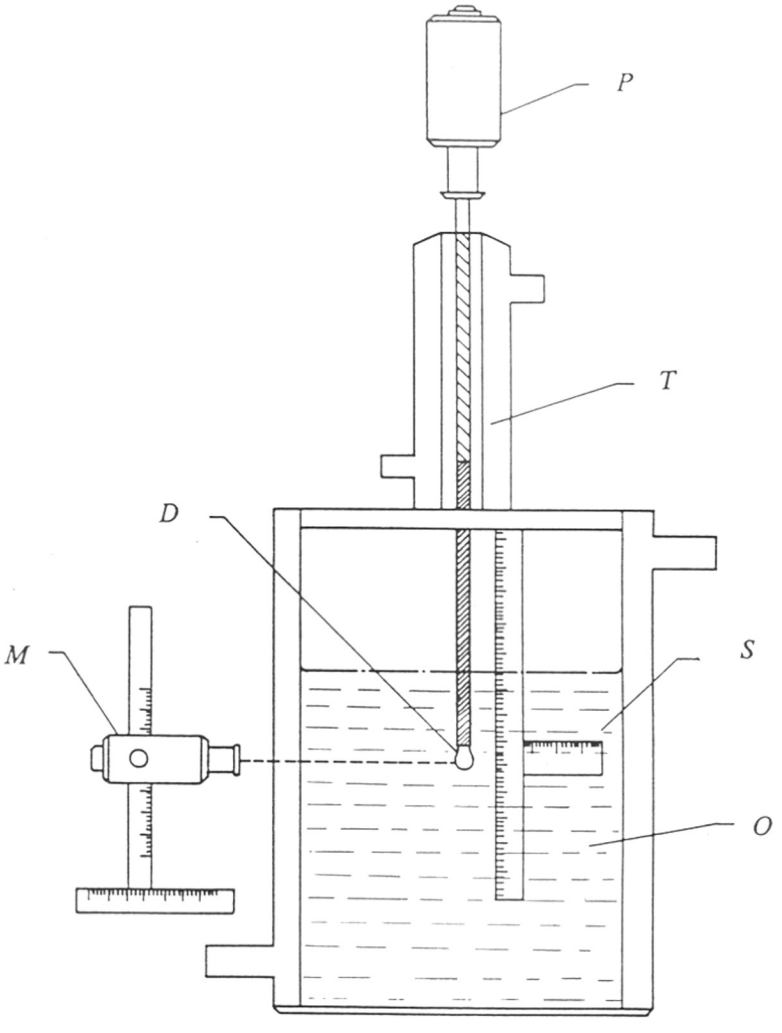

Fig. 2.5 **Apparatus for measuring interfacial tension by pendant drop method:** *P* :- automatic plunger; *T* :- thermostatic syringe; *D* :- the drop; *S* :- scale; *O* :- the lighter liquid; *M* :- microscope.

have been used as per the requirements of the experiments. The range of dimensions of the needles have been : i) outer diameter 0.2 to 0.45 mm, and ii) inner diameters 0.1 to 0.2 mm respectively. The aqueous phase drop has been formed by plunging slowly for over 10 min. in the organic phase. The diameters, d_e and d_s have been measured for the drop. The interfacial tensions were calculated for each drop using equation 1.

2.4.3 Interfacial tension measurements (capillary method)

The apparatus used for measuring the interfacial tension by capillary method is shown in *fig.* 2.6. The apparatus consists of two cylindrical glass containers joined by a capillary of internal diameter about 1 mm. The two liquids have been filled in the two cylinders such that the interfacial meniscus was in between the two ends of the capillary. The capillary has been set in an exact vertical position. The vertical distance of the menisci of the organic and the aqueous phases with respect to the interfacial meniscus have been measured by the microscope provided with vertical and horizontal micrometer screw gauge. Knowing the densities of both the phases, the equation for interfacial tension have been given as,[12]

$$\gamma_{ao} = \frac{rg}{2}(h_a\rho_a - h_o\rho_o) \qquad (3)$$

where γ_{ao} is the interfacial tension, r the capillary radius, g the gravitational acceleration, h_a and h_o the respective vertical distances of the menisci, and ρ_a and ρ_o the densities of aqueous and organic phases respectively.

The densities of both the phases have been measured by using an automated vibrating tube density meter (DMA 60/602 Anton Paar) which has been calibrated at the required temperature. The internal diameter of the capillary has been measured to be 0.1006 cm. Knowing the densities and h_a and h_o, the interfacial tensions have been calculated for various systems shown in Table 2.3.

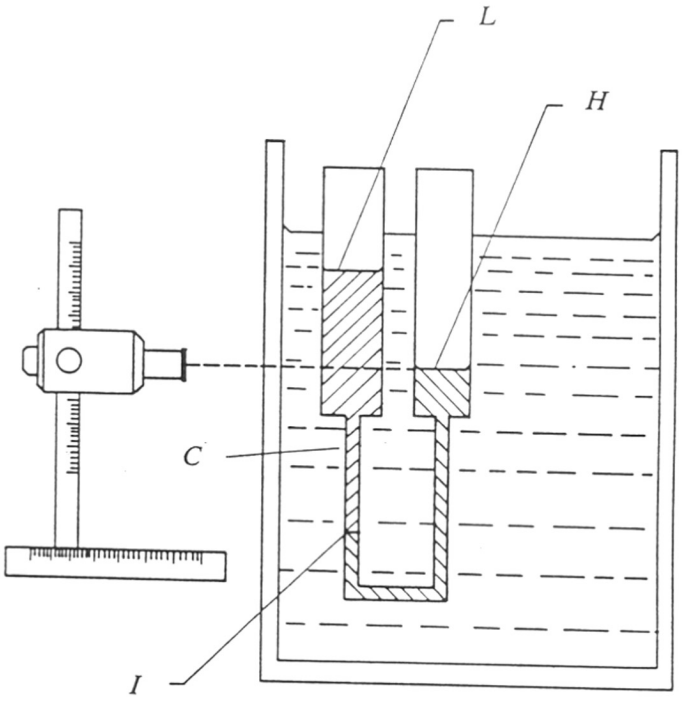

Fig. 2.6 **Apparatus for measuring interfacial tension by capillary method:** H :- heavier liquid; L :- lighter liquid; C :- capillary; I :- interface meniscus.

Table 2.3 Systems used for interfacial tension measurements

No.	Aqueous phase	Organic phase
a)	Water	Benzene
b)	0.02 mol/lit SDBS in water	n-heptane
c)	0.08 mol/lit SDBS in water	n-heptane
d)	0.16 mol/lit SDBS in water	n-heptane
e)	0.02 mol/lit SDBS in water	toluene
f)	0.08 mol/lit SDBS in water	toluene
g)	0.16 mol/lit SDBS in water	toluene
h)	0.26 N (0.13 mol/lit) H_2SO_4	kerosene
i)	0.52 N (0.26 mol/lit) H_2SO_4	kerosene
j)	0.73 N (0.365 mol/lit) H_2SO_4	kerosene
k)	SDS + 1-pentanol/ (0.05 mol/lit) H_2SO_4/ Kerosene	excess kerosene
l)	CTAB + 1-pentanol/ (0.13 mol/lit) H_2SO_4/ Kerosene	excess kerosene
m)	CTAB + 1-pentanol /(0.26 mol/lit) H_2SO_4/ Kerosene	excess kerosene
n)	CTAB + 1-pentanol/ (0.365 mol/lit) H_2SO_4/ Kerosene	excess kerosene
o)	TX-100 + 1-pentanol/ (2.5 mol/lit) H_2SO_4/ Kerosene	excess kerosene

2.5 Micellar reactions

Amino acid esters have been extensively used as intermediate compounds in the resolution of amino acids like phenyl glycine and p-hydroxy phenyl glycine which are used in the manufacture of important drugs like Ampicillin and Amoxycillin. The esterification of amino acids and their resolution process have been reported[13-16] in the presence of mineral acids and alcohol as a medium of the reaction, under reflux conditions. Due to poor solubility of amino acids in methanol or ethanol, its esterification normally requires a large amount of mineral acid (sulfuric acid for example) to first convert the amino acid into its sulfate. The sulfate is then solubilized into the alcohol and the batch is refluxed to obtain the esterified product (for example in case of phenyl glycine methyl ester, 2 moles of conc. sulfuric acid are required per mole of phenyl glycine; methanol required is 20 moles, and the time required to attain equilibrium is 3 hours). The product formed has to be treated with an excess of alkali (liq. ammonia for example) to neutralize the acid and also to remove any unreacted amino acid. This results in formation of salt (ammonium sulfate) which is an unnecessary by-product of the reaction. The reaction is usually carried out in batch mode and equilibrium considerations restrict the extent to about 90% conversion under condition of operation. In the present work the earlier process has been improvised. A method to solubilize the amino acid in alcohol has been developed and the esterification has been carried out using only catalytic amounts of mineral acid. It has been found that this has circumvented the formation of by-products, and the isolation of the product from the reaction mixture has been simplified. The surfactant used has been AOT which has been first dissolved in the alcohol such that the concentration of the solution has been well above the critical micelle concentration (CMC). The amount of AOT used has been 2 gm in 25 gm alcohol. 2 gm of the amino acid has been then solubilized into this solution by initially treating it with catalytic amount (0.2 gm) of sulfuric acid, adding it to the micellar solution and by mild stirring.

The solubilized amino acid has been treated with the ion exchange resin Indion CXC-125 in presence of the acid. The whole mixture has been maintained at the reflux temperature of 78°C for 2 hours. The product has been filtered to remove the spent resin. The filtrate has been demulsified to remove the unconverted amino acid and analyzed by HPLC technique. The HPLC method was developed on a Millipore-Waters (Milford, MA, USA) High Performance Liquid Chromatography system consisting of a model 510 dual head reciprocating solvent delivery pump, a Rheodyne (Cotati, CA, USA) model 7125 injector and a Model 440 filter photometric absorbance detector operating at 254 nm. The analogue output of the detector was recorded and processed with a Hewlett-Packard (Avondale, CA, USA) model 3390A integrator. A Waters Radial-PAK μ Bondapak phenyl (1 dp 10 mμ) cartridge column (8 mm i.d. × 10 cm) with Waters Z-module radial compression mounting system was used. The mobile phase consisted of a mixture of methyl alcohol-10 mmol triethyl ammonium phosphate buffer (pH 2.6) in the ratio of 10:80. The flow rate of the mobile was maintained at 2.0 ml/min.

2.6 Results

The first four systems, namely SDS + 1-pentanol/ water/ benzene, SDS + 1-pentanol/ water/ toluene, SDS + 1-pentanol/ water/ p-xylene, and TX-100 + 1-pentanol/ (2.5 mol/lit) H_2SO_4/ toluene were studied as model pseudo-ternary systems. The isothermal pseudo-ternary phase behavior of these systems have been shown in *figs*. 2.7 to 2.10 respectively. It has been found that these diagrams could be, in general, divided into 5-6 distinct regions. Some of these regions have been marked on the diagrams as i) $S + L$: solids in equilibrium with an excess micellar solution, ii) *Type I* : an excess organic phase in equilibrium with a microemulsion iii) *Type II* : an excess aqueous phase in equilibrium with a microemulsion iv) *Type III* : a three phase behavior v) *Type IV* : an isotropic, transparent microemulsion and vi) G : liquid crystalline phase.

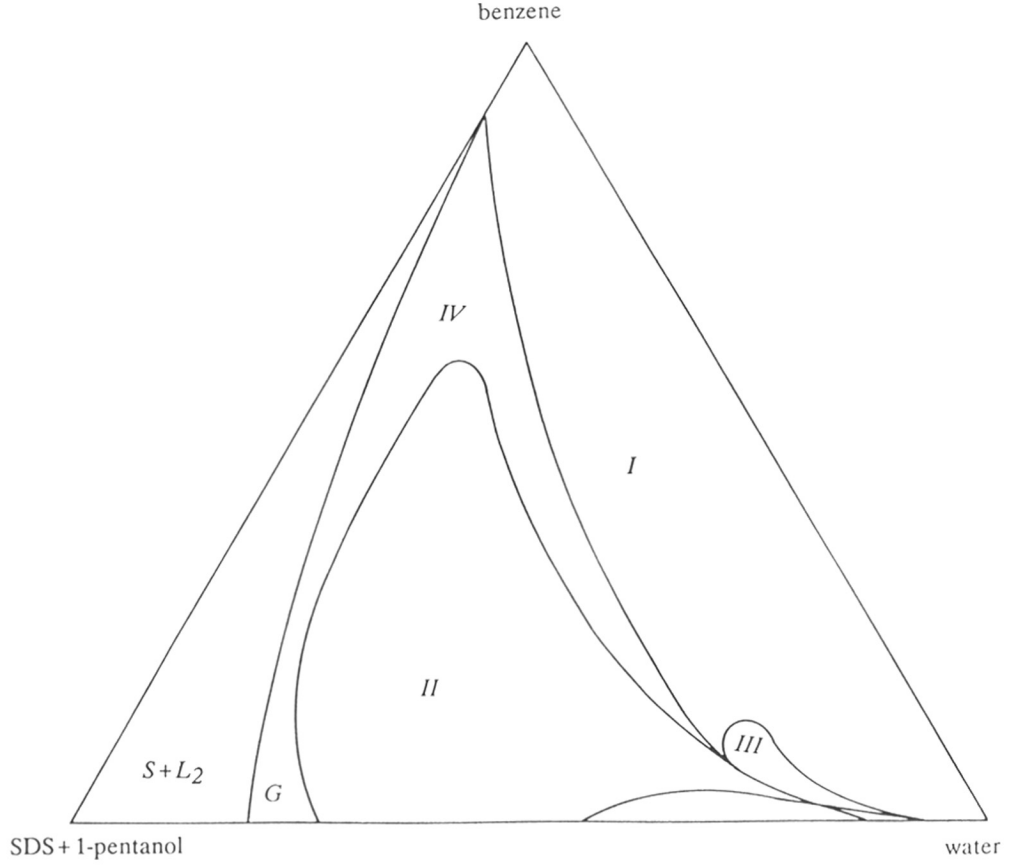

Fig. 2.7 **Complete phase diagram for the pseudo-ternary system SDS + 1-pentanol/ water/ benzene at 25°C:** *I* :- type *I* system; *II* :- type *II* system; *III* :- type *III* system; *IV* :- type *IV* system; $S + L_2$:- solids + w/o emulsion; *G* :- gel phase.

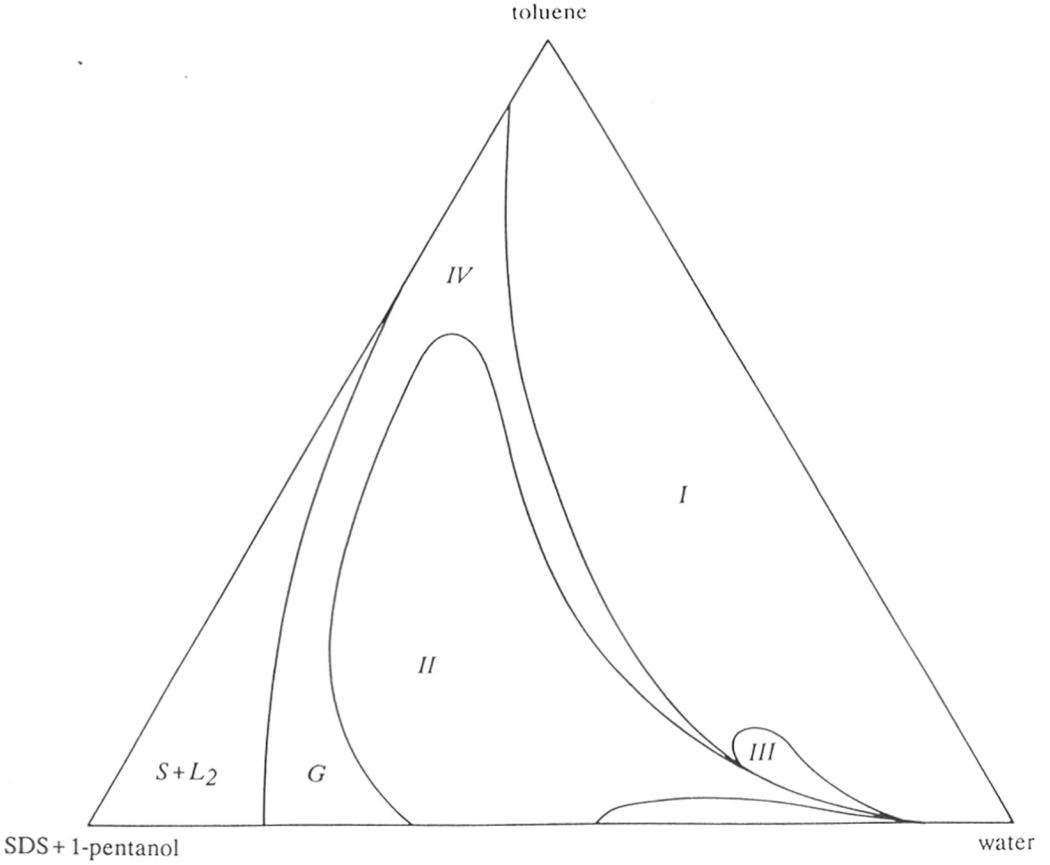

Fig. 2.8 **Complete phase diagram for the pseudo-ternary system SDS + 1-pentanol/ water/ toluene at 25°C:** *I* :- type *I* system; *II* :- type *II* system; *III* :- type *III* system; *IV* :- type *IV* system; $S + L_2$:- solids + w/o emulsion; *G* :- gel phase.

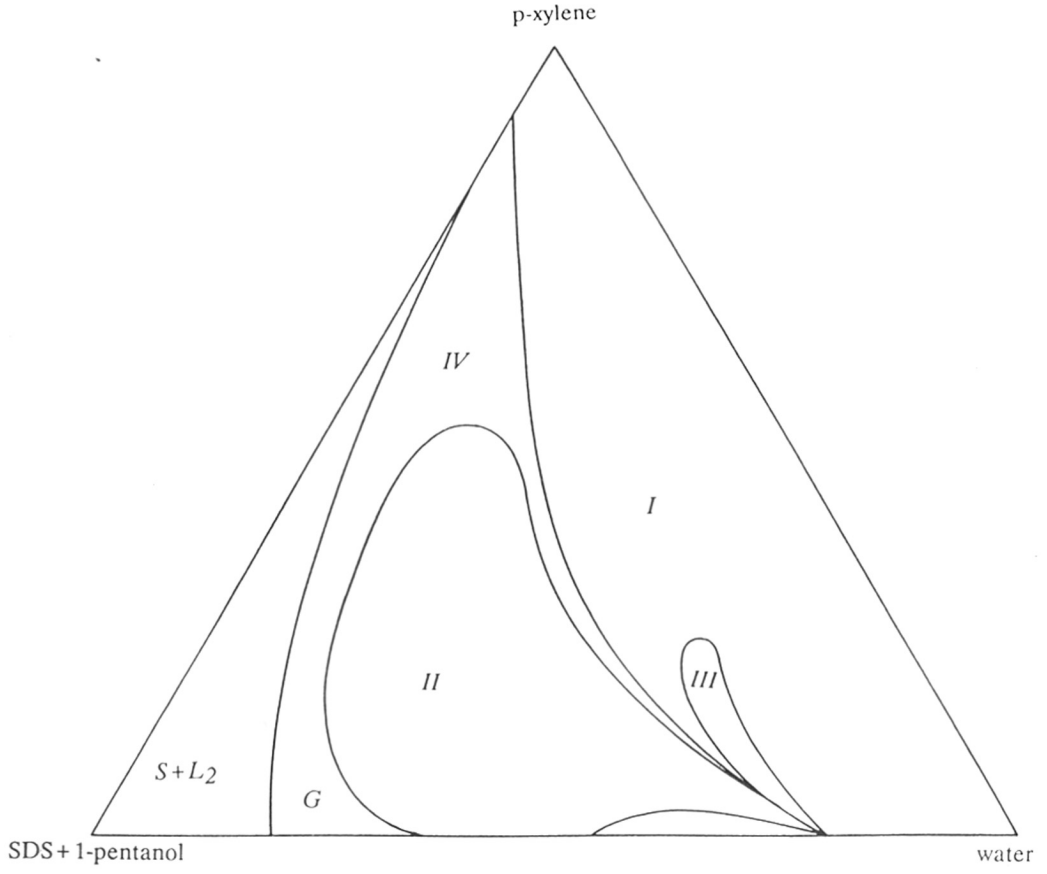

Fig. 2.9 **Complete phase diagram for the pseudo-ternary system SDS + 1-pentanol/ water/ p-xylene at 25°C:** *I* :- type *I* system; *II* :- type *II* system; *III* :- type *III* system; *IV* :- type *IV* system; $S + L_2$:- solids + w/o emulsion; *G* :- gel phase.

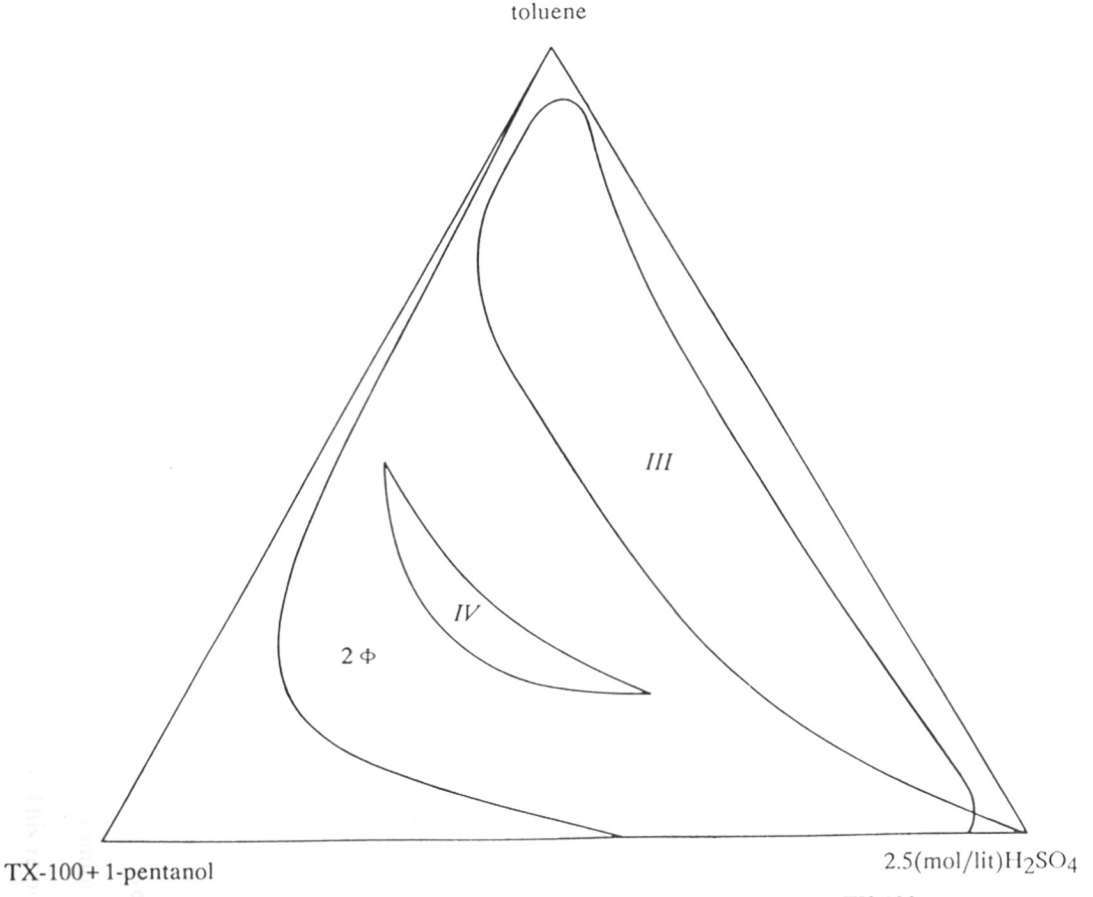

Fig. 2.10 **Complete phase diagram for the pseudo-ternary system TX-100 + 1-pentanol/ 2.5 (mol/lit) H2SO4/ toluene at 25°C:** 2 Φ :- two phase system; *III* :- three phase system; *IV* :- microemulsion system.

2.6.1 Effect of acid concentration on phase behavior

The isothermal pseudo-ternary phase diagrams for systems containing TX-100, which has been reported in *figs.* 2.11 through 2.13 clearly exemplify the differences that exist between the microemulsion domains of the phase diagrams on changing the acid concentration. Surprisingly, the area covered by the microemulsion domain has been found to appear as all-in-one block, denoted as *N*. The percentages of the areas covered by this region *N*, for water , 0.5 mol/lit H_2SO_4 and 2.5 mol/lit H_2SO_4 have been calculated to be 34%, 18% and 38% respectively, of the total area of the pseudo-ternary domain. In such a situation, no solubilization gap has been found to exist between the "direct" and the "inverse" type of micelles. This type of case has been denoted as type "*U*" by Clausse, *et al* [17]. A three phase region, denoted by *T* has been found to be surrounded by a two phase region (2ϕ) in these systems. As expected, the phase boundaries have not been straight lines, since these systems have not been truly ternary. In the case of 0.5 mol/lit sulfuric acid, a cusp has been observed at a point denoted by *C* on the phase diagram. This point represents a micellar solution in equilibrium with excess acid and oil phases.

On changing the surfactant to SDS and using water as aqueous phase, two strikingly dissimilar regions (N_1 and N_2), each single phase, have been found to appear on the phase diagram. (*fig.* 2.14). These regions are separated by a so called solubilization gap, which is composed of a range of compositions, corresponding to the existence of mesophases (*B*). on changing the concentration of the acid from zero (water) to 0.05 mol/lit H_2SO_4 (*fig.* 2.15), the areas of N_1 and N_2 have been found to decrease. Simultaneously, a lenticular region which is continuous with the N_1 region has been found to appear on the phase diagram. This region has been denoted by *l*. Considering the relative locations of each, it has been asserted that N_1 is the realm-of-existence of the "direct" kind of microemulsion, and N_2 that of the "inverse" kind. Such a case has been classified as *type "S"* by Clausse, *et*

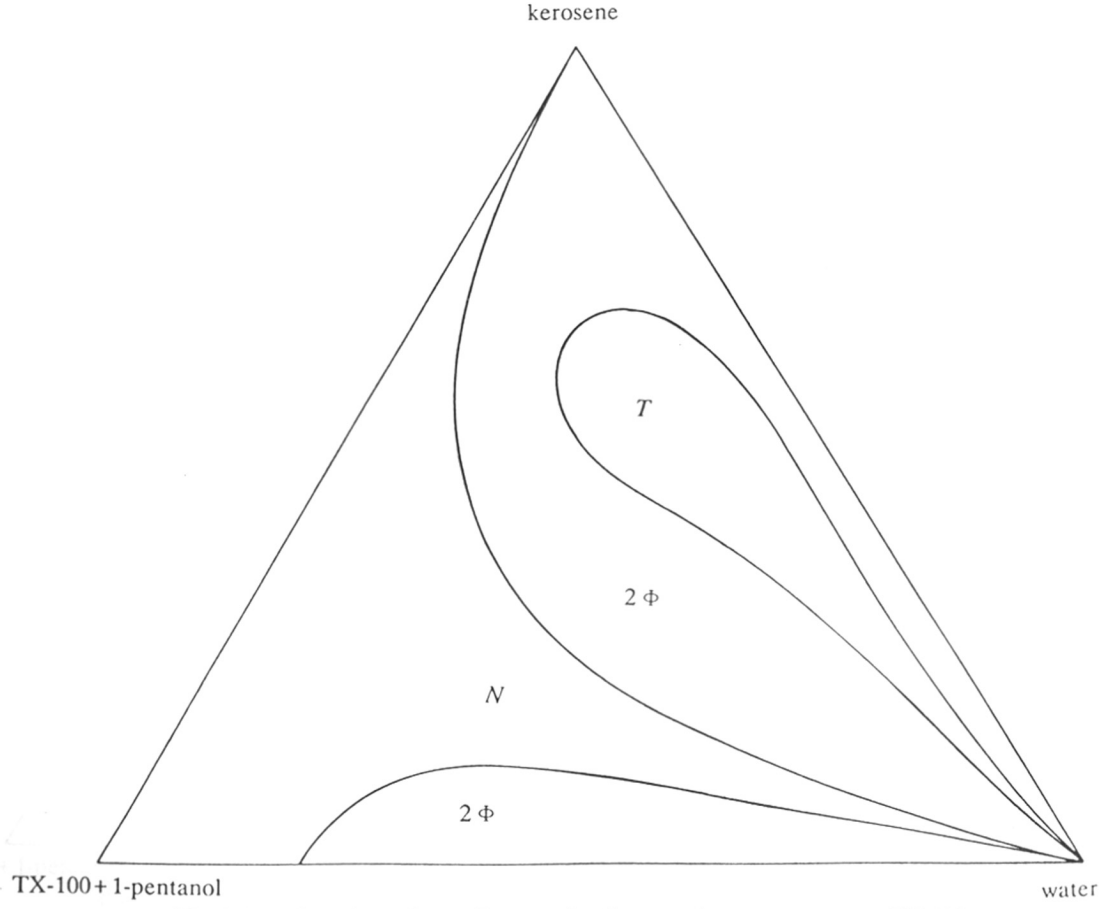

Fig. 2.11 **Complete phase diagram for the pseudo-ternary system TX-100 + 1-pentanol/ water/ kerosene at 30°C:** *N* :- micellar system; 2 Φ :- two phase system; *T* :- three phase system.

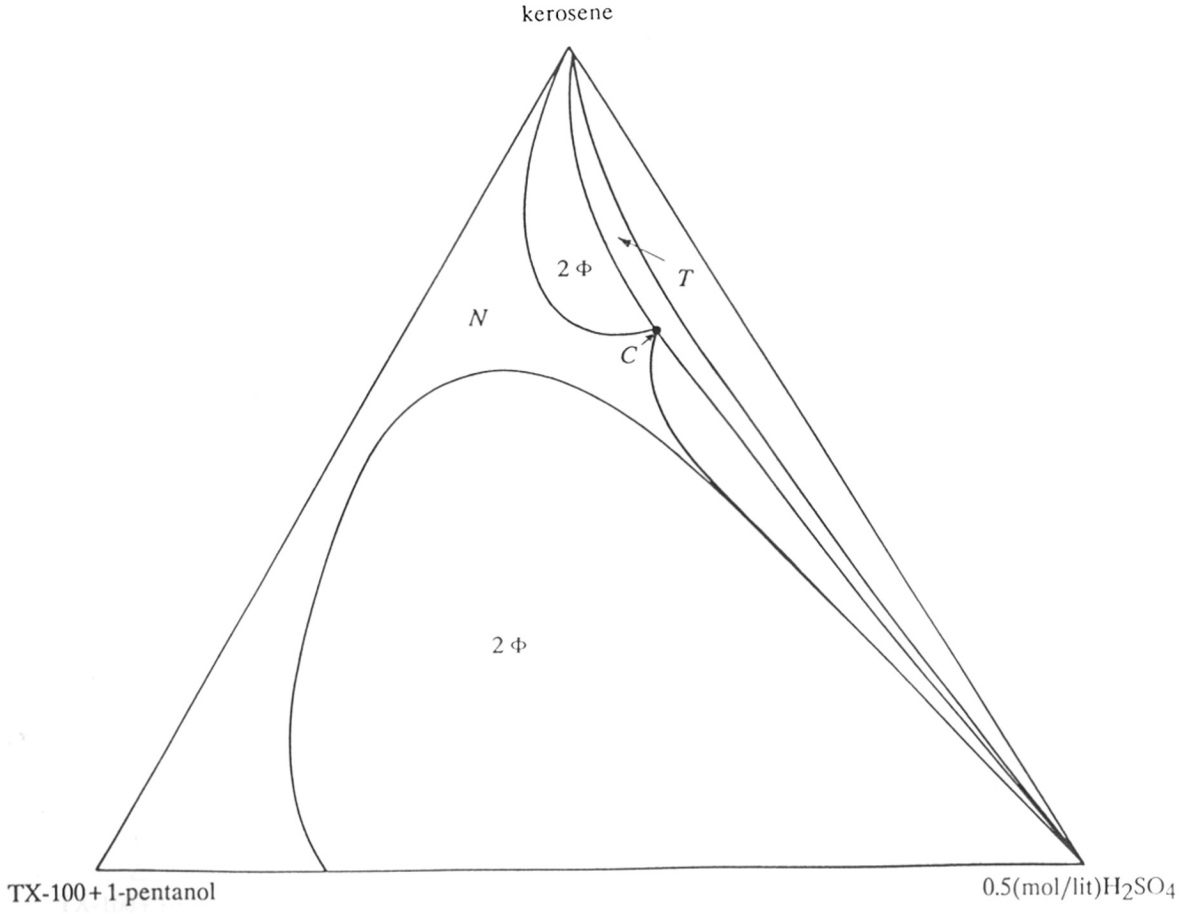

Fig. 2.12 **Complete phase diagram for the pseudo-ternary system TX-100 + 1-pentanol/ 0.5 (mol/lit) H2SO4/ kerosene at 30°C:** *N* :- micellar system; 2 Φ :- two phase system; *T* :- three phase system; *C* :- cusp.

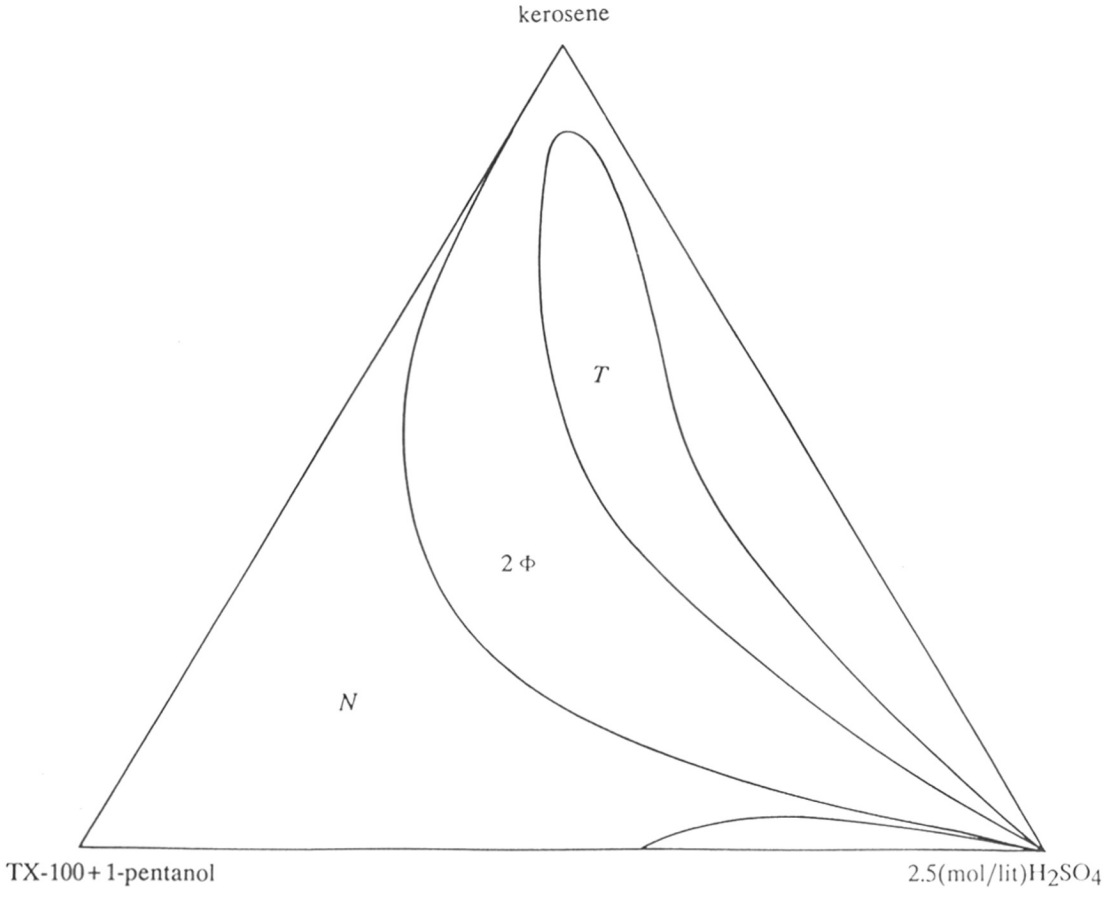

Fig. 2.13 **Complete phase diagram for the pseudo-ternary system TX-100 + 1-pentanol/ 2.5 (mol/lit) H2SO4/ kerosene at 30°C:** *N* :- micellar system; 2 Φ :- two phase system; *T* :- three phase system.

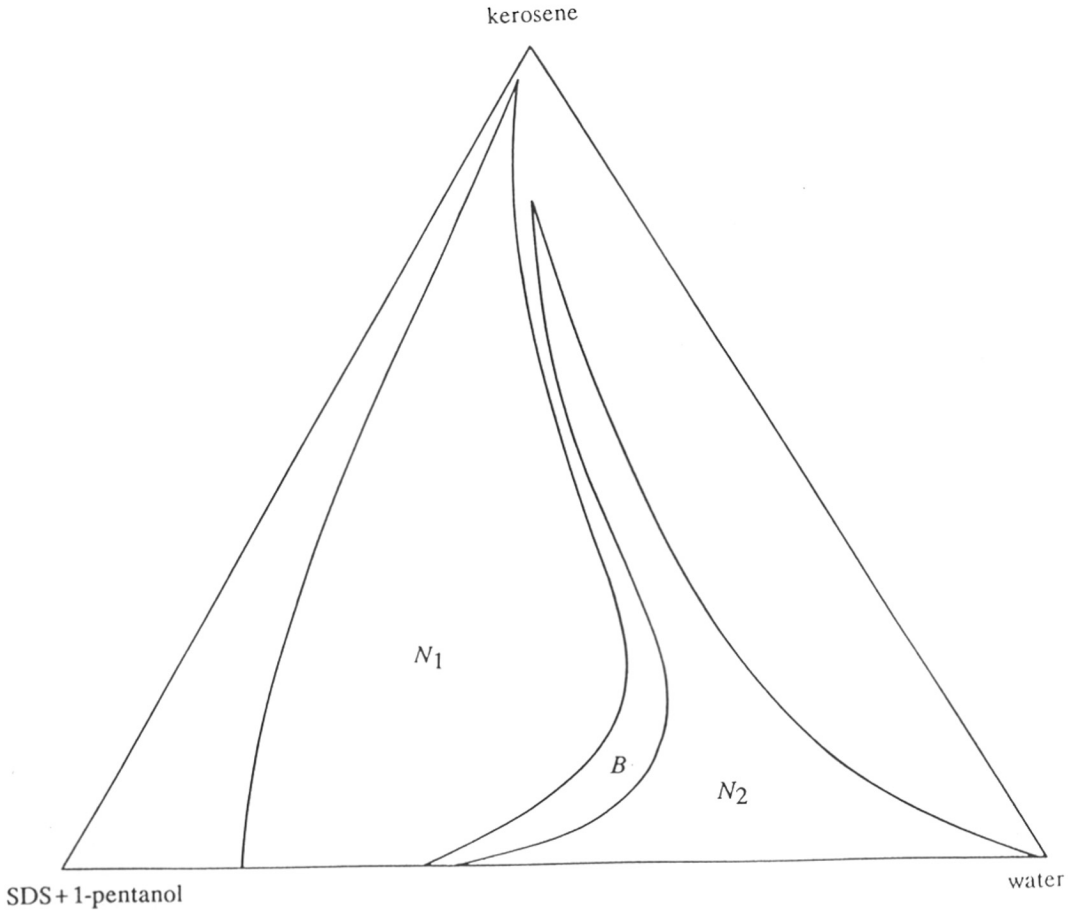

Fig. 2.14 **Complete phase diagram for the pseudo-ternary system SDS + 1-pentanol/ water/ kerosene at 30°C:** N_1, N_2 :- one phase micro-emulsion systems; B :- mesophase.

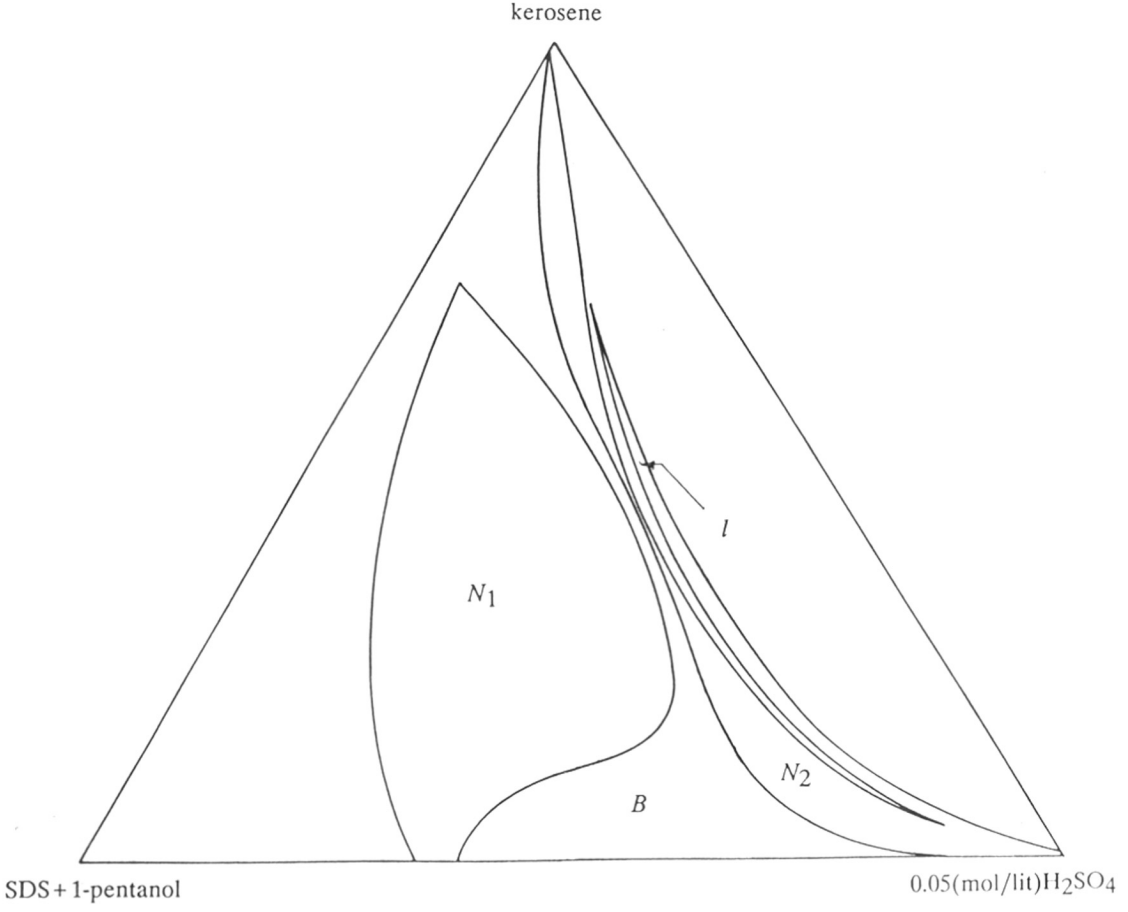

Fig. 2.15 **Complete phase diagram for the pseudo-ternary system SDS + 1-pentanol/ 0.05 (mol/lit) H2SO4/ kerosene at 30°C:** N_1, N_2 :- one phase microemulsion systems; B :- mesophase; l :- lamellar phase.

al [17]. Considering the areas covered by the microemulsion regions in the above systems, it has been stated that TX-100 along with pentanol can withstand up to about 2.5 mol/lit H_2SO_4, as in comparison with SDS + 1-pentanol mixture.

The isothermal pseudo-ternary phase diagrams for systems containing CTAB + 1-pentanol, acid and kerosene at 30°C have been reported in *figs.* 2.16 through 2.21. The observed phase behavior on equilibration could be either a single phase (*L1*), a single phase in equilibrium with a precipitated solid (*S* + *L2*), an oil-in-water microemulsion phase in equilibrium with an excess oil phase (*type I*), or a water-in-oil microemulsion phase in equilibrium with an excess aqueous phase (*type II*). In some cases a three phase region, consisting of a microemulsion in equilibrium with an excess oil and an excess aqueous phase was found to exist (*type III*). An optically transparent liquid crystalline phase has been found in the region denoted by *G*. These diagrams clearly exemplify the differences that exist between the microemulsion domains of the phase diagrams on changing the acid concentration. On each of the diagrams have been marked points *p* through *t*. Points *p* and *q* represent two compositions having surfactant concentrations of respectively 8% and 10% by weight, whereas points *r* and *s* represent two compositions having the same surfactant concentration of 8.5% by weight. As is evident from *fig.* 2.16, for zero concentration of acid (water), two phases are observed at all the points. Since these phases are respectively an excess kerosene phase in equilibrium with a micellar solution of kerosene in water, they have been denoted as a *type I* system. It has been found that on increasing the acid concentration to 0.13 mol dm^{-3} (*fig.* 2.17) points *p* and *q* undergo a *type I* to *type III* transition, whereas points *r* and *s* are still under a *type I* regime. On increasing the acid concentration further to 0.26 mol dm^{-3} (*fig.* 2.18), points *p* and *q* undergo a type III to type II transition, whereas points *r* and *s* undergo a *type I* to *type III* transition. At 0.365 mol dm^{-3} sulfuric acid (*fig.* 2.19), points *r* and *s* also undergo a *type III* to *type II* transition. Another notable feature of the sequence of these systems concerns the point marked *t* on

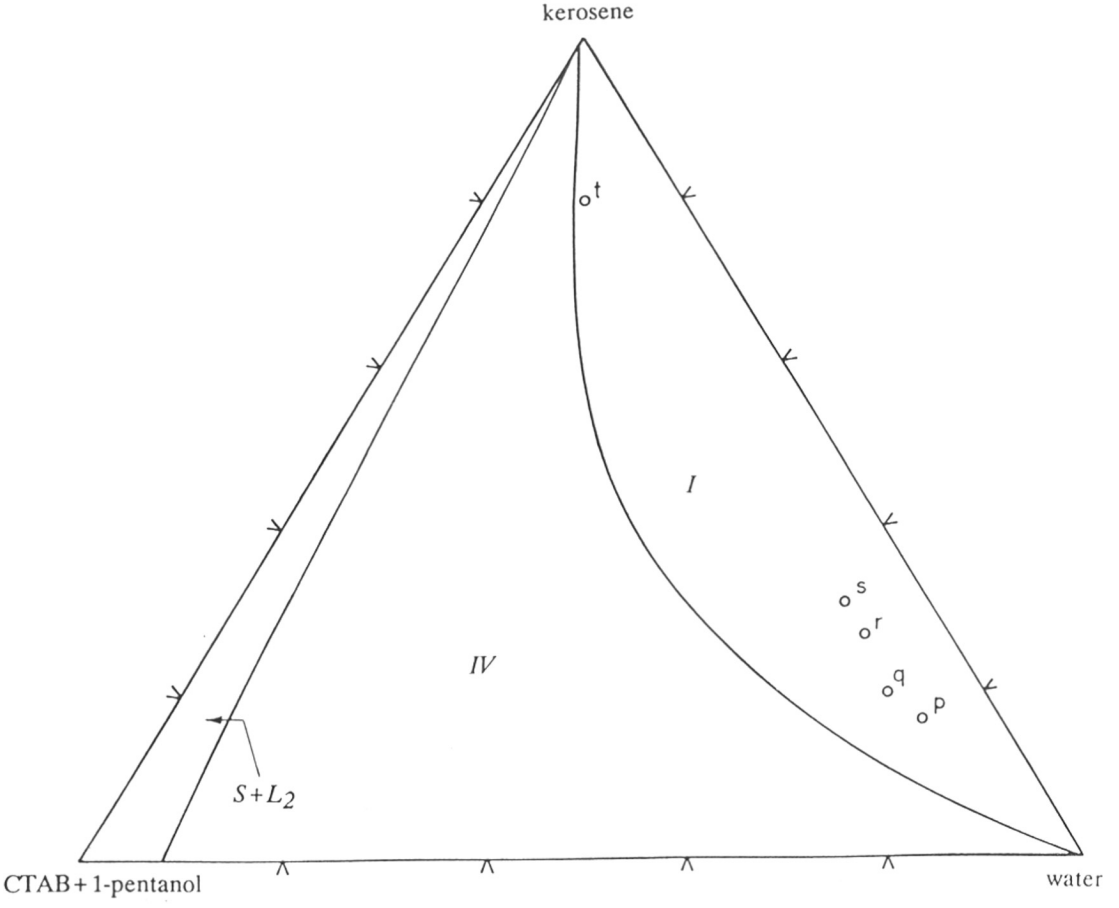

Fig. 2.16 **Complete phase diagram for the pseudo-ternary system CTAB + 1-pentanol/water/ kerosene at 30°C:** *I* :- type *I* system; *IV* :- type *IV* system; $S + L_2$:- solids + w/o emulsion

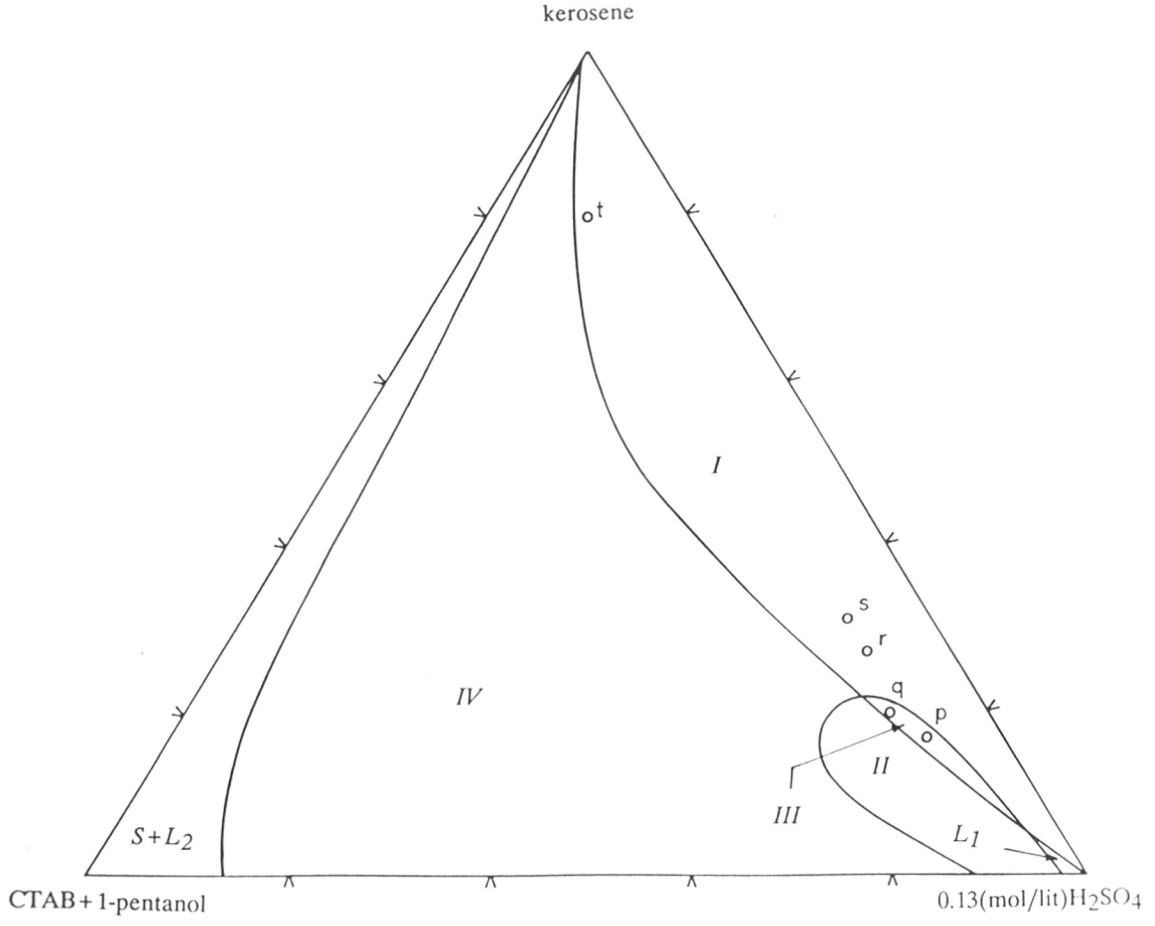

Fig. 2.17 **Complete phase diagram for the pseudo-ternary system CTAB + 1-pentanol/ 0.13 (mol/lit) H2SO4/ kerosene at 30°C:** *I* :- type *I* system; *II* :- type *II* system; *III* :- type *III* system; *IV* :- type *IV* system; L_1 :- solids + o/w emulsion; $S + L_2$:- solids + w/o emulsion.

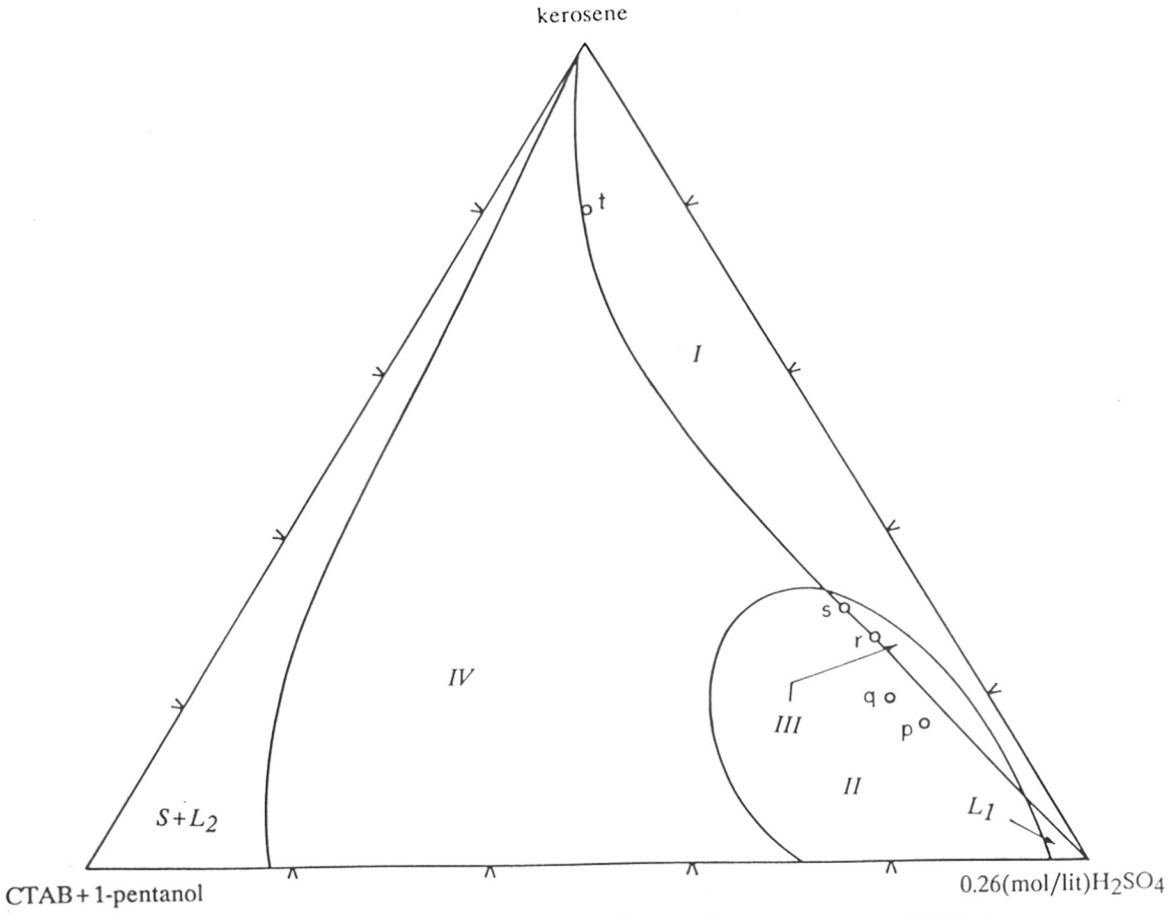

Fig. 2.18 **Complete phase diagram for the pseudo-ternary system CTAB + 1-pentanol/ 0.26 (mol/lit) H2SO4/ kerosene at 30°C:** *I* :- type *I* system; *II* :- type *II* system; *III* :- type *III* system; *IV* :- type *IV* system; L_1 :- solids + o/w emulsion; $S + L_2$:- solids + w/o emulsion.

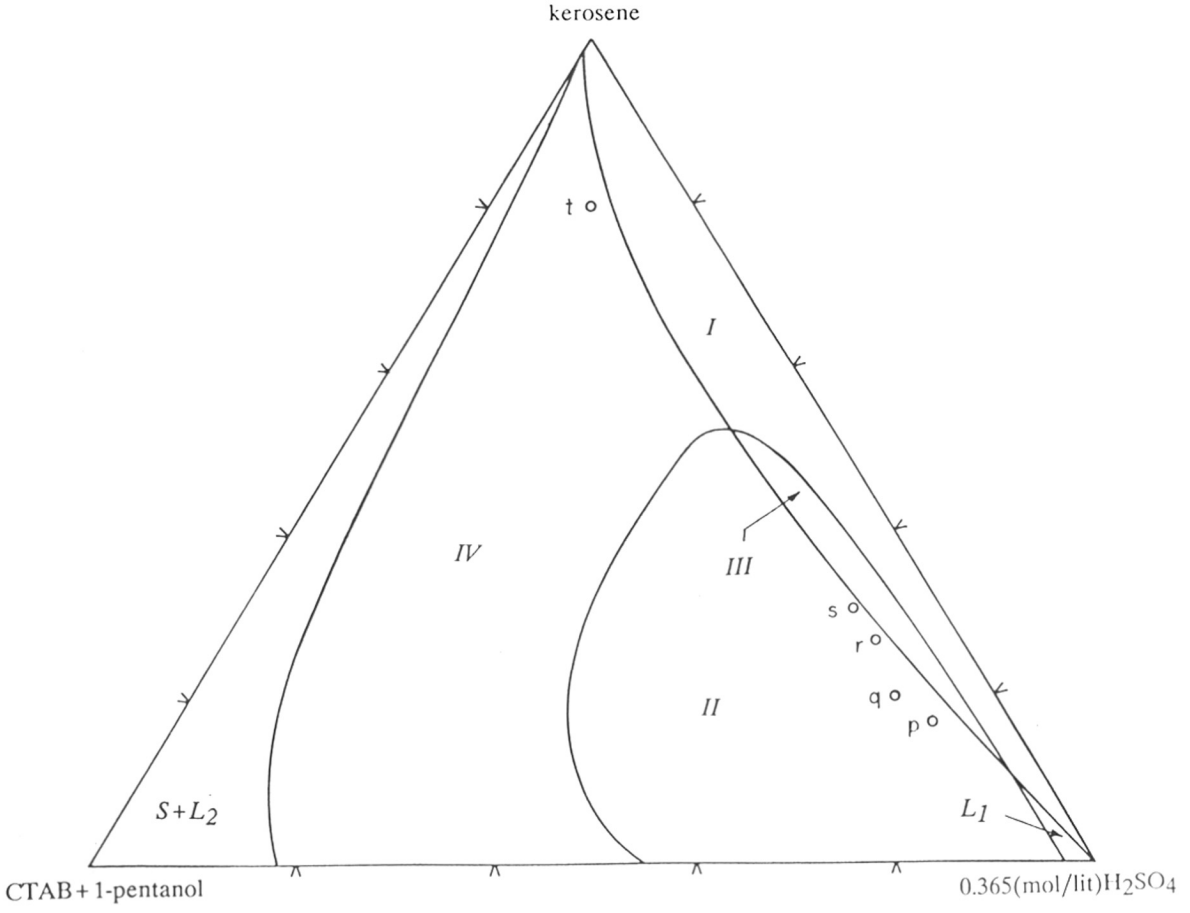

Fig. 2.19 **Complete phase diagram for the pseudo-ternary system CTAB + 1-pentanol/ 0.365 (mol/lit) H2SO4/ kerosene at 30°C:** *I* :- type *I* system; *II* :- type *II* system; *III* :- type *III* system; *IV* :- type *IV* system; L_1 :- solids + o/w emulsion; $S + L_2$:- solids + w/o emulsion.

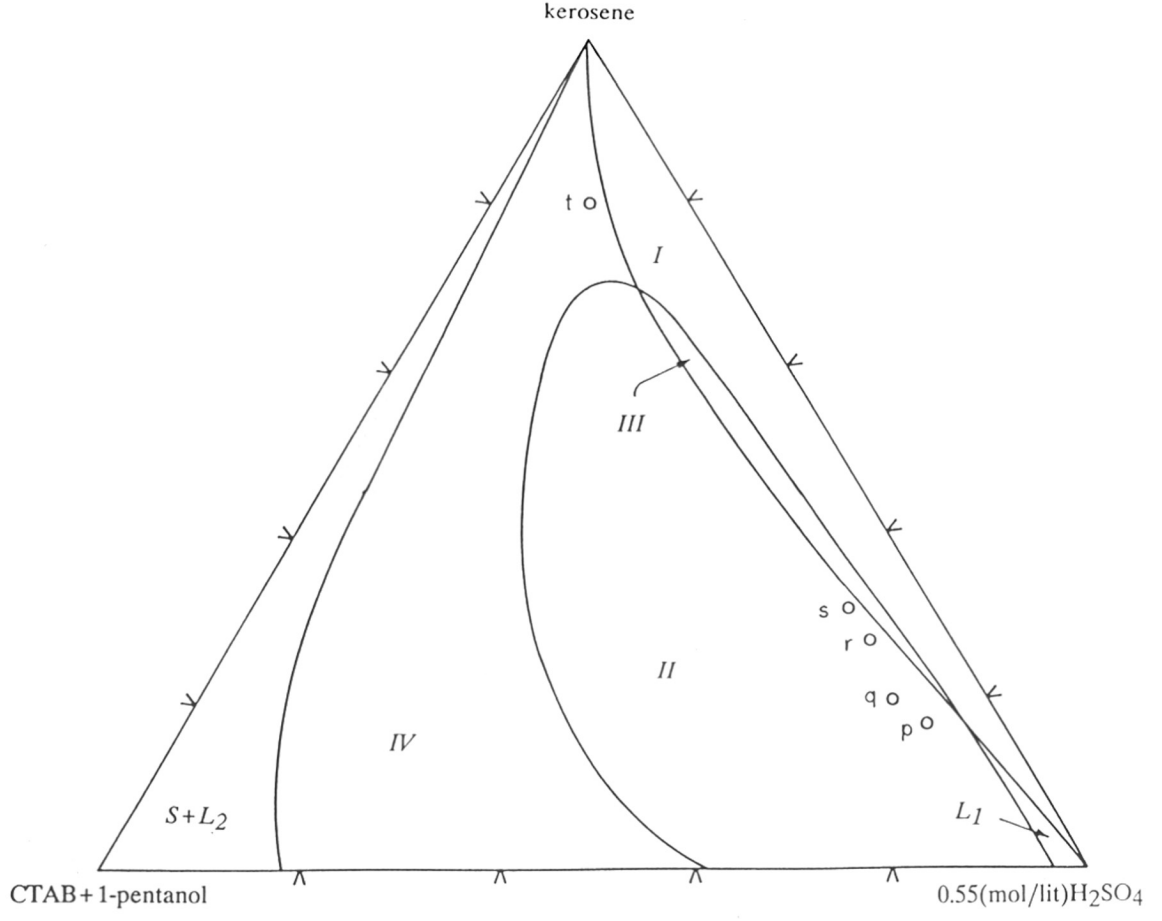

Fig. 2.20 **Complete phase diagram for the pseudo-ternary system CTAB + 1-pentanol/ 0.55 (mol/lit) H2SO4/ kerosene at 30°C:** *I* :- type *I* system; *II* :- type *II* system; *III* :- type *III* system; *IV* :- type *IV* system; L_1 :- solids + o/w emulsion; $S + L_2$:- solids + w/o emulsion.

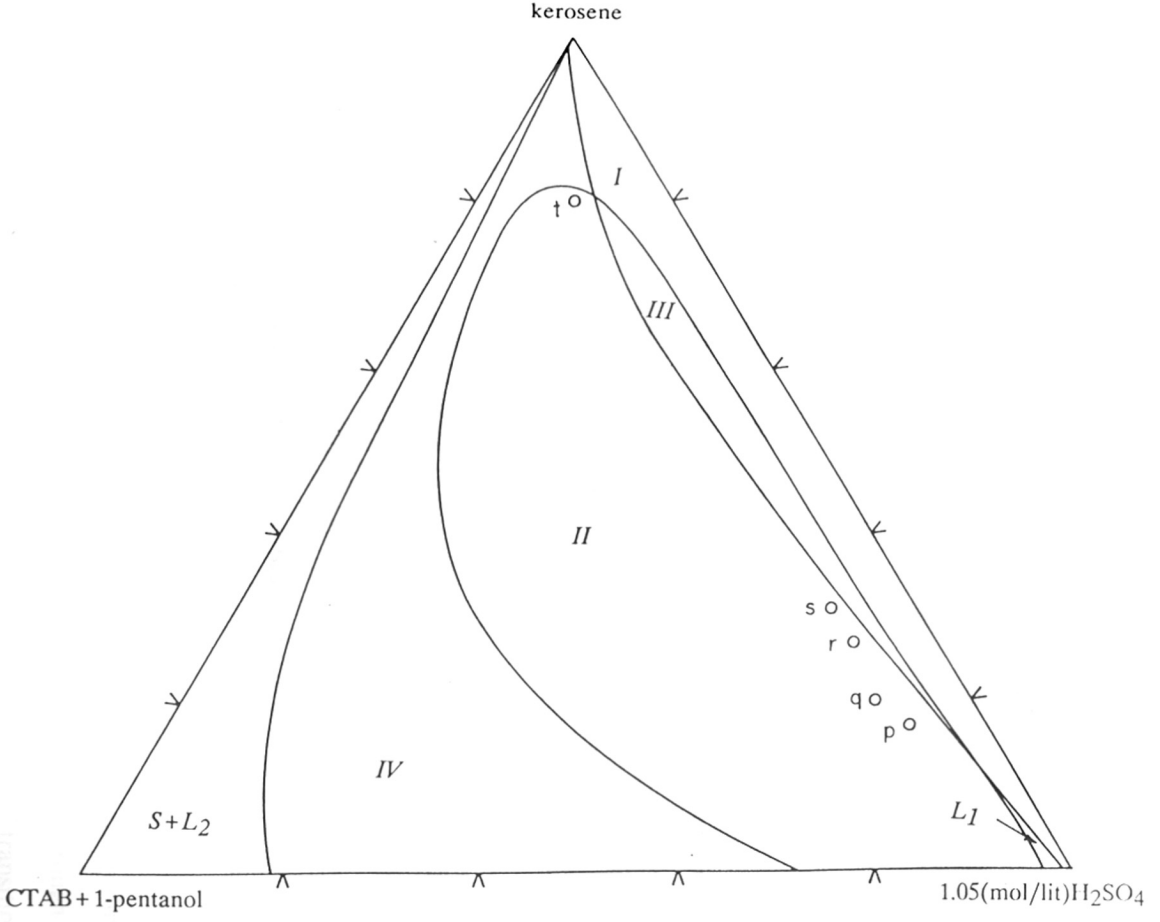

Fig. 2.21 **Complete phase diagram for the pseudo-ternary system CTAB + 1-pentanol/ 1.05 (mol/lit) H2SO4/ kerosene at 30°C:** *I* :- type *I* system; *II* :- type *II* system; *III* :- type *III* system; *IV* :- type *IV* system; L_1 :- solids + o/w emulsion; $S + L_2$:- solids + w/o emulsion.

the phase diagram. It has been observed that at zero concentration of the acid, point *t* falls in the *type I* regime. At higher concentrations of the acid the excess kerosene starts solubilizing into the micellar phase, and subsequently at 0.365 mol dm^{-3} sulfuric acid (*fig.* 2.19) a single phase has been obtained. This single phase which is isotropic in nature and optically transparent has been denoted as *type IV* [18]. Finally on increasing the acid concentration to 1.05 mol dm^{-3} (*fig.* 2.21), the single phase splits into a *type II* system which is an excess aqueous phase in equilibrium with a micellar solution of an aqueous phase in kerosene. Thus at the point *t* we get a type *I-IV-II* type of transition. This is similar to the one described by Bourrel, *et al* [19].

2.6.2 Effect of change in temperature on phase behavior

The system TX-100 + 1-pentanol/(2.5 mol/lit) H_2SO_4/ kerosene has been found to behave differently, when the temperature has been raised from 30°C to 40°C, as shown in *fig.* 2.22. and *fig.* 2.23. Points marked *m* through *w* represent different overall compositions with 10% by weight of the surfactant mixture. A *I-III-II* type of transition has been observed at point marked as *t* on the phase diagram. This point represents an overall composition of 10% by weight of the surfactant mixture, 70% by weight of 2.5 mol/lit H_2SO_4, and 20% by weight of kerosene. This type of transition observed on changing the temperature, may be due to the entropic contribution to the free energy of the micellar system, similar to that observed by Kunieda, *et al* [20].

The system CTAB + 1-pentanol/ 0.55 mol dm^{-3} H2SO4/ kerosene has been chosen for a study of the effect of change in temperature. The temperature range scanned has been 30°C to 60°C with intervals of 10°C (*figs.* 2.24 through 2.27). It has been found from the diagrams that we get a *II-III-I* type of transition at the points marked *u* through *w* on increasing the temperature.

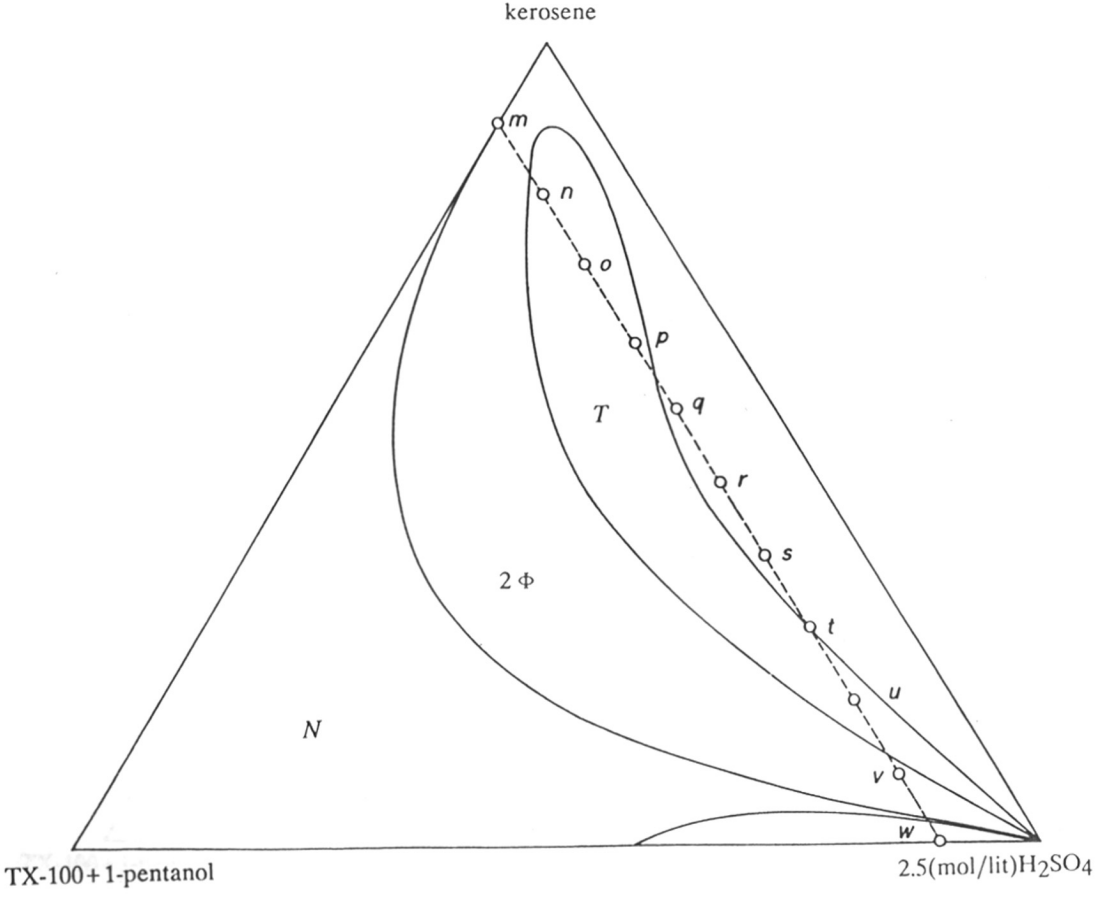

Fig. 2.22 **Complete phase diagram for the pseudo-ternary system TX-100 + 1-pentanol/ 2.5 (mol/lit) H2SO4/ kerosene at 30°C:** *N* :- micellar system; 2 Φ :- two phase system; *T* :- three phase system.

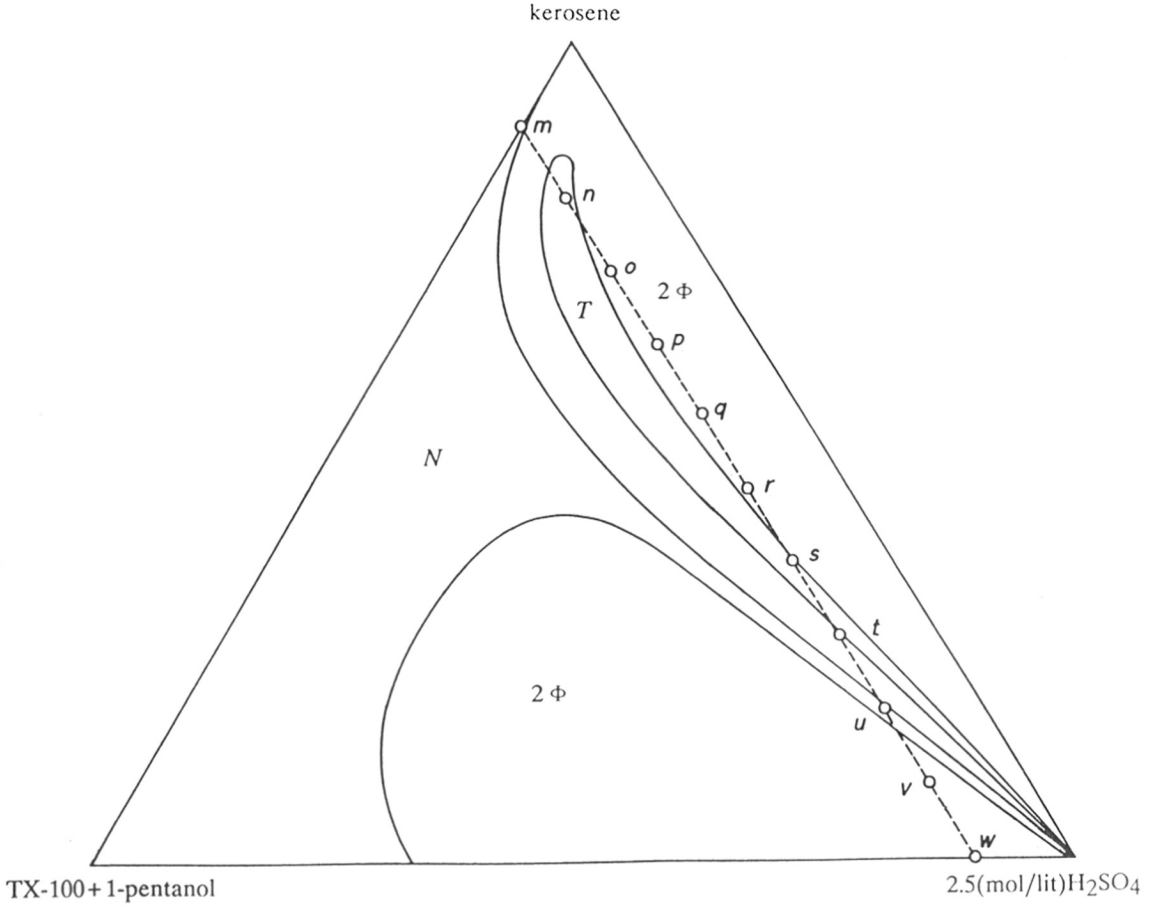

Fig. 2.23 **Complete phase diagram for the pseudo-ternary system TX-100 + 1-pentanol/ 2.5 (mol/lit) H2SO4/ kerosene at 40°C:** *N* :- micellar system; 2 Φ :- two phase system; *T* :- three phase system.

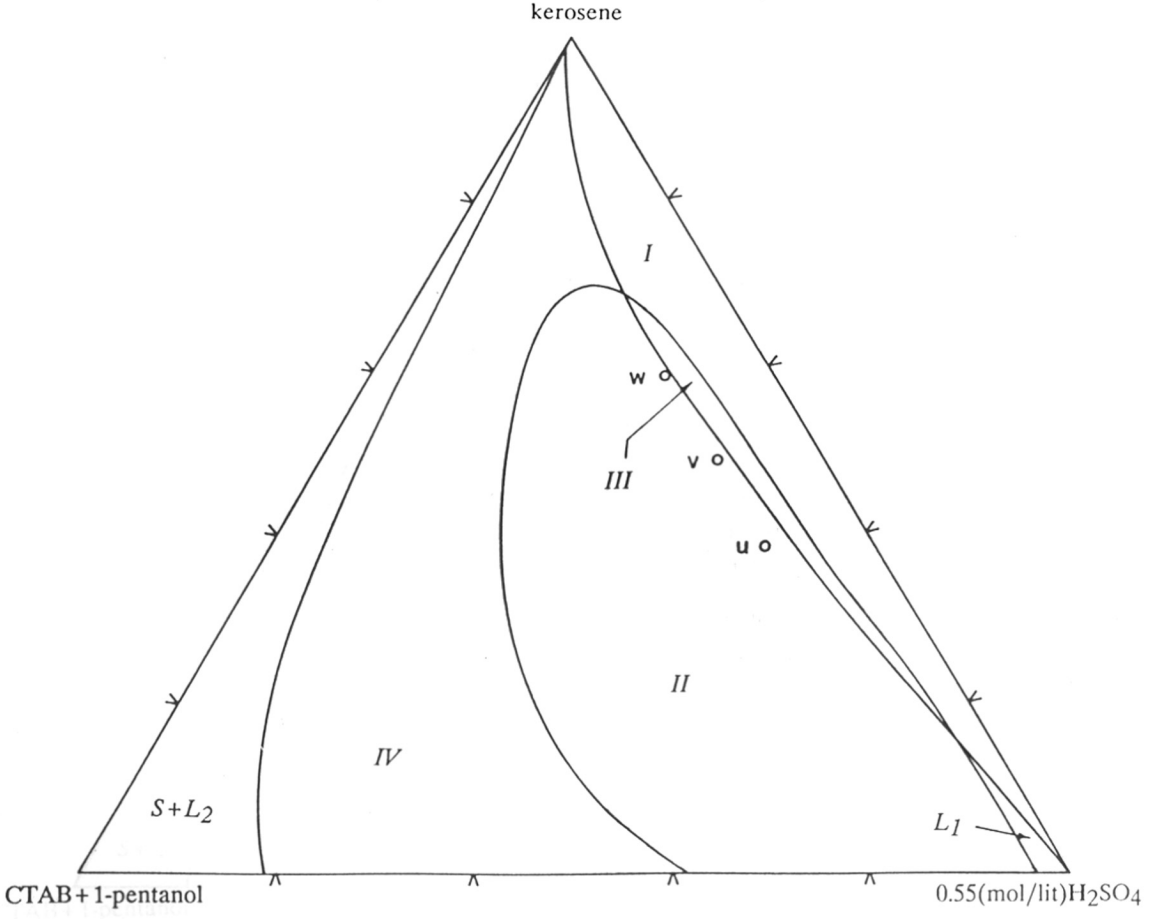

Fig. 2.24 **Complete phase diagram for the pseudo-ternary system CTAB + 1-pentanol/ 0.55 (mol/lit) H2SO4/ kerosene at 30°C:** *I* :- type *I* system; *II* :- type *II* system; *III* :- type *III* system; *IV* :- type *IV* system; L_1 :- solids + o/w emulsion; $S + L_2$:- solids + w/o emulsion.

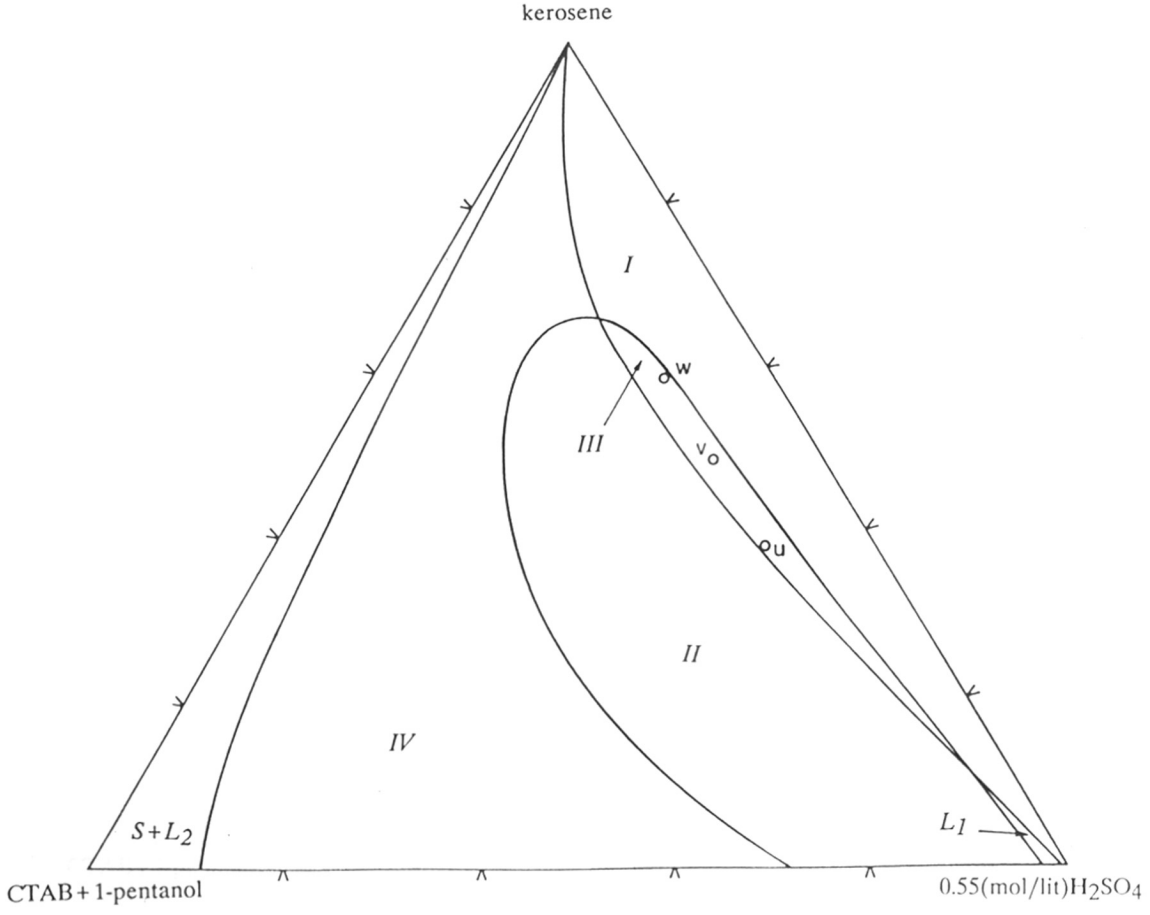

Fig. 2.25 **Complete phase diagram for the pseudo-ternary system CTAB + 1-pentanol/ 0.55 (mol/lit) H2SO4/ kerosene at 40°C:** *I* :- type *I* system; *II* :- type *II* system; *III* :- type *III* system; *IV* :- type *IV* system; L_1 :- solids + o/w emulsion; $S + L_2$:- solids + w/o emulsion.

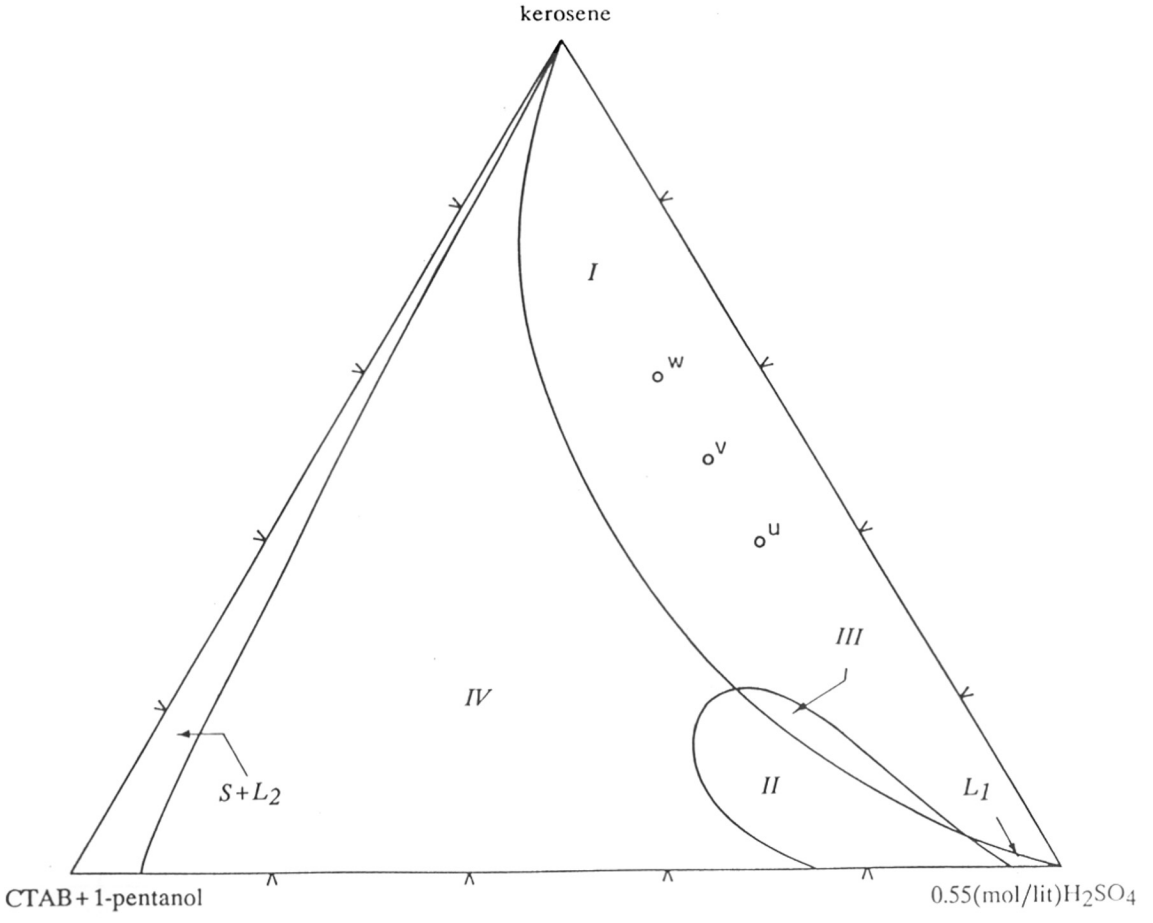

Fig. 2.26 **Complete phase diagram for the pseudo-ternary system CTAB + 1-pentanol/ 0.55 (mol/lit) H2SO4/ kerosene at 50°C:** *I* :- type *I* system; *II* :- type *II* system; *III* :- type *III* system; *IV* :- type *IV* system; L_1 :- solids + o/w emulsion; $S + L_2$:- solids + w/o emulsion.

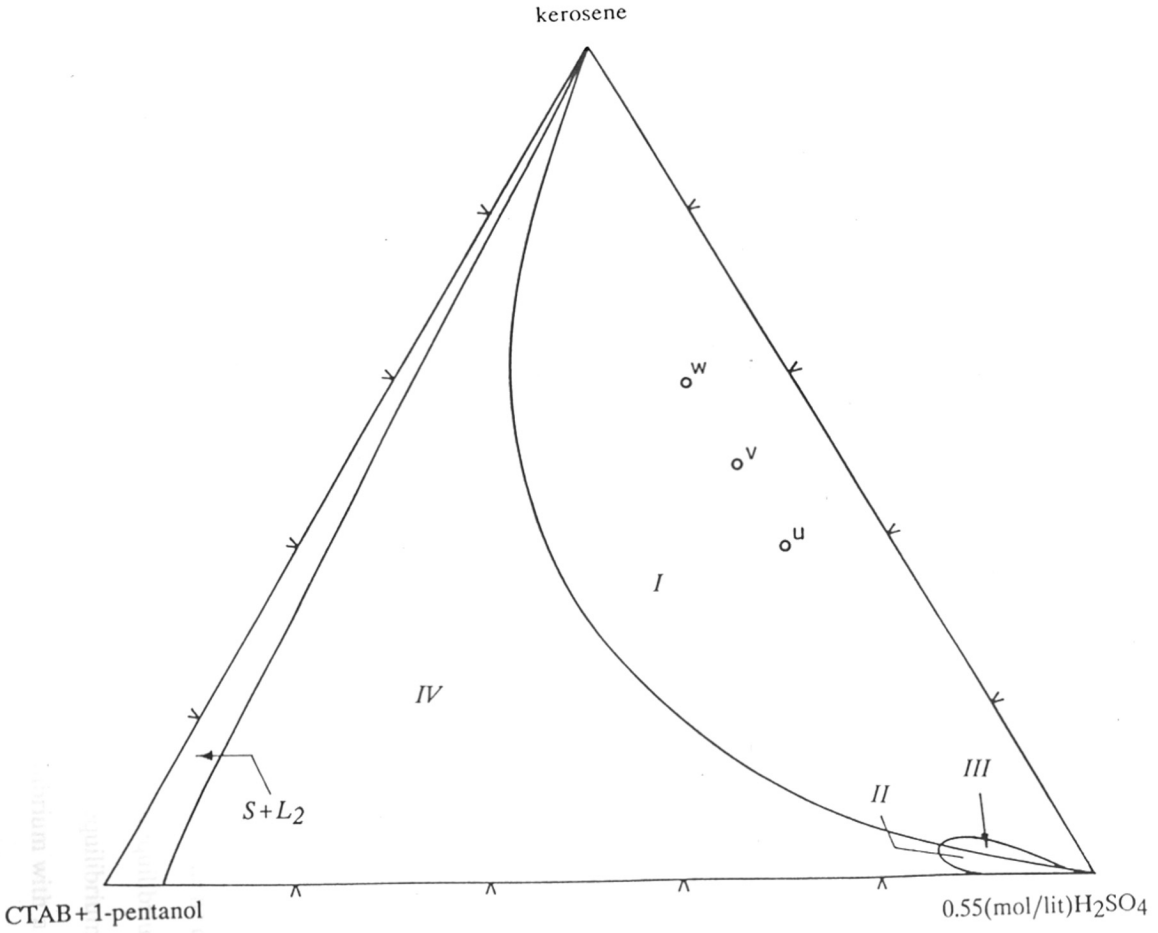

Fig. 2.27 **Complete phase diagram for the pseudo-ternary system CTAB + 1-pentanol/ 0.55 (mol/lit) H2SO4/ kerosene at 60°C:** *I* :- type *I* system; *II* :- type *II* system; *III* :- type *III* system; *IV* :- type *IV* system; L_1 :- solids + o/w emulsion; $S + L_2$:- solids + w/o emulsion.

2.6.3 Interfacial tensions

The measured parameters for the experiments by pendant drop method have been tabulated (Table 2.4). Table 2.5 shows the measured parameters values for the experiments on the capillary method. The calculated values of interfacial tension and those reported in literature have been shown in Table 2.6. It has been estimated that the average uncertainty in the measurements has been less than about 0.5%

2.6.4 Esterification reaction

The HPLC analysis of the product of the reaction carried under micellar conditions shows about 70% formation of the phenyl glycine methyl ester in the reaction mixture. The analysis report also shows some solubilized but unreacted DL-phenyl glycine in the reaction product. In contrast, the analysis report of the reaction carried out under normal conditions (no surfactant) shows about 3% phenyl glycine methyl ester and the remaining unreacted phenyl glycine. It has been found that the filtrate could be treated further with fresh resin, alcohol, and the amino acid in order to make it a continuous process.

2.7 Discussions

It has been assumed that in case of systems involving aqueous solution of sulfuric acid, the sulfuric acid and water partition into various phases in nearly a fixed ratio [21]. Also, the co-surfactant 1-pentanol being amphiphilic in nature partitions at the interface and various phases in the same ratio as that of the surfactant. A general pseudo-ternary phase diagram or a phase map can be divided into various distinct regions. Various regions like $S + L$ (solids in equilibrium with an excess micellar solution) *Type I* (an excess organic phase in equilibrium with a microemulsion), *Type II* (an excess aqueous phase in equilibrium with a micro-emulsion), *Type III* (a three phase behavior) *Type IV* (an isotropic, transparent microemulsion) and G (liquid crystalline phase) can be found.

Table 2.4 Measured parameters for the pendant drop method

No.	ρ_a /(gm/cc)	ρ_o /(gm/cc)	d_e/cm	d_s/cm
a)	0.9978	0.8711	0.3822	0.2083
b)	1.0042	0.6791	0.2123	0.1606
c)	1.0093	0.6791	0.2215	0.2069
d)	1.0161	0.6791	0.1105	0.1005
e)	1.0042	0.8653	0.2102	0.1246
f)	1.0093	0.8653	0.1891	0.1171
g)	1.0161	0.8653	0.1515	0.0976
h)	1.0037	0.7861	0.3312	0.1811
i)	1.0106	0.7861	0.3301	0.1837
j)	1.0161	0.7861	0.3295	0.1875
k)	1.0263	0.7865	0.1019	0.0949
l)	0.9162	0.7865	0.1002	0.0743
m)	0.8970	0.7864	0.1008	0.0704
n)	0.8706	0.7864	0.1015	0.0940
o)	1.1722	0.8484	0.0628	0.0388

Table 2.5 Measured parameters for the capillary method

No.	ρ_a /(gm/cc)	ρ_o /(gm/cc)	h_a/cm	h_o/cm
a)	0.9978	0.8711	6.9015	9.3504
b)	1.0042	0.6791	6.0782	8.3665
c)	1.0093	0.6791	4.2909	6.1009
d)	1.0161	0.6791	5.6507	8.3223
e)	1.0042	0.8653	4.2218	4.4843
f)	1.0093	0.8653	6.8368	7.6869
g)	1.0161	0.8653	7.0688	8.1114
h)	1.0037	0.7861	8.9253	9.6314
i)	1.0106	0.7861	8.7599	9.4136
j)	1.0161	0.7861	8.0586	8.6612
k)	1.0263	0.7865	5.9709	7.7172
l)	0.9162	0.7865	4.4558	5.1411
m)	0.8970	0.7864	7.6496	8.6661
n)	0.8706	0.7864	8.3027	9.1076
o)	1.1722	0.8484	6.1282	8.3132

Table 2.6 Interfacial tension values calculated

γ_{ao} / (dynes/cm)

No.	Pendant drop method	Capillary method	literature	Reference
a)	28.254	31.05	28.25	ref.29
b)	9.399	10.41	9.40	
c)	5.949	4.63	5.94	
d)	1.622	2.22	1.64	
e)	7.502	8.86	7.54	
f)	5.608	6.14	5.60	
g)	3.395	4.04	3.40	
h)	36.123	34.21	-	this work
i)	35.341	35.83	-	
j)	33.996	34.03	-	
k)	0.922	1.44	-	
l)	0.881	0.96	-	
m)	0.889	1.15	-	
n)	0.902	1.63	-	
o)	1.400	3.22	-	

The *I-III* type of transition observed on increasing the acid concentration have been be attributed to the coacervation of the "normal micelles" [22]. Similarly the *III-II* type of transitions in these cases have been attributed to the percolation phenomena of the "inverse micelles" [23-25]. Both these transitions have been associated with the critical phenomena [26]. These phenomena have been explained as follows. At low acidity, the water soluble CTAB molecules form charged micelles, which has been a well known process. These micelles are somewhat swollen due to the kerosene. The approach of these micelles towards each other is prevented by electric repulsion. On increasing the acidity the electric double-layer repulsion is strongly reduced, which makes the attractive London-van der Waals forces more dominant. The swollen micelles therefore tend to minimize their free energy inside the core by solubilizing more kerosene from the upper excess phase. This process of solubilization proceeds until the acidity is so high that the attractive forces exceed the entropic forces, thus favouring the formation of a single lower microemulsion phase. Thereafter the system separates into a three phase region. On increasing the acid concentration further, the oil-in-water structure in the middle phase of the *type III* system is destabilized. A Donnan-type equilibrium may exist between the middle phase and the lower phase [27]. This is due to the fact that the acid content of the aqueous phase in the middle phase is lower than that in the lower phase of the *type III* system. Destabilization of the microemulsion in the middle phase leads to an inversion of the microemulsion structure thus causing a *III-II* type of transition.

The precipitation of CTAB has been influenced by increasing the acid concentration. As a consequence of this, the phase boundary between the microemulsion domain and the so called $S + L2$ domain has been found to shift towards the acid apex of the pseudo-ternary diagram. Also, the *type I* domain has been found to become narrower while the *type II* region extends over a larger surfactant range.

The *II-III-I* type of phase transition which has been observed on increasing the temperature (*figs*. 2.24 through 2.27) has been found to be exactly opposite to the one for a system incorporating a nonionic surfactant [28]. This may be due to the fact that ionic amphiphiles are more soluble in the upper oil-rich phase at lower temperatures. Hence at lower temperatures *type II* systems have been predominant. On the other hand the amphiphiles being more soluble in the lower aqueous phase at higher temperatures, *type I* systems have been predominant at higher temperatures.

2.8 Conclusions

The anionic surfactant SDS, alongwith cosurfactant pentanol forms a surfactant mixture, that can withstand up to about 0.05 mol/lit sulfuric acid to form a microemulsion. At higher concentrations of the acid, the microemulsion region of the phase diagram disappears. The nonionic surfactant Triton X-100 alongwith pentanol forms a surfactant mixture, which can withstand up to about 2.5 mol/lit sulfuric acid, to form a microemulsion. A *I-III-II* type of transition is also observed upon changing the temperature, by about 10°C. This behavior has been due to the entropic contributions to the free energy of the micellar solutions. Comparison between the areas covered by the microemulsion regions on the phase diagrams, reveal that nonionic surfactants are best suited to withstand lower pH conditions. In case of CTAB systems the notable features have been as follows. The three phase microemulsion region have been found to be sandwiched between a *type I* region at a relatively high surfactant concentration and a *type II* region at relatively low surfactant concentrations. The extent of this region has been found to depend upon the acidity and temperature of the system. A *I-III-II* type of phase transition has been observed on increasing the acidity of the system. At relatively high kerosene contents, a *I-IV-II* type of transition can be expected. A *II-III-I* type of transition has been observed on increasing the temperature of the system.

It has been found that the pendant drop technique has been a better method than the capillary method in measuring the interfacial tensions between two immiscible phases since the reported values in case of the pendant drop method match with those from the literature[29].

From the HPLC analysis of the esterification reaction it has been concluded that micellar reactions are best for the esterification of amino acids. The study of phase diagrams of pseudo-ternary systems containing benzene, toluene, p-xylene and kerosene have been carried out keeping in view, their extensive uses as common solvents for chemical reactions in the industry. The microemulsion system studied here envisages quite a large range of sulfuric acid concentration, thus increasing the diversity of the microemulsion structure.

2.9 Notations

g	gravitational acceleration
ρ_a , ρ_o	density of aqueous and organic phases
$\Delta\rho$	density difference
γ_{ao}	interfacial tension
d_e	maximum equatorial diameter of the drop
d_s	diameter of the drop at distance d_e from the apex
S	ratio (d_e/d_s)
H	parameter defined by equation 2
r	internal radius of capillary
h_a, h_O	vertical distance of the aqueous and organic menisci from the interface

2.10 References

1 R. Leung, M. J. Hou, C. Manohar, D. O. Shah, and P. W. Chun, in *Macro- and Microemulsions: Theory and applications* ed. D. O. Shah, ACS Symp. Ser. 272, Am. Chem. Soc. Washington D.C., 1985 p. 325

2 Martin C. A., McCrann P.M., Angelos G. H., and Jaeger D. A. *Tetrahedron Letters*, **23(45)**, 4651, (1982)

3 J. H. Fendler and E. J. Fendler in *Catalysis in micellar and macromolecular systems*, Academic press, New York (1975)

4 Gonzalez A. and Holt S. L. *J. Org. Chem.*, **47**, 3186, (1982)

5 M. L. Moya, C. Izquierdo and J. Casado, *J. Phys. Chem.*, **95**, 6001, (1991)

6 R. Schomacker, K. Stickdorn and W. Knoche, *J. Chem. Soc. Faraday Trans.*, **87(6)**, 847, (1991)

7 Robinson B. H., *Nature*, **320**, 309, (1986)

8 Prince L. M. in *Microemulsions*, Academic press, New York, (1977)

9 J. Th. G. Overbeek, P. L. de Bruyn, and F. Verhoeckx, in *Surfactants*, ed. Th.F. Tadros, Academic press, New York, p.111, (1984)

10 Martin C. A., McCrann P. M., Angelos G. H., and Jaeger D. A. *Tetrahedron Letters*, **23(45)**, 4651-54 (1982)

11 Paul C. Hiemenz in "Principles of Colloid and Surface Chemistry" II edition, Marcel Dekker Inc., New York, (1986), p. 326.

12 F. E. Bartell and F. L. Miller, *J. Am. Chem. Soc.* **50**, 1961, (1928)

13 G.Ovakimian, M.Kuna and P.A.Levene, *J. Biol. Chem.* **135**, 91, (1940)

14 H.Adkins and A.A.Pavlic, *J. Am. Chem. Soc.* **69**, 3039, (1947)

15 L.Peter, C.Gyorgy, S.Andrea, G.Ferenc, L.Gabor and H.Andras, Hung. Teljes. **HU 24118** (Cl. C07 C101/06) 28 Dec. 1982

16 J.C.Clark, G.H.Phillipps, M.R.Steer, L.Stephenson and A.R.Cooksey, *J. Chem. Soc. Perkin Trans. I.*, 471, (1976)

17 Clausse M., Peyrelasse J.,Boned C., Heil J., Nicolas-Morgantini, and Zradba A., *in* "Surfactants in Solution" ,Vol III p. **2583,**(Mittal K. L. and Lindman B. Eds.), Plenum press, New York, (1984)

18 Winsor P. A. *Trans. Farad. Soc.*, **44**, 376 (1948)

19 M. Bourrel and R. S. Schechter in *Microemulsions and related systems* Surfactant Science Series Vol. 30, Marcel Dekker, Inc. New York and Basel (1988)

20 Kunieda H., and Friberg S. E., *Bull. Chem. Soc. Jpn.*, **54**, 1010 (1981)

21 A. M. Bellocq, J. Biais, B. Clin, A. Gelot, P. Lalanne and B. Lemanceau, *J. Colloid Interface Sci.*, **74**, 311, (1980)

22 D. O. Shah, Proc. Europ. Symp. Enhanced Oil Recovery, Bournemouth, England, Sept. 21-23, 1981, Elsevier, Amsterdam (1982)

23 A. M. Cazabat, D. Langevin, J. Meunier and A. Pouchelon, *J. Phys. Paris Lett.*, **43**, L-89, (1982)

24 A. M. Cazabat, D. Chatenay, D. Langevin, and A. Pouchelon, *J. Phys. Paris Lett.*, **41**, L-441, (1980)

25 M. Laques and C. Sauterey, *J. Phys. Chem.*, **84**, 3503, (1980)

26 A. M. Cazabat, D. Langevin J. Meunier and A. Pouchelon, *Adv. Colloid Interface Sci.*, **16**, 175, (1984)

27 Guggenheim, E. A. in *Thermodynamics* North-Holland, Amsterdam, p. 305, (1967)

28 M. Kahlweit, R. Strey, R. Schomacker and D. Haase, *Langmuir*, **5**, 305, (1989)

29 Estimated from the data presented by O. N. Anand, V. P. Malik and A. K. Singh in "*Surfactants in Solution*" Vol. , K. L. Mittal ed., Plenum Press, New York (1989), page 99.

CHAPTER 3

NICOTINE SULFATION USING SULFURIC ACID IN A MICROEMULSION MEDIUM CASE - STIRRED CELL REACTOR

3.1 Introduction

Nicotine sulfate has been an important chemical used in pesticide industry. It has been available commercially as a 40% aqueous solution. This solution is diluted to around 0.1% in order to use for agricultural spraying. The current process of preparation of nicotine sulfate involves extraction of nicotine from the macerated tobacco waste stream using kerosene, and treating the extract with concentrated sulfuric acid in a bubble column reactor [1] to form nicotine sulfate. Owing to mass transport limitations, the overall rate of the reaction has been low, due to which multiple columns are used in series to get the desired concentration of the product. In the present chapter we report and analyze the experimental results on the reaction of the extract with sulfuric acid in a suitably prepared microemulsion medium. The phase behavior of microemulsion system consisting of kerosene, various surfactants and cosurfactants, and sulfuric acid has been studied [2,3]. A surfactant : co-surfactant ratio of 1:1 has been used in the study of such a phase diagram. For carrying out the reaction between nicotine and sulfuric acid, a *type I* microemulsion system which comprises of an excess kerosene phase in equilibrium with a microemulsion of kerosene in sulfuric acid has been used. The reaction has been carried out using a simple stirred cell reactor. The product (nicotine sulfate) has been found to be water soluble and remains into the aqueous phase in solubilized state. The advantages in carrying out this reaction under microemulsion medium have been i) enhancement in the overall rate of reaction, ii) formation of an *insitu* product which can be used directly for field applications, and iii) the process can be made continuous and hence any desired concentration of nicotine sulfate can be obtained to suit individual requirements.

3.2 Materials

Cetyl trimethyl ammonium bromide (CTAB), Sodium dodecyl sulfate (LR grade) and Triton X-100 (Isooctyl phenoxy polyethoxy ethanol) have been

obtained from SD chemicals and have been used as received. 1-pentanol (AR grade) has been a Fluka guaranteed material. Kerosene has been obtained from local markets and has been used without further purification. The approximate composition of the kerosene used (volume %) has been a) Aromatics [1. Mono-nuclear (single ring aromatic hydrocarbons) - 15% and 2. Dinuclear (double ring aromatic hydrocarbons) - 6%] b) Naphthenic rings [1. Monocyclic (single ring aliphatic hydrocarbons) - 26% and 2. Dicyclic (double ring aliphatic hydrocarbons) - 9%] and c) Paraffins [1. Normal (straight chain aliphatic hydrocarbons) - 25% and 2. Branched (aliphatic hydrocarbons with side chains) - 19%]. Water used for the experiments has been doubly distilled, and deionized. Concentrated sulfuric acid and potassium sulfate crystals have been obtained from SD chemicals and aqueous solutions of these have been used. The exact concentrations of sulfuric acid have been determined by titration with standard 0.5*N* and 1.0*N* sodium hydroxide solutions.

3.3 Method

3.3.1 Phase diagram study

In all the experiments for studies of phase behavior, kerosene has been used as an oil phase. Triton X-100 (TX-100), Sodium dodecyl sulfate (SDS) or Cetyl trimethyl ammonium bromide (CTAB) are used as surfactants, and 1-pentanol as a co-surfactant. Distilled water, or different concentrations of sulfuric acid has been used as an aqueous phase. The boundaries of the microemulsion domain have been determined for surfactant : cosurfactant mass ratio of 1:1 by weight for all the systems. This has been done by progressive 'dynamic' titration of mixture of two pseudo-components, viz. surfactant + cosurfactant, and kerosene versus water or acid. These boundaries have been then confirmed by titrating mixtures of surfactant + cosurfactant, and water or acid, versus kerosene. The end points have been noted for a clear to turbid or a turbid to clear type of change in the

appearance of the mixture. Usually, the titration paths followed in the triangular diagrams have been discussed in chapter 2. Only in some cases, when the phase boundaries used to be almost parallel to these paths, the titrations have been followed along paths as shown earlier in chapter 2, with the end points towards a "macroscopically homogeneous" composition. The concentrations of the titrant added, at which different transitions occurred, have been derived from precise weight measurements. All the titrations have been performed at a fixed temperature accurate to within ± 0.5°C. In some cases, it has been necessary to carry 'static' titration experiments. For this purpose, samples, whose overall composition has been close to the transition composition determined by 'dynamic' titration, have been prepared and stored in a temperature controlled bath for at least a week. The phase behavior of these samples has been checked at regular intervals, until no change in the physical condition has been observed. It has been estimated that on an average, the relative uncertainty on the components' mass fraction corresponding to transition point has been less than 1 %. Finally the phase diagrams have been drawn on a triangular graph paper in order to locate various types of regions in the system. The boundary demarcating the *type I* and *type IV* regions has been used to decide the initial composition of the reaction mixtures

3.3.2 Stirred cell reactor

The experiments have been divided into two sets, each comprising of five different runs. In the first set (runs 1-5), pure aqueous sulfuric acid of known strength has been equilibrated with excess kerosene and then used for the reaction after discarding the excess kerosene. In the second set (runs 6-10), five different microemulsion systems of *type I* have been used for the reaction. The composition of these systems has been shown in Table 3.1. The microemulsion has been prepared by equilibrating excess of the organic solvent (kerosene) with a micellar aqueous solution of sulfuric acid, using 1:1 (wt/wt) surfactant-cosurfactant mixtures. Thus a two phase *type I* system has been formed, wherein the upper

Table 3.1 Composition of various phases used in Sets 1 and 2

Composition of aqueous phase for Set 1

Run 1 : 0.13 mol/lit H_2SO_4; Run 2 : 0.26 mol/lit H_2SO_4; Run 3 : 0.365 mol/lit H_2SO_4; Run 4 : 2.5 mol/lit H_2SO_4; Run 5 : 0.05 mol/lit H_2SO_4; Negligible amounts of kerosene found in all the aqueous phases.

Composition of excess organic phase for Set 1

Runs 1-5 : Kerosene containing negligible amounts of acid

Composition of aqueous phase (microemulsion) for Set 2

Run No.	Surfactant mixture	Surfactant mixture		Kerosene		H_2SO_4		Strength of H_2SO_4
		wt%	vol%	wt%	vol%	wt%	vol%	mol/lit
6	CTAB + 1-pentanol	15	15.1	29	33.8	56	51.1	0.13
7	CTAB + 1-pentanol	12	11	43	49.1	45	39.9	0.26
8	CTAB + 1-pentanol	10	9.1	55	61	35	30	0.365
9	TX-100 + 1-pentanol	8	6.2	20	27.3	72	66.5	2.5
10	SDS + 1-pentanol	10	5.9	6	7.8	84	86.3	0.05

Composition of excess organic phase for Set 2

Run No.	Surfactant mixture	Surfactant mixture		Kerosene	
		wt%	vol%	wt%	vol%
6	CTAB + 1-pentanol	1.1	0.9	98.9	99.1
7	CTAB + 1-pentanol	0.6	0.5	99.4	99.5
8	CTAB + 1-pentanol	0.6	0.5	99.4	99.5
9	TX-100 + 1-pentanol	1.2	0.6	98.8	99.4
10	SDS + 1-pentanol	1.0	0.4	99.0	99.6

organic layer has been in equilibrium with an oil-in-water type of microemulsion. The excess organic layer as obtained above has been used to prepare the organic phase for the reaction in all the runs by dissolving in it a known amount of nicotine. The initial concentration of nicotine has been adjusted to around 4.748×10^{-5} mol/cc for all the runs. The microemulsion being saturated with kerosene, most of the resistance to mass transfer of nicotine has been expected to lie in the organic phase [4]. The product nicotine sulfate being water soluble has been found to remain in the aqueous phase. The contact between 50 cc of the microemulsion and 50 cc of the organic solution has been achieved in a simple jacketed stirred cell reactor, shown in *fig.* 3.1. The stirred cell reactor has been maintained at a constant temperature of 30°C by circulating thermostated water through its jackets. A four-blade stirrer has been placed in such a way that half the width of the blades lie into the organic phase, while the other half lie into the microemulsion. The speed of rotation of the stirrer has been maintained at 50 ± 2 rpm. The partition ratios of nicotine between various phases have been determined as follows. For determining the partition ratio of nicotine between kerosene phase and pure acid phase, equal volumes of the organic phase and aqueous solution of K_2SO_4 of appropriate molarity have been equilibrated at 30°C by vigorous shaking in a separating funnel. The organic phase which separated from the aqueous phase has been analyzed for its nicotine content. In the case of determination of the partition ratio of nicotine between kerosene phase and the surfactant phase, equal volumes of both the phases have been taken in a stoppered test tube, and have been equilibrated at 30°C by vigorous shaking. The phases have been separated by ultracentrifugation after which the kerosene phase has been analyzed for its nicotine content. The concentration of nicotine in the organic phase has been determined by withdrawing small alliquots of the organic phase, diluting the alliquot with kerosene and analyzing the diluted solution by UV spectrophotometric methods at $\lambda_{max} = 281$ nm. A Shimadzu make UV-visible spectrophotometer has been used for this

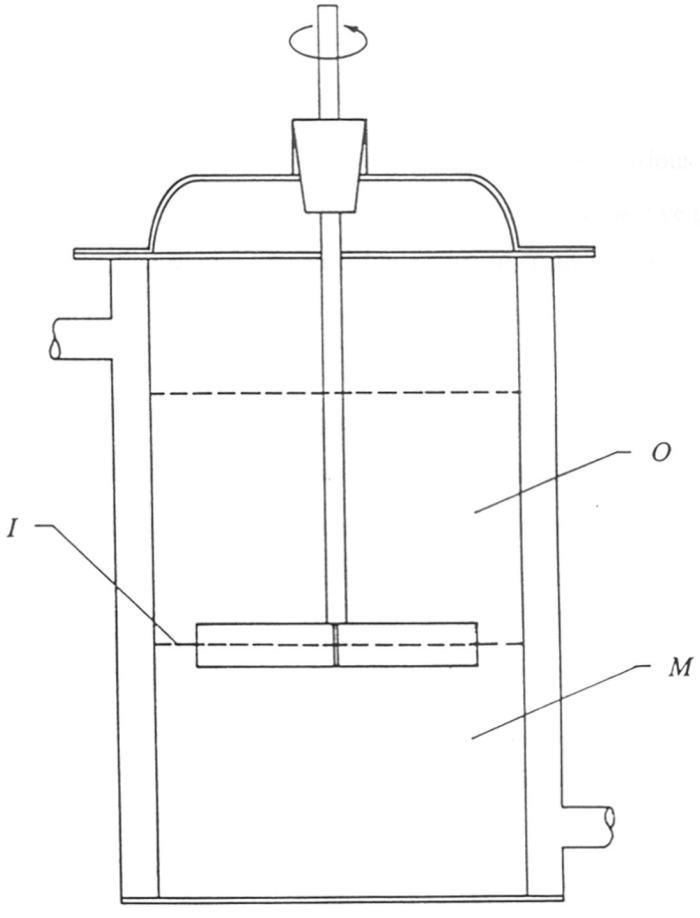

Fig. 3.1 **Stirred cell reactor for sulfation of nicotine:** *O* :- excess organic phase; *M* :- *type I* microemulsion; *I* :- interface.

purpose. The partition ratios thus obtained are shown in table 3.2. It has been estimated that the average relative uncertainty in the measurement of the organic phase concentration in set 1, has been less than about 1% and that in set 2 has been about 2%.

3.4 Results

Figures 3.2 to 3.6 show the partial phase diagrams for various microemulsion systems used. Points marked as numbers 1 to 5 on the respective phase diagrams denote the actual compositions used in runs 6-10. Table 3.3 shows values of concentration of the organic phase measured with time. A plot of concentration of the organic phase versus time for runs 1-5 has been shown in *fig.* 3.7 and that for runs 6-10 in *fig.* 3.8. A plot of log concentration of the organic phase versus time for runs 1-5 shown in *fig.* 3.9 reveals the first order nature of the reaction. Figure 3.10 shows a plot of log concentration versus time for runs 6-10. Considering the rates of reaction obtained in case of microemulsion (runs 6-10) as compared to those obtained in the corresponding case of no surfactant (runs 1-5) an enhancement factor E has been defined as,

$$E = \frac{(d[B]/dt)_{[B]}^{\text{microemulsion}}}{(d[B]/dt)_{[B]}^{\text{no surfactant}}} \qquad (1)$$

where $(d[B]/dt)_{[B]}^{\text{microemulsion}}$ is the rate at a known value of *[B]* in the case of microemulsion (runs 1-5), and $(d[B]/dt)_{[B]}^{\text{no surfactant}}$ is the rate of reaction at that concentration, in the case of no surfactant (runs 6-10). Figure 3.11 shows a plot of the enhancement factor thus obtained versus concentration of organic phase.

The influence of micelles in enhancing the reaction rate has been of significant interest and models appropriate for hydrophilic or hydrophobic solutes have been formulated [5-8]. These models treat the micellar solution as a multiphase system, wherein the reacting species distribute themselves between various phases. The

Table 3.2 Partition ratios of nicotine between kerosene and aqueous K_2SO_4

Conc.(mol/lit)	Partition ratio
7 E-5 moles/lit K_2SO_4	163
1.4 E-4 moles/lit K_2SO_4	184
2.8 E-4 moles/lit K_2SO_4	261
3.5 E-4 moles/lit K_2SO_4	288
4.2 E-4 moles/lit K_2SO_4	344
0.05 moles/lit K_2SO_4	1101.0
0.13 moles/lit K_2SO_4	1214.2
0.26 moles/lit K_2SO_4	1283.7
0.365 moles/lit K_2SO_4	1301.4
2.5 moles/lit K_2SO_4	1422.3

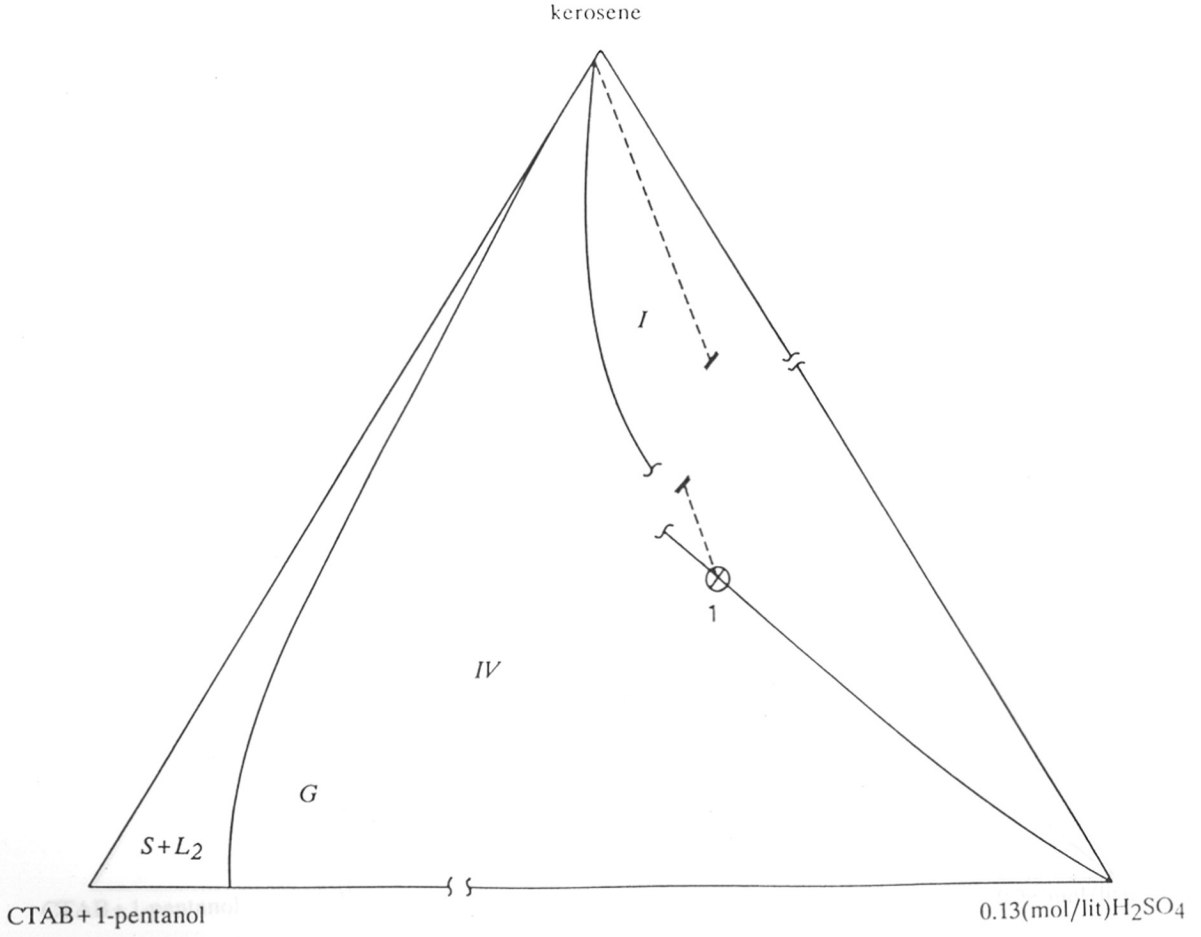

Fig. 3.2 **Partial phase diagrams of the pseudo-ternary system CTAB + 1-pentanol/ 0.13 (mol/lit) H2SO4/ kerosene at 30°C:** *I* :- type *I* system; *II* :- type *II* system; *IV* :- type *IV* system; L_1 :- solids + o/w emulsion; $S + L_2$:- solids + w/o emulsion; *G* :- gel phase; (note break in scale)

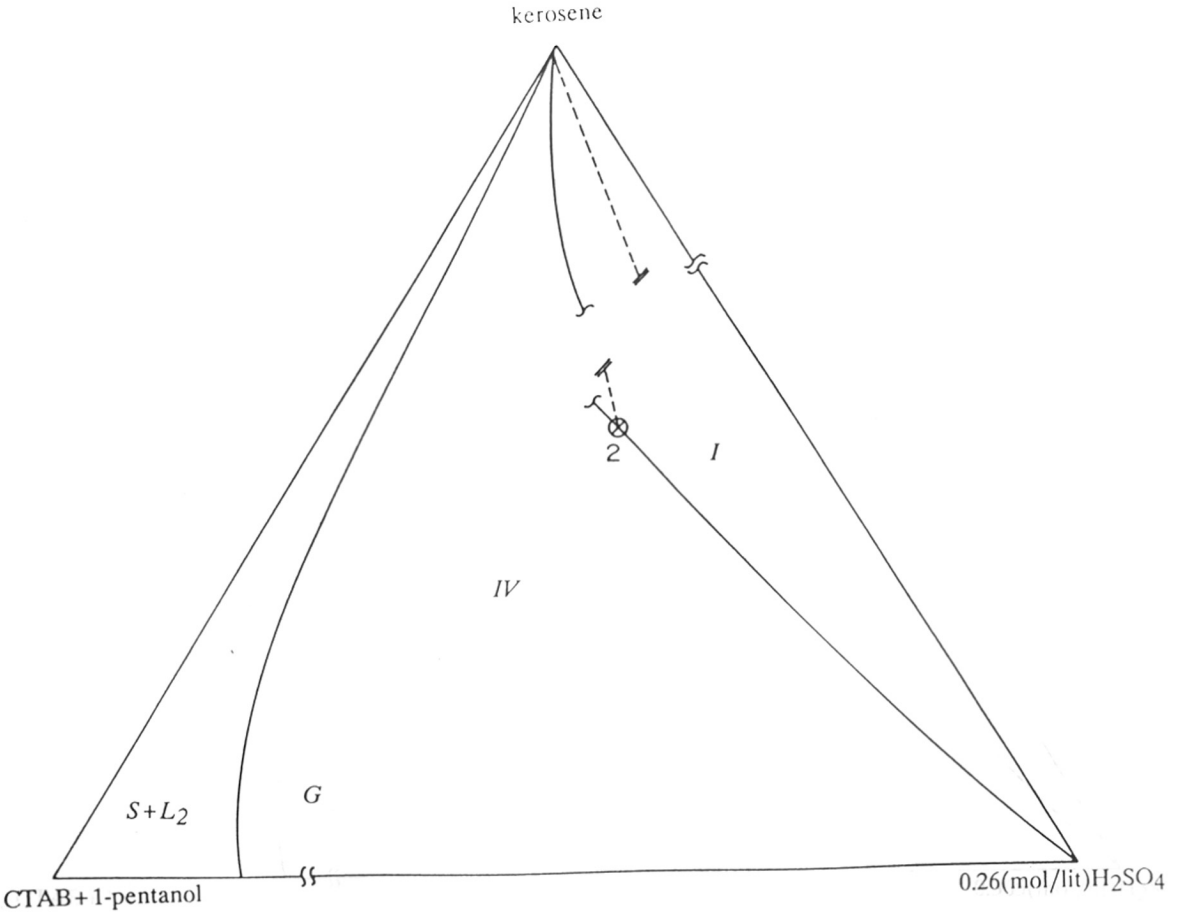

Fig. 3.3 **Partial phase diagrams of the pseudo-ternary system CTAB + 1-pentanol/ 0.26 (mol/lit) H2SO4/ kerosene at 30°C:** *I* :- type *I* system; *II* :- type *II* system; *IV* :- type *IV* system; L_1 :- solids + o/w emulsion; $S + L_2$:- solids + w/o emulsion; *G* :- gel phase; (note break in scale)

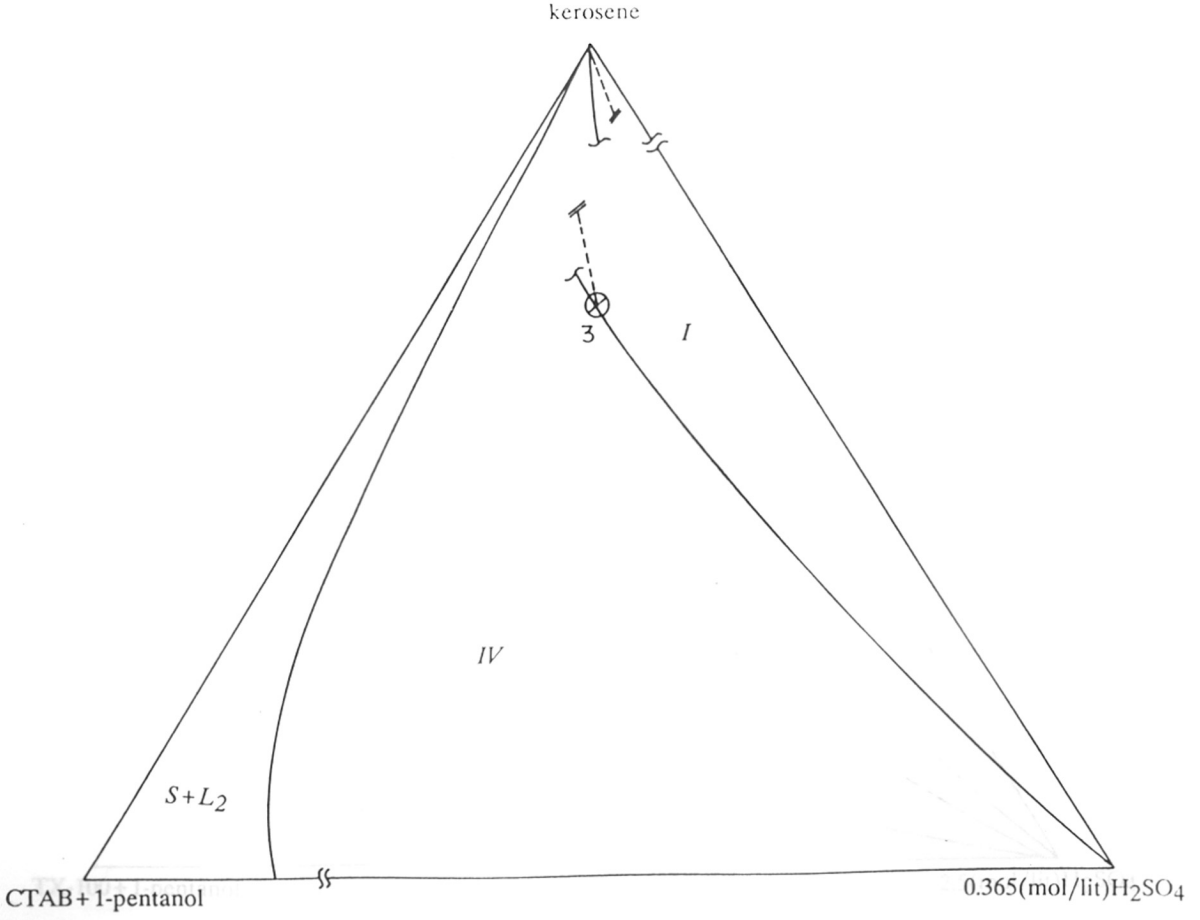

Fig. 3.4 **Partial phase diagrams of the pseudo-ternary system CTAB + 1-pentanol/ 0.365 (mol/lit) H2SO4/ kerosene at 30°C:** *I* :- type *I* system; *II* :- type *II* system; *IV* :- type *IV* system; L_1 :- solids + o/w emulsion; $S + L_2$:- solids + w/o emulsion; *G* :- gel phase; (note break in scale)

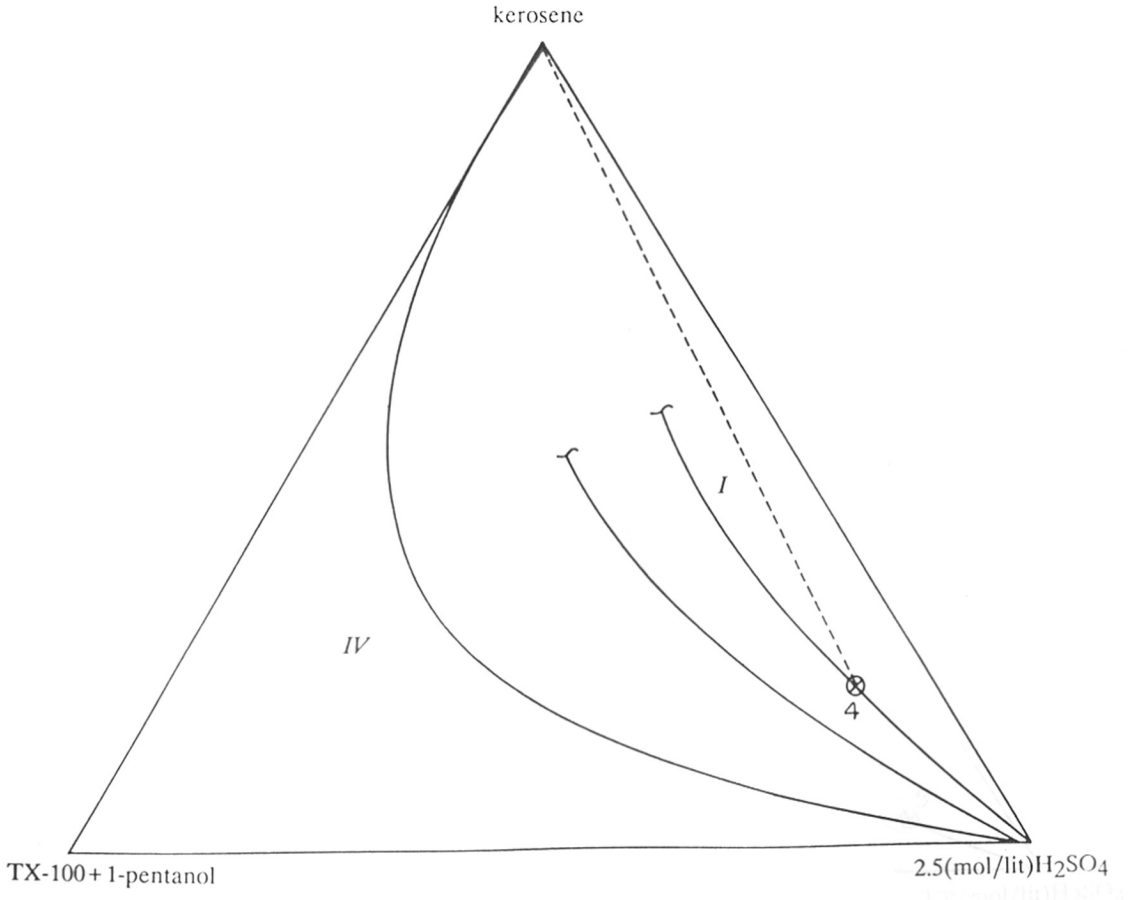

Fig. 3.5 Partial phase diagrams of the pseudo-ternary system TX-100 + 1-pentanol/ 2.5 (mol/lit) H2SO4/ kerosene at 30°C: *I* :- *type I* system; *IV* :- *type IV* system.

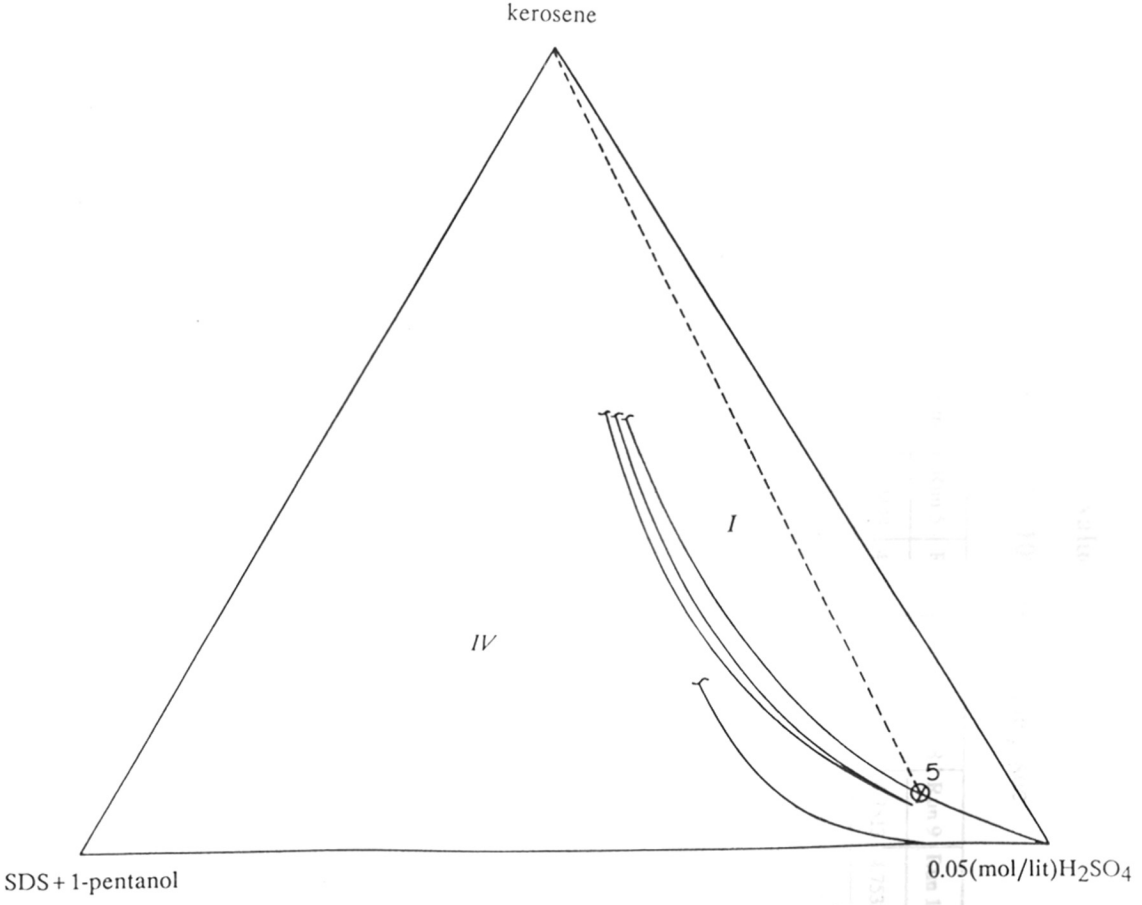

Fig. 3.6 **Partial phase diagrams of the pseudo-ternary system SDS + 1-pentanol/ 0.05 (mol/lit) H2SO4/ kerosene at 30°C:** *I* :- *type I* system; *IV* :- *type IV* system.

Table 3.3 Measured values of nicotine concentration/(mol $cm^{-3} \times 10^{-5}$) with Time / sec

Time/sec	Run 1	Run 2	Run 3	Run 4	Run 5	Run 6	Run 7	Run 8	Run 9	Run 10
0	4.7488	4.7474	4.7487	4.7485	4.7499	4.7501	4.7492	4.7466	4.7513	4.7533
120	4.0391	4.0379	4.0422	4.0319	4.0433	2.8660	3.2057	3.0646	1.4657	2.7262
240	3.4356	3.4335	3.4409	3.4234	3.4428	1.8888	2.3023	2.2863	0.4690	1.6536
360	2.9222	2.9196	2.9290	2.9067	2.9315	1.2814	1.7383	1.7558	0.1530	1.0130
480	2.4856	2.4826	2.4932	2.4680	2.4961	0.8693	1.3323	1.4020	0.0536	0.6144
600	2.1142	2.1110	2.1223	2.0956	2.1254	0.6011	1.0366	1.1410	0.0182	0.3727
720	1.7983	1.7951	1.8066	1.7793	1.8098	0.4168	0.8105	0.9445	0.0061	0.2283

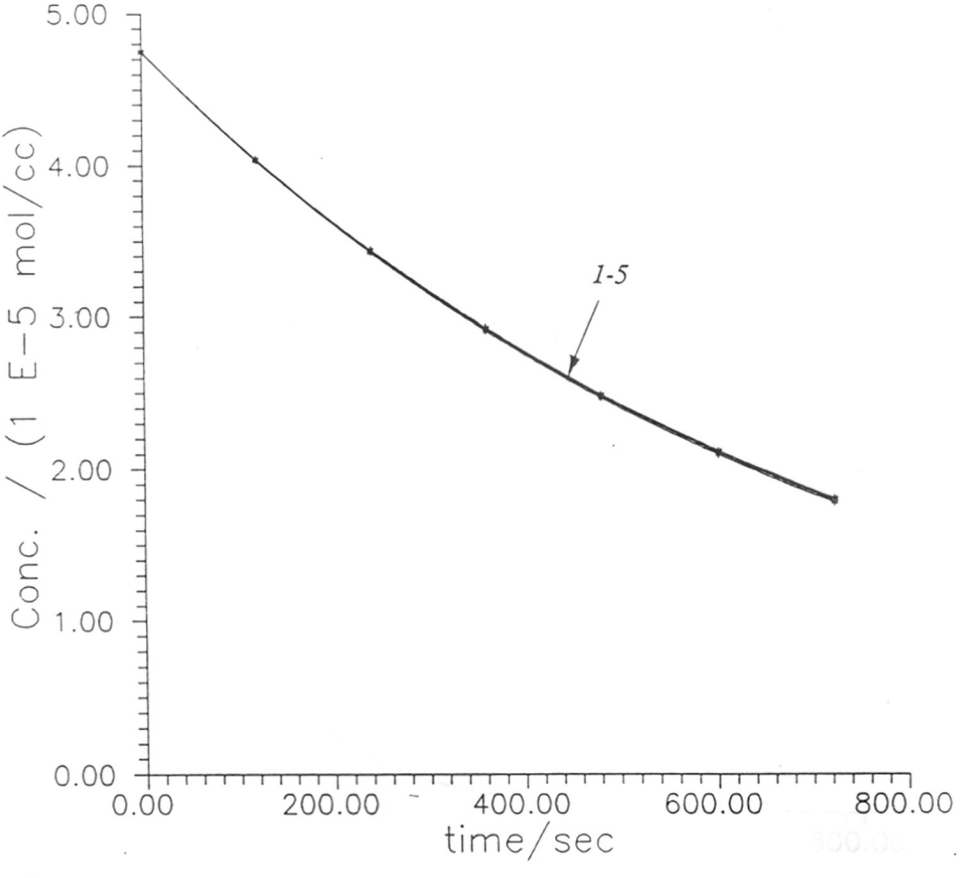

Fig. 3.7 Concentration (mol/cc) versus time (sec) for runs 1-5: *1-5* runs 1-5

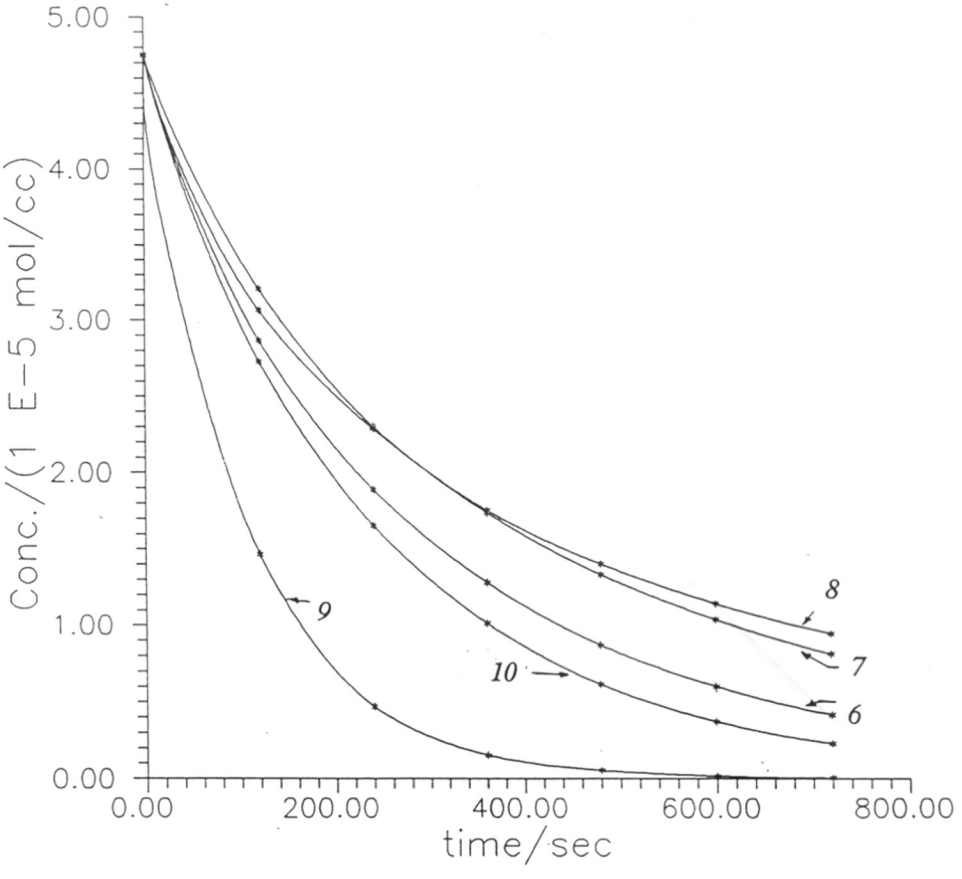

Fig. 3.8 **Concentration (mol/cc) versus time (sec) for runs 6-10:** *6-10* runs 6-10

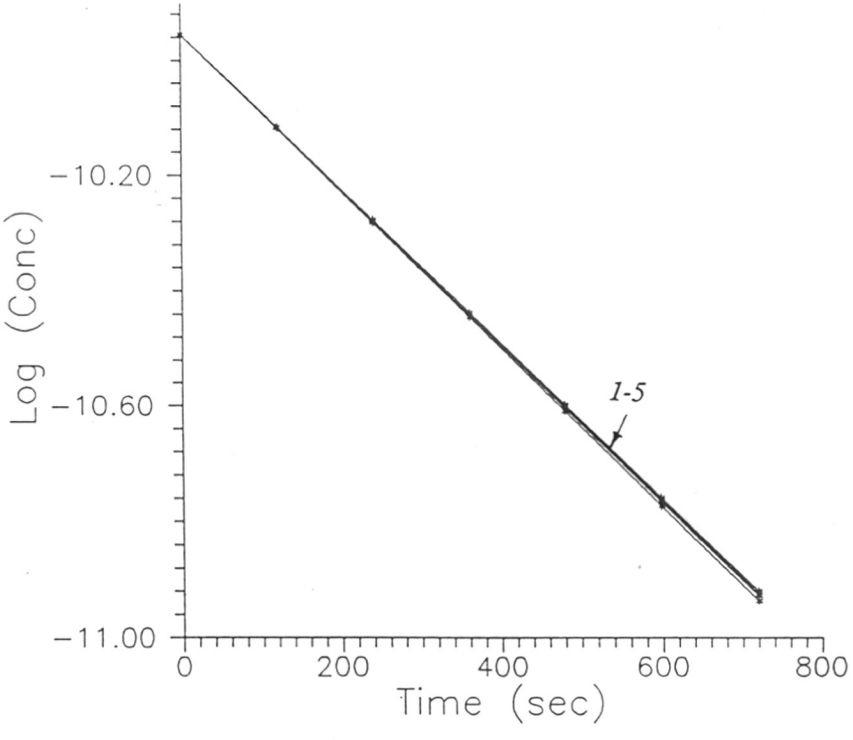

Fig. 3.9 **Ln(Conc.) versus time (sec) for runs 1-5:** *1-5* runs 1-5

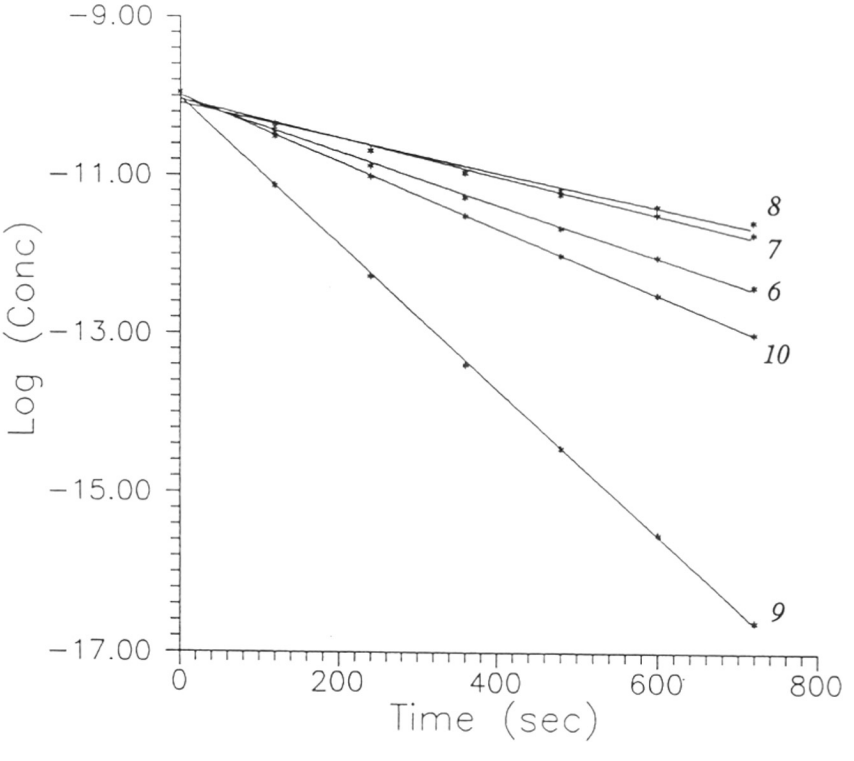

Fig. 3.10 **Ln(Conc.) versus time (sec) for runs 6-10:** *6-10* runs 6-10

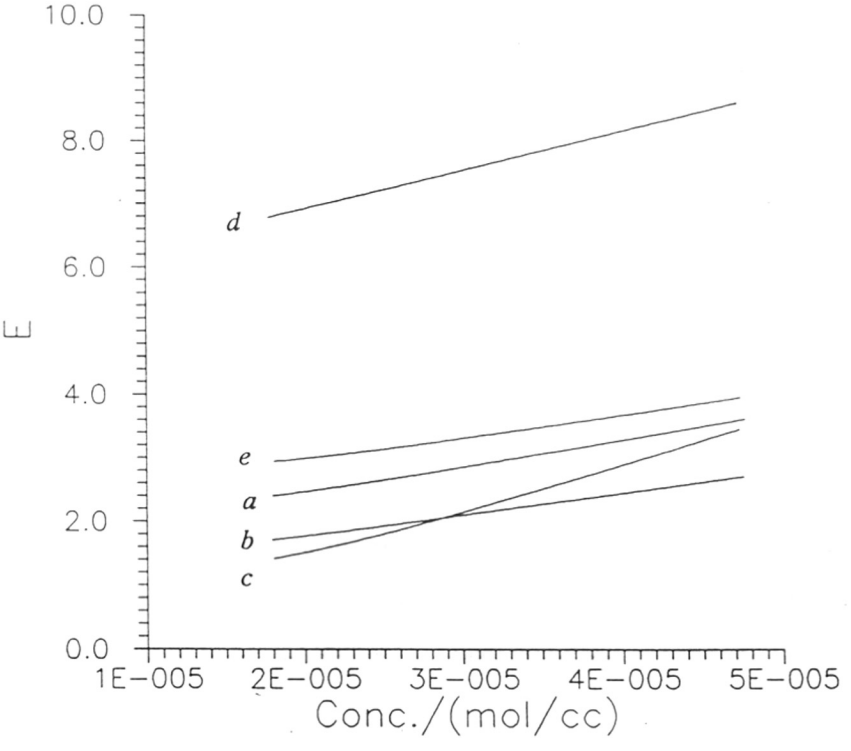

Fig. 3.11 **Enhancement (E) versus Concentration (mol/cc):** E :- enhancement factor defined as in equation 1

presence of micelles has been found to influence the rates of reactions due to the simultaneous course of the reaction in all the pseudo-phase sub-volumes. It is conceivable to divide the micellar solution into three sub-volumes: the organic phase volume (o), the interfacial volume (s) and bulk aqueous phase volume (w), and a reaction may proceed in all the three sub-volumes. The scheme for such reaction can be given as,

$$A_o + B_o \rightarrow P_o \qquad \text{(oil phase)}$$

$$\uparrow\downarrow \qquad\qquad \uparrow\downarrow$$

$$A_s + B_s \rightarrow P_s \qquad \text{(interface)}$$

$$\uparrow\downarrow \qquad\qquad \uparrow\downarrow$$

$$A_w + B_w \rightarrow P_w \qquad \text{(water phase)}$$

where A (here sulfuric acid) has been assumed to be predominantly water-soluble and B (nicotine) the oil-soluble reagent. The overall balance of species such as B can then be written as,

$$n_B = n_B^o + n_B^s + n_B^w \qquad (2)$$

$$= V_o[B]_o + V_s[B]_s + V_w[B]_w \qquad (3)$$

where o, w, and s denote the respective phases and the square brackets represent concentrations. The rate law for the irreversible reaction has been expressed by change in n_B, the number of moles of organic reagent as,

$$-\frac{dn_B}{dt} = V_o k_o [B]_o [A]_o^2 + V_s k_s [B]_s [A]_s^2 + V_w k_w [B]_w [A]_w^2 \qquad (4)$$

On assuming that the hydrophilic reagent A cannot penetrate into the oil phase, the above equation reduces to,

$$-\frac{dn_B}{dt} = V_s k_s [B]_s [A]_s^2 + V_w k_w [B]_w [A]_w^2 \qquad (5)$$

Under pseudo-first order conditions, $[A]_w >> [B]_w$ giving $K_w = k_w[A]_w^2$ and $K_s = k_s[A]_s^2$. Further defining the distribution ratio of the organic reagent between the aqueous and oil phase as

$$R_{w,o} = \frac{V_w[B]_w}{V_o[B]_o} = \frac{n_B^w}{n_B^o} \tag{6}$$

and that between the surfactant phase and the oil phase as

$$R_{s,o} = \frac{V_s[B]_s}{V_o[B]_o} = \frac{n_B^s}{n_B^o} \tag{7}$$

the equation for rate of the reaction has been written as,

$$-\frac{dn_B}{dt} = n_B^o(R_{w,o}K_w + R_{s,o}K_s) \tag{8}$$

where now K_W has been regarded as the pseudo-first order rate constant of the reaction between the oil phase and pure aqueous phase, and K_S that between the oil phase and the surfactant phase.

On integrating the above equation,

$$n_{B,i}^o = n_{B,f}^o \exp\{-K(t_f - t_i)\} \tag{9}$$

where $n_{B,i}^o$ and $n_{B,f}^o$ are the moles of B at times t_i and t_f respectively, and K represents the overall rate constant observed for the reaction, which has been given as

$$K = R_{w,o}k_w[A]_w^2 + R_{s,o}K_s \tag{10}$$

K_W has been calculated from the experimental data of reaction between oil phase and pure acid. Knowing the values of $R_{W,O}$, $R_{S,O}$ and K one can determine the values of K_S as

$$K_s = \frac{K - R_{w,o}k_w[A]_w^2}{R_{s,o}} \tag{11}$$

3.5 Discussion

Equation 11 implies that the presence of micelles may influence the rate of chemical reactions in two different ways : (i) the rate constants in the interface region, K_S, differ from those in the bulk aqueous region, K_W and (ii) the reacting species A and B partition into the aqueous and surfactant sub-volumes to different extents, thus increasing or decreasing the overall rate of the reaction. In the later case, the equilibrium has been also influenced. Using the concentration-time data, and the values of $R_{W,O}$, $R_{S,O}$, K and K_W reported in Table 3.4, the rate constant K_S has been estimated.

3.6 Conclusions

It has been evident from *fig.* 3.11 that the enhancement obtained in case of TX-100 + 1-pentanol has been the greatest, whereas that obtained in case of CTAB + 1-pentanol has been the lowest. This is because $R_{S,O}$ has been predominantly greater in the case of TX-100 + 1-pentanol/ 2.5 mol lit^{-1} H_2SO_4/ kerosene system in comparison with CTAB + 1-pentanol/ H_2SO_4/ kerosene system. However on comparison between the plots of E versus concentration in case of SDS + 1-pentanol and CTAB + 1-pentanol it becomes evident that $R_{S,O}$ has not only been the factor which decides the enhancement E. Besides the volume fraction of the surfactant phase of the microemulsion system, the mechanism of reaction taking place at the interface also decides the magnitude of E. Since the value of K_S has been entirely decided by these factors, the trend shown by K_S has been found to match exactly with that shown by E.

The aqueous phase which has been an oil-in-water microemulsion contains the product nicotine sulfate. The excess sulfuric acid if any can be reacted with fresh organic phase, in order to get the desired concentration of the product in

Table 3.4 Measured values of K, $R_{w,o}$, $R_{s,o}$, and K_w and estimated values of K_s

No.	k_w $\times 10^3$ sec	K $\times 10^3$ sec	$R_{w,o}$ $\times 10^4$	$R_{s,o}$ $\times 10^{-4}$	K_w $\times 10^{10}$ sec	K_s $\times 10^7$ sec
1	1.35	3.30	8.236	1.2812	0.228	2.58
2	1.35	2.40	7.79	1.2812	.913	1.87
3	1.34	2.13	7.68	1.2812	1.78	1.67
4	1.36	9.16	7.03	1.9938	85.21	4.59
5	1.34	4.19	9.08	1.0163	0.0335	4.11

the aqueous phase. Since the microemulsion contains a mixture of surfactant and cosurfactant alongwith nicotine sulfate, it can be used directly for field applications by merely diluting to the desired concentration

3.7 Notations

$[A]$, $[B]$: Concentration of species A, B (mol/cc)

E : Enhancement factor as defined by equation 1

k_O, k_S, k_W : Rate constants of reaction in organic, surfactant and aqueous phases respectively

K_S, K_W : Pseudo order rate constants of reaction in surfactant and aqueous phases respectively, (sec^{-1})

K : Overall pseudo order rate constant of the reaction

n_B^o, n_B^s, n_B^w : Moles of species B in organic, surfactant and aqueous phases respectively, (gm moles)

$n_{B,i}^o$: Moles of species B in organic phase before reaction, (gm moles)

$n_{B,f}^o$: Moles of species B in organic phase after reaction, (gm moles)

$R_{W,O}$: Partition ratio of species B between aqueous and organic phases

$R_{S,O}$: Partition ratio of species B between surfactant and organic phases

t : Time, (sec)

t_i : Initial time, (sec)

t_f : Final time, (sec)

V_O, V_S, V_W : Volumes of organic, surfactant and aqueous phases respectively, (cc)

3.8 References

1 E. L. Griffin,Jr., G. W. Macpherson Phillips, J. B. Claffey, J. J. Skalamera and E. O. Strolle, *Ind. Eng. Chem.*, **44**, 274, (1952)

2 A. S. Chhatre and B. D. Kulkarni, *J. Colloid Interface Sci.*, (in press)

3 A. S. Chhatre and B. D. Kulkarni, *J. Chem. Res.* (in press)

4 A. P. Colburn and D. B. Welsh, *Trans. Am. Inst. Chem. Engrs.* **38**, 179, (1942)

5 I. V. Berezin, I. Martinek and A. K. Yatsimirskii, *Dokl. Akad. Nauk SSSR*, **194**, 840, (1970)

6 L. S. Romsted, in *Micellization, Solubilization and Microemulsions*, ed. K. L. Mittal, Plenum Press, New York, (1977)

7 Victoria-R. Hanke, W. Knoche and E. Dutkiewicz, *J. Chem. Soc. Faraday Trans. I*, **83(9)**, 2847, (1987)

8 R. Schomacker, K. Stickdorn and W. Knoche, *J. Chem. Soc. Faraday Trans. I*, **87(6)**, 847, (1991)

CHAPTER 4

NICOTINE SULFATION USING SULFURIC ACID IN A MICROEMULSION MEDIUM CASE - SINGLE DROP COLUMN REACTOR

4.1 Introduction

The reaction between nicotine and sulfuric acid has been found to be pseudo-first order as seen from the results presented in Chapter 3. The reaction between nicotine in the kerosene phase and sulfuric acid in the aqueous phase of various microemulsion media has been carried out using a *type I* microemulsion system, in a stirred cell reactor, wherein the excess aqueous phase containing nicotine has been contacted with a microemulsion of kerosene in sulfuric acid. In the work presented in this chapter the same technique has been used in a single drop column reactor. A solution of nicotine in kerosene has been introduced dropwise into the reactor from the bottom of the reactor which contained a microemulsion of kerosene in sulfuric acid. The microemulsion systems used as stagnant phase and their compositions are shown in Table 4.1. The drops exchange the solute nicotine with the microdroplets of the stagnant phase microemulsion and the reaction takes place at the surface of either of the two. It has been found that in case of single drop containing substantial amounts of surfactant at the interface, the mass transfer is hindered if the surfactant film is stagnant. Even the internal circulation in the drop is drastically reduced due to the film. A simple equation for flux across the drop interface has been used in the calculations. The local mass transfer coefficient has been calculated using existing model proposed by Ruckenstein, *et al*[1]. The mass transfer coefficients thus calculated also suggest that internal circulation and interfacial film rigidity are the major factors responsible for the observed fluxes in case of reaction between the solute nicotine in the drop and sulfuric acid in the stagnant phase.

4.2 Single drop column reactor

4.2.1 Droplet velocity

Drops falling or rising freely under influence of gravity in an infinite medium have been classified according to their shapes, as spherical, ellipsoidal and spherical caps. A generalized correlation in terms of Eotvos number (*Eo*), Morton number (*M*), and Reynolds' number (*Re*), has been given by Grace, *et al*[2]. It is a well known fact that for a drop falling or rising freely in a stagnant medium the presence of surfactants at the drop interface have a retarding effect on its motion. Also, the interface is rendered immobile due to which internal circulation drops drastically. This may lead to a decreased mass transfer across the drop interface. For an ellipsoidal drop whose volume-equivalent-sphere diameter is d_e and which has a substantial amounts of surfactant on its surface a correlation for the terminal velocity (U_t) with the system properties has been given as follows[2].

For $M < 10^{-3}$, $Eo < 40$, $Re > 0.1$, and $H \leq 59.3$

$$J = 0.94 \quad H^{0.757} \tag{1}$$

For $M < 10^{-3}$, $Eo < 40$, $Re > 0.1$, and $H > 59.3$

$$J = 3.42 \quad H^{0.441} \tag{2}$$

where H is given as,

$$H = (4/3)Eo \quad M^{-0.149}(\mu_c/\mu_w)^{-0.14} \tag{3}$$

U_t is thus calculated from the expression

$$U_t = (\mu_c/\rho_c d_e) \quad M^{-0.149} \quad (J - 0.857) \tag{4}$$

It has been noted here that the drop diameter d_e is sufficiently small as compared to the reactor diameter, so that the wall effects can be neglected. It has been assumed that the drop assumes terminal velocity as soon as it is detached from the bottom. It is a well known phenomena that drops change shapes when

rising or falling freely in an infinite medium. Due to this, the effective surface area of the drop is increased. The deformation of drops is due to inertial effects. This deformation has been found to depend not only on Eo, but also on M. The mean aspect ratio, denoted as $\overline{E}$ where E is the ratio of maximum vertical dimension to the maximum horizontal dimension of the drop, and serves as a better measure of the deformation of the drop. For low Morton numbers, a simple correlation between $\overline{E}$, Eo and M has been proposed by Wellek *et al*[3] as,

$$\overline{E} = 1/(1 + 0.163 Eo^{0.757}) \qquad (5)$$

for $Eo < 40$ and $M <\approx 10^{-6}$

Using the above correlation the height-to-width of the ellipsoidal drop can be calculated. Knowing this ratio, which is the ratio of length of the minor axis to that of the major axis of the ellipsoidal drop, and knowing the volume of the drop, the surface area of the ellipsoidal drop can be calculated from geometry.

4.2.2 Mass transfer from single drops

A kerosene solution of nicotine has been used in place of pure nicotine. If pure nicotine were directly contacted with the microphase in a drop column reactor, the rate of change in the volume of the single drop due to depletion of nicotine from the drop would be significant[1] in case of a fast reaction. The rate of change in the drop volume which is determined by the overall rate of reaction and hence by rate of mass transfer of the reacting species, would be difficult to measure in that case. Hence we have preferred to use a diluted solution of nicotine instead of pure one. Any changes in volume of the drop due to mass transfer effect would be quite small so that the change in radius of the drop has been neglected.

Mass transfer during drop formation and during its translation through the stagnant medium has been treated separately. The following assumptions have been made in the analysis of the present work. i) The droplet shape is spherical when it is forming at the nozzle. ii) Immediately after its release from the nozzle,

it assumes an ellipsoidal shape, and translates with terminal velocity. Under these circumstances, the expression for mean surface area available for mass transfer during drop formation can be given[4] as

$$A_m = \frac{1}{t_f} \int_0^{t_f} \frac{[3t_f(dV/dt)]^{2/3}}{(1/4\pi)^{1/3}} \, dt \qquad (6)$$

where A_m is the mean surface area, t_f is the time of drop formation, and dV/dt is the volumetric flow rate of the solution. The drop when released assumes ellipsoidal shape, and the surface area (A_S) has been calculated as described earlier.

Assuming Fick's law to be valid here, the flux across any surface can be given as

$$N = -D_a \, (-dC/dx) \qquad (7)$$

where D_a is the diffusivity, C denotes the concentration, and x denotes a characteristic length. Alternatively, given the number of moles transferred across a known area in known time the flux equation can be written as,

$$N = \frac{(n_1 - n_2)}{(t_2 - t_1)(A)} \qquad (8)$$

where N is the flux (mol/cm^2 sec), n_1 and n_2 are the number of moles at times t_1 and t_2 (sec) respectively, and A (cm) is the area across which the transfer has taken place.

The flux across the drop surface when it is forming can be given as,

$$F_1 = \frac{(n_i - n_1)}{(A_m)(t_f)} \qquad (9)$$

where n_i is the initial number of moles in the droplet, n_1 is the number of moles present after the drop has formed, t_f is the time of formation of the drop, and A_m is the mean surface area of the drop. Similarly the flux across the drop surface when it is translating can be given as,

$$F_2 = \frac{(n_1 - n_f)}{(A_s)(t_r)} \qquad (10)$$

where n_f is the number of moles in the droplet after it has translated for time t_r, n_1 is the initial number of moles present and A_s is the mean surface area of the ellipsoidal drop.

Since the reaction taking place is the same these fluxes can be equated to obtain the value of n_1, which when substituted back in any of the above equations gives the value of overall flux.

In case of a two component drop, molecular diffusivities of the solute in the drop phase and that in the stagnant phase are comparable. Since the exact analysis of mass transfer to binary drops is quite complicated due to several effects discussed later, a quasi-steady state assumption (QSSA) has been introduced. It implies the use of the steady state mass transfer coefficient for the stagnant phase, even though these transient effects exist, coupled with the unsteady state mass balance over the drop phase. For a chemical reaction occurring in the stagnant phase the Sherwood number has been given as[1],

$$Sh = 2\sqrt{R}\ erf(\sqrt{(0.5R)/Pe}) + 4\sqrt{(Pe/3\pi)}\exp(-0.5R/Pe) \qquad (11)$$

where Pe is the Peclet number given as $Pe = (3\ a\ U_{obs})/\ 2\ D_C$ for potential flow and R is given as, $R = k_2\ a^2\ /\ D_C$

In this case, the QSSA is valid if $\Phi\sqrt{Pe} \gg 1$ for $(R/Pe) \ll 1$ and $\Phi\sqrt{R} \gg 1$ for $(R/Pe) \gg 1$. The QSSA may introduce serious errors if either $\Phi\sqrt{R} < 10$ or $\Phi\sqrt{Pe} < 10$.

The pseudo-first order rate constant (k_2) of the reaction between nicotine and sulfuric acid has been measured in chapter 2. Using this rate constant and the above equations the Sherwood number can be calculated from which the mass transfer coefficient (k) have been deduced using the equation

$$k = (D_c Sh)/2a \qquad (12)$$

4.3 Experimental procedure

All the experiments have been carried out at 30°C by circulation of thermostated water through the jackets of the drop column reactor. The reactor used in the present work has been shown in *fig.* 4.1. The systems studied here have been as shown in Table 4.1. The organic solution of the solute nicotine has been introduced dropwise from the bottom of the reactor into the stagnant phase microemulsion containing the water-soluble reactant at a constant flow rate. The flow rate ($\overline{V} = dV/dt$) has been measured by noting the time required for the flow of definite volume of the organic solution. The time required for the formation of one drop (t_f), the total time (t) for which these droplets have been introduced and the volume of the organic solution introduced into the reactor (V) have been measured. From this, the total number of drops, and hence the volume per drop (v) have been calculated. The residence time of the drop inside the reactor (t_r) has also been measured accurately. The volume-equivalent-sphere diameter (d_e) of the drop has been calculated as,

$$d_e = (6v/\pi)^{1/3} \qquad (13)$$

The reaction has been followed by collecting the organic phase form the top of the reactor and analyzing for its constituents by using an automated Shimadzu make UV Spectrophotometer at λ_{max} = 281 nm.

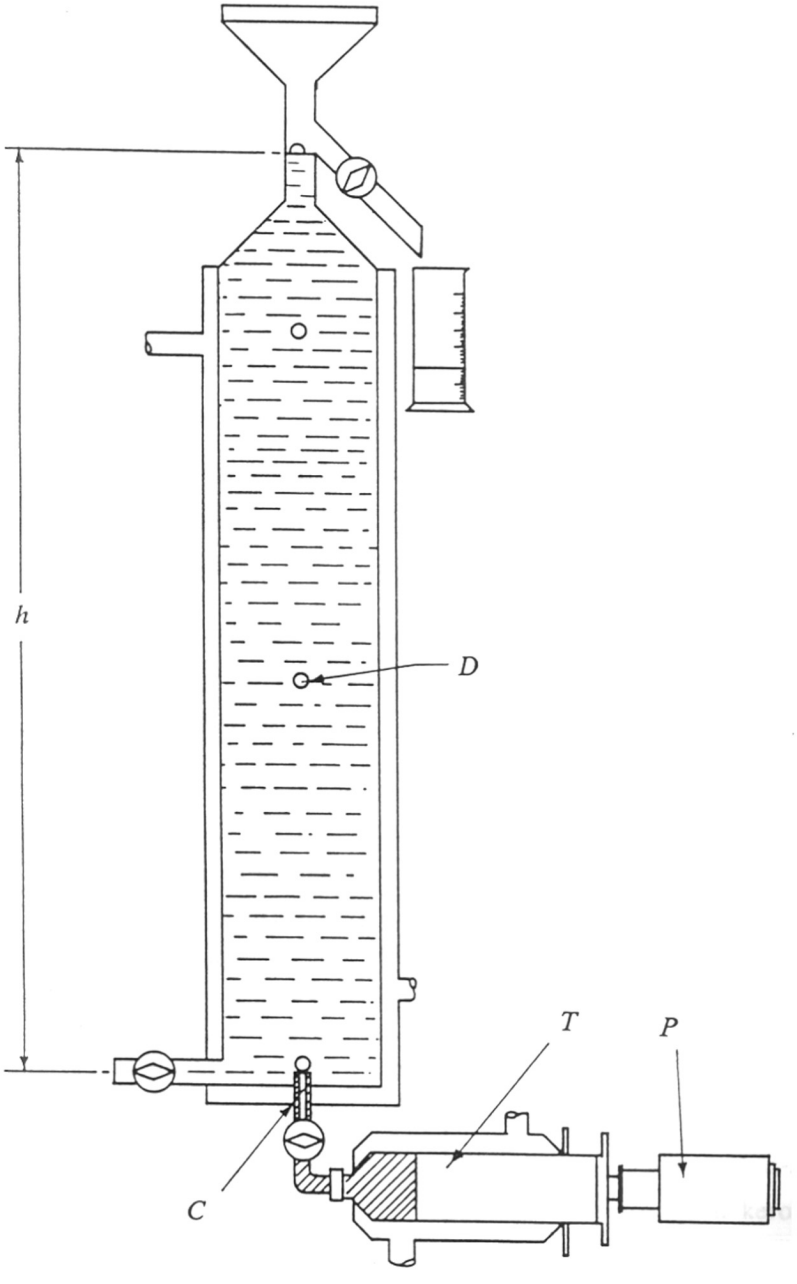

Fig. 4.1 **Single drop column reactor for nicotine sulfation:** h :- height of the reactor; C :- capillary of known diameter; P :- automatic plunger; T :- thermostatic syringe; D :- the rising drop

Table 4.1 Composition of systems studied

No.	System studied	Stagnant phase	Drop phase
1	0.26 N (0.13 mol/lit) H_2SO_4	100%	100% (4.748E-5 mol/cc) nicotine in kerosene
2	0.52 N (0.26 mol/lit) H_2SO_4	100%	100% (4.748E-5 mol/cc) nicotine in kerosene
3	0.73 N (0.365 mol/lit) H_2SO_4	100%	100% (4.748E-5 mol/cc) nicotine in kerosene
4	SDS + 1-pentanol (0.05 mol/lit) H_2SO_4 Kerosene	10% 84% 6%	1% 0% 99% (4.753E-5 mol/cc) nicotine in kerosene
5	CTAB + 1-pentanol (0.13 mol/lit) H_2SO_4 Kerosene	15% 56% 29%	1.1% 0.0% 98.9% (4.750E-5 mol/cc) nicotine in kerosene
6	CTAB + 1-pentanol (0.26 mol/lit) H_2SO_4 Kerosene	12% 45% 43%	0.6% 0.0% 99.4% (4.749E-5 mol/cc) nicotine in kerosene
7	CTAB + 1-pentanol (0.365 mol/lit) H_2SO_4 Kerosene	10% 35% 55%	0.6% 0.0% 99.4% (4.747E-5 mol/cc) nicotine in kerosene
8	TX-100 + 1-pentanol (2.5 mol/lit) H_2SO_4 Kerosene	8% 72% 20%	1.2% 0.0% 98.8% (4.751E-5 mol/cc) nicotine in kerosene

4.4 Physical properties measurements

The densities of the stagnant phase (ρ_c) and the organic phase (ρ_d) have been measured by using an automated vibrating tube density meter (DMA 60/602 Anton Paar) which has been calibrated at the reaction temperature. Viscosity of the microemulsion (μ_c) and the organic solution (μ_d) have been measured by using a simple Ostwald viscometer which has also been calibrated earlier at the reaction temperature. Interfacial tension (σ) measurements have been carried out using the pendant drop technique. Molar volume of nicotine at normal boiling point has been estimated by the method given by Tyn and Calus[5], and the critical volume has been determined by the group contribution method of Vetere[6]. Average molecular weights of kerosene (M_d) and the stagnant phase (M_C) microemulsions have been estimated from the respective compositions, with an accuracy of 1%. The molecular diffusivities of nicotine into the organic solution (D_d) and microemulsion (D_C) have been estimated by using the Wilke-Chang equation[7]. Distribution coefficient (Φ) of nicotine in various phases has been determined by equilibrating equal volumes of the organic solution of nicotine in kerosene and aqueous solution of potassium sulfate of appropriate strengths.

4.5 Results

The composition (by weight%) of microemulsion systems and the organic phase used in the experiments have been as given in Table 4.1. The general properties of the systems used have been tabulated in Table 4.2. Measured system parameters have been tabulated in Table 4.3. The empirically calculated and estimated parameters have been tabulated in Table 4.4.

4.6 Discussions

The problem of mass transfer from a single drop has been more complex than that in the case of a solid particle. This is because in case of a drop moving freely in a stagnant phase, the tangential component of drop velocity at the

Table 4.2 General properties (all property measurements at 303°K)

1) Molar volume of Nicotine at normal B.P. = 198.2 cc/gm mole

2) Association factor of Drop phase (Kerosene) = 1.0

3) Association factor of Stagnant phase (Acid) = 2.6

4) Mol. Wt. of Nicotine = 162.2

5) Mol. Wt. of Kerosene = 190 (approx.)

6) Distribution coefficient of nicotine between Kerosene and aqueous K_2SO_4

Conc.(mol/lit)	Φ
0.05 moles/lit K_2SO_4	1101.0
0.13 moles/lit K_2SO_4	1214.2
0.26 moles/lit K_2SO_4	1283.7
0.365 moles/lit K_2SO_4	1301.4
2.5 moles/lit K_2SO_4	1422.3

Table 4.3 Measured parameters

No.	Parameter	System number							
		1	2	3	4	5	6	7	8
1	V/cc	18.2	17.9	17.6	18.1	18.6	18.1	17.9	18.3
2	t/sec	1800	1800	1800	1800	1800	1800	1800	1800
3	t_f/sec	1.2	1.1	1.1	1.1	1.5	1.2	1.1	1.1
4	t_r/sec	2.8	2.8	2.9	3.8	4.3	4.8	4.6	3.2
5	h/cm	30	30	30	30	30	30	30	30
6	ρ_d/(gm/cc)	0.7861	0.7861	0.7861	0.7865	0.7865	0.7864	0.7864	0.8484
7	ρ_c/(gm/cc)	1.0037	1.0106	1.0161	1.0263	0.9162	0.897	0.8706	1.1722
8	μ_d/poise	0.0082	0.0082	0.0082	0.0083	0.0083	0.0083	0.0084	0.0087
9	μ_c/poise	0.0106	0.0112	0.0129	0.0144	0.0112	0.0106	0.0104	0.0288
10	σ/(dyne/cm)	36.123	35.341	33.996	0.922	0.881	0.889	0.902	1.4
11	Temperature/°K	303	303	303	303	303	303	303	303
12	M_d/(gm/mole)	190	190	190	190	190	190	190	190
13	M_C/(gm/mole)	18.209	18.398	18.553	21.072	30.28	37.32	47.26	25.182
14	C_i/(1E-5 mole/cc)	4.748	4.748	4.748	4.753	4.750	4.749	4.747	4.751
15	C_O/(1E-5 mole/cc)	2.361	2.341	2.383	2.001	1.998	1.695	1.670	1.214

Table 4.4 Calculated and Estimated parameters

No	Calculated parameters	System No.							
		1	2	3	4	5	6	7	8
1	$\overline{V}$ /(cc/sec)	0.01011	0.0099	0.0098	0.0101	0.0103	0.0101	0.0099	0.0102
2	$\Delta\rho$/(gm/cc)	0.218	0.225	0.230	0.240	0.130	0.111	0.084	0.324
3	v/cc	0.0121	0.0109	0.0108	0.0111	0.0155	0.0121	0.0109	0.0112
4	d_e/cm	0.285	0.275	0.274	0.276	0.309	0.285	0.275	0.277
5	Eo	0.480	0.472	0.497	19.51	13.85	9.90	6.96	17.40
6	M	5.7E-11	7.7E-11	1.5E-10	1.2E-5	3.5E-6	2.4E-6	1.7E-6	5.8E-5
7	H	21.03	19.63	18.3	131.4	116.4	88.6	65.6	84.3
8	J	9.43	8.95	8.48	29.4	27.9	24.7	21.6	24.2
9	$U_{t,obs.}$ /(cm/sec)	10.71	10.71	10.34	7.89	6.98	6.25	6.52	9.38
10	$U_{t,calc.}$ /(cm/sec)	10.68	10.46	10.24	7.81	6.94	6.80	6.50	8.84
11	Re	289.2	266.3	223.2	155.5	176.6	150.5	150.4	105.9
12	$\overline{E}$	0.915	0.915	0.912	0.393	0.456	0.520	0.585	0.381
13	A_s/(cm^2)	0.25572	0.23864	0.23599	0.28334	0.33796	0.27596	0.25153	0.28848

Table 4.4 Calculated and Estimated parameters (contd.)

No	Calculated parameters	System No.							
14	$A_m/(cm^2)$	0.1532	0.1430	0.1413	0.1440	0.1803	0.1526	0.1429	0.1451
15	F/(1E-7 mol/cm^2 sec)	2.605	2.616	2.496	2.148	2.096	2.144	2.250	3.123
16	D_d /(1E-5cm^2/sec)	1.578	1.578	1.578	1.578	1.578	1.578	1.578	1.578
17	D_c /(1E-6cm^2/sec)	6.092	5.795	5.053	4.824	7.435	8.721	10.003	2.637
18	Pe	375782	381180	420517	338563	217568	153186	134435	738982
19	Sh	802.1	800.3	845.3	757.2	608.8	533.6	479.4	1115.4
20	k/(1E-2 cm/sec)	1.714	1.684	1.560	1.321	1.463	1.635	1.741	1.06

interface, with respect to the drop centre may take a non-zero value due to internal circulation[8]. This value is dependant upon various parameters like drop velocity, viscosity of the two phases as well as presence of any surface active material at the interface[9,10]. Also the Marangoni effect complicates the problem further[11]. As stated earlier, the drop surface is rendered immobile, due to which internal circulation drops down drastically, as compared to the case where no surfactant is present. It has been seen from Table 4.4, that since the presence of the surfactant film over the drop surface, the overall flux in case of system nos. 4 to 7 has been less as that in comparison with the corresponding systems with no surfactant (systems 1-3). In the case of the system 8, which involves TX-100 + 1-pentanol as surfactant mixture, the flux has been increased. The film rigidity, and hence its stability, has been one of the factors which plays an important role in the determination of the overall flux. It is for this reason that the flux across the interface have been found to be lowered in presence of the surfactant film made of either SDS + 1-pentanol, or CTAB + 1-pentanol. Therefore in case of TX-100 + 1-pentanol, the film being weaker than the other two, results in an increased flux.

4.7 Notations

a	radius of drop
A_m	Mean surface area of drop during its formation
A_S	Surface area of translating drop
C	Concentration of species
C_i	Initial concentration of nicotine in bulk drop phase
C_i	Final concentration of nicotine in bulk drop phase
d_e	Volume equivalent sphere diameter of the drop
D_a	Molecular diffusivity of a
D_d	Molecular diffusivity of nicotine in drop phase
D_c	Molecular diffusivity of nicotine in stagnant phase
$erf\,(x)$	$= \frac{2}{\sqrt{\pi}} \int_0^x e^{-m^2}\, dm$
E	Aspect ratio
$\overline{E}$	Mean aspect ratio
Eo	Eotvos number ($= \frac{g d_e^2 \Delta\rho}{\sigma}$)
F_1, F_2	Molar fluxes across the drop surface (F)
g	gravitational acceleration
h	height of reactor
H	Parameter defined by equation 3
J	Parameter defined by equations 1 and 2
k	Local mass transfer coefficient

k_2	Reaction rate constant in stagnant phase
M	$(\frac{g\mu_c^4\Delta\rho}{\rho_c^2\sigma^3})$ Morton number
M_d, M_C	Molecular weights of drop, stagnant phases
n_1, n_2	number of moles of nicotine in the drop
n_i, n_f	Initial and final moles of the reactant
N	Overall flux
P_e	Peclet number ($= \frac{1}{4}\frac{\mu_c}{\mu_d+\mu_c}\frac{2aU_t}{D_A}$ for Hadamard flow
	$= \frac{3}{2}\frac{aU_t}{D_A}$ for potential flow)
R	$= k_2a^2/D_c$
Re	Reynolds number ($= \frac{\rho_c d_e U_t}{\mu_c}$)
Sh	Sherwood number
t, t_1, t_2	Time
t_f	Time of drop formation
t_r	Residence time of drop in the column
$U_{t,calc.}$	Terminal velocity of drop (calculated)
$U_{t,obs.}$	Terminal velocity of drop (observed)
v	volume of one drop
V	Volume of organic phase
$\overline{V}$	Volumetric flow rate ($= dV/dt$)
x	Characteristic length

Greek symbols

$\Delta\rho$	$= \lvert\rho_c - \rho_d\rvert$
μ_d	viscosity of drop phase
μ_c	viscosity of stagnant phase
μ_w	viscosity of water (0.9 cP)
ρ_c	density of stagnant phase
ρ_d	density of drop phase
σ	Interfacial tension
Φ	Distribution coefficient

4.8 References

1 Ruckenstein E., Dang Vi-Duong and Gill W. N. *Chem. Engng. Sci.* **26**, 647, (1971)

2 Grace J. R., Wairegi T., and Nguyen T. H., *Trans. Inst. Chem. Engrs.* **54**, 167, (1976)

3 Wellek R. M., Agrawal A. K. and Skelland A. H. P. *AIChEJ.*, **12**, 854-862, (1966)

4 Licht W. and Conway J. B. *Ind. Eng. Chem.*, **42**, 1151, (1950)

5 Tyn M. T. and Calus W. F., *Processing*, **21(4)**, 16, 1975

6 For the method, refer to Perry's Chemical Engineers Handbook, VI edition, Mc.Graw Hill Book Company, pp 3-266, 1984

7 Wilke, C. R., and Chang P., *AIChEJ*, **1**, 264 (1955)

8 Ruckenstein E. *Chem. Engng. Sci.*, **19**, 131 (1964)

9 Hadamard J. C. R. *Acad. Sci. Paris*, **152**, 1735, (1911)

10 Frumkin A. N. and Levich V. G. *Zh. Fiz. Khim., SSSR* **21**, 1183, (1947)

11 Ruckenstein E. and Berbente C. *Chem. Engng. Sci.* **19**, 329, (1964)

CHAPTER 5

SELECTIVE NITRATION OF PHENOL TO O-NITROPHENOL USING A NOVEL MICROEMULSION MEDIUM

5.1 Introduction

Nitration of aromatic compounds has been a challenging unit process since long. The conventional nitrating agent is a mixture of concentrated sulfuric and nitric acids. In other commercial processes, nitrating agents like mixture of acetic acid and concentrated nitric acid, or nitric acid in acetic anhydride have been used [1]. Use of other acids such as perchloric acid and hydrofluoric acid, or boron trifluoride have also been studied but its commercial applications have been limited. Nitrating reactions require inert solvents such as chlorohydrocarbons to give homogeneous reaction mixtures. A typical nitrating agent for large-scale aromatic mononitration consists of 20% nitric acid, 60% sulfuric acid and 20% water. It has been noted that when on one hand stronger nitric acid leads to oxidative side reactions, on the other hand high reaction temperatures lead to formation of NO_2 gas and thus a decreased nitronium ion concentration. It therefore becomes necessary to carry out these reactions in a medium wherein the contact between the two phases is maximized, as well as the reaction temperature is controlled. Also well mixed conditions minimize the resistance to mass transfer, since the liquid aromatic substrate and the nitrated product together form a separate phase from the aqueous mixed acid phase. Microemulsions seem to provide such an efficient reaction medium.

It is known that the components of a microemulsion readily establish an equilibrium with each other. The microdroplets in a typical microemulsion exchange matter with other droplets on a nanosecond time scale. The microemulsion droplet can be considered as a micro-reactor where chemical reactions can occur within the small domain provided by the droplet. This can facilitate and regulate the growth process for particles as exemplified during crystallization and polymer formation. In addition, microemulsions have recently been used to effect separation and purification[2]. The molecular scale reactors offered by microemulsions have been of interest from a technology viewpoint, since the associated

kinetic effects and the presence of droplets can enhance or retard chemical rates by large factors[3-6]. Despite these advantages only a few studies highlight the beneficial effects of microemulsions in enhancing the reaction rates and the related issue of selectivity to the desired product. In the present chapter it has been shown that suitably prepared *type I* microemulsions facilitate selective transformation of reactants. It may be noted that *type II* microemulsions which contain excess aqueous phase in equilibrium with a water-in-oil type of microemulsion can also be used for the purpose depending upon the limiting component used in the reaction.

The nitration process of highly reactive aromatic compounds such as phenol, resorcinol, etc. using concentrated nitric acid (under homogeneous conditions) has been technologically important but very difficult from an operation and control viewpoint. The high reaction rates and the consequent release of heat causes oxidation and resinification of these compounds. Also, conventional strategies yield mixed nitrates at ortho- and para- positions and higher nitrated compounds. Direct nitration of such compounds using dilute nitric acid appears to be attractive although studies so far indicate that they have been technically difficult and uneconomical. Therefore, as a common practice, these compounds are first sulfonated and then nitrated[7]. Kaloshin[8] suggested that the nitration may be carried out in a heterogeneous liquid-liquid system. Other methods using nitrating agents such as graphite nitrate[9], tetranitromethane[10], nitrates in trifluoroacetic acid[11], sodium nitrate in presence of hydrochloric acid and lanthanum nitrate[12] have also been reported in literature. Gaude, *et al*[13] carried out the nitration in a two-phase media and suggested a diffusion controlled mode of operation to control the reaction rate. This study revealed that in a mixture of phenol and its derivatives, the more reactive compounds can get selectively nitrated. However, no notable regioselectivity have been observed in the nitration. In the work reported in the present chapter a *type I* microemulsion has been employed to carry out the nitration

of phenol using dilute nitric acid. The investigation indicated that the process rates have been selectively regulated and the oxidation and resinification have been largely avoided when the reaction has been carried out under microemulsion conditions.

It has been of interest to note that the conventional processes have been making use of concentrated nitric acid for the purpose of nitration and that dilute nitric acid has been known more as a oxidizing rather than a nitrating agent in organic chemistry. Since a *type I* microemulsion has been used, the excess organic phase which remains as a separate phase, can be re-used as a solvent, so that the process of nitration can be made continuous.

5.2 Materials

Phenol crystals obtained from SD chemicals have been purified by re-crystalization. Benzene (AR grade) procured from Sigma has been distilled and used as a solvent for phenol. AR grade Sodium salt of dioctyl sulfosuccinate (AOT) has been obtained from Aldrich and used as a surfactant without further purification. Nitric acid procured from SD chemicals has been used in a diluted form. The exact concentrations of the diluted acid solutions have been determined by titrating the acid solution with standard sodium hydroxide solutions. Diethyl ether used for extraction of nitrophenol has been obtained from SD chemicals, and has been distilled before use. The initial concentrations of organic phase have been determined by analyzing the organic phase on an automated Chemito 3800 make Gas chromatograph provided with a flame ionization detector. Nitrogen has been used as a carrier gas with flow rate of 30 ml/min. A 3 mt. long 0.8 mm internal diameter stainless steel column has been packed with 10% SE30 on Chromosorb W(HP) 80/100 mesh, and has been used in all the GC measurements. The aqueous phase in each reaction has been analyzed for its components, by using an automated Shimadzu make UV-visible spectrophotometer at λ_{max} around 430 nm.

5.3 Method

Experiments for determination of the phase behavior of microemulsion system consisting of nitric acid, benzene and the surfactant have been carried out at 30°C in the usual way. The experiments for reaction have been divided into three sets. In the first set (Runs 1-18), three different microemulsions of type I have been prepared corresponding to points marked *a*, *b* and *c* on the partial phase diagrams (*figs.* 5.1 to 5.3). The reactions have been carried out under these microemulsion media in different runs. In the second set (runs 19-36) aqueous solution of nitric acid with concentrations corresponding to those in runs 1-18 has been used. The composition of 400 ml of the aqueous phase used in each set has been shown in Table 5.1. The stock microemulsion solution has been prepared as follows. To a fixed amount of the dilute nitric acid, a pre-calculated amount of the surfactant (AOT) has been added such that the concentration of AOT was more than its critical micelle concentration (CMC). This ensured the formation of micelles of the type oil-in-water. Then the micellar solution has been equilibrated with an excess of pure benzene. Some of the benzene solubilized into the micelles and the excess has then been used to prepare the phenol-benzene mixtures of varying concentrations. The micellar solution thus prepared has been an oil-in-water type of microemulsion. In the third set of experiments (Table 5.2), 100 ml of an organic phase of concentration 0.716 mol/lit phenol in benzene, has been reacted with 400 ml of 7.66 mol/lit HNO_3, with varying stirrer speeds in 6 different runs (runs 37-42). In all the experimental runs 400 ml of the aqueous phase has been reacted with 100 ml of the organic phase. A jacketed cylindrical reactor shown in figure 5.4 has been used for all the reactions. The reactor has been provided with a four blade stirrer, a reflux condenser and has been maintained at 30°C by circulation of thermostated water through the jacket. The temperature has been maintained with an accuracy of ± 2°C . All the experiments except those reported in Table 5.2 have been carried out at a fixed stirring rate of 50 rpm. The stirring

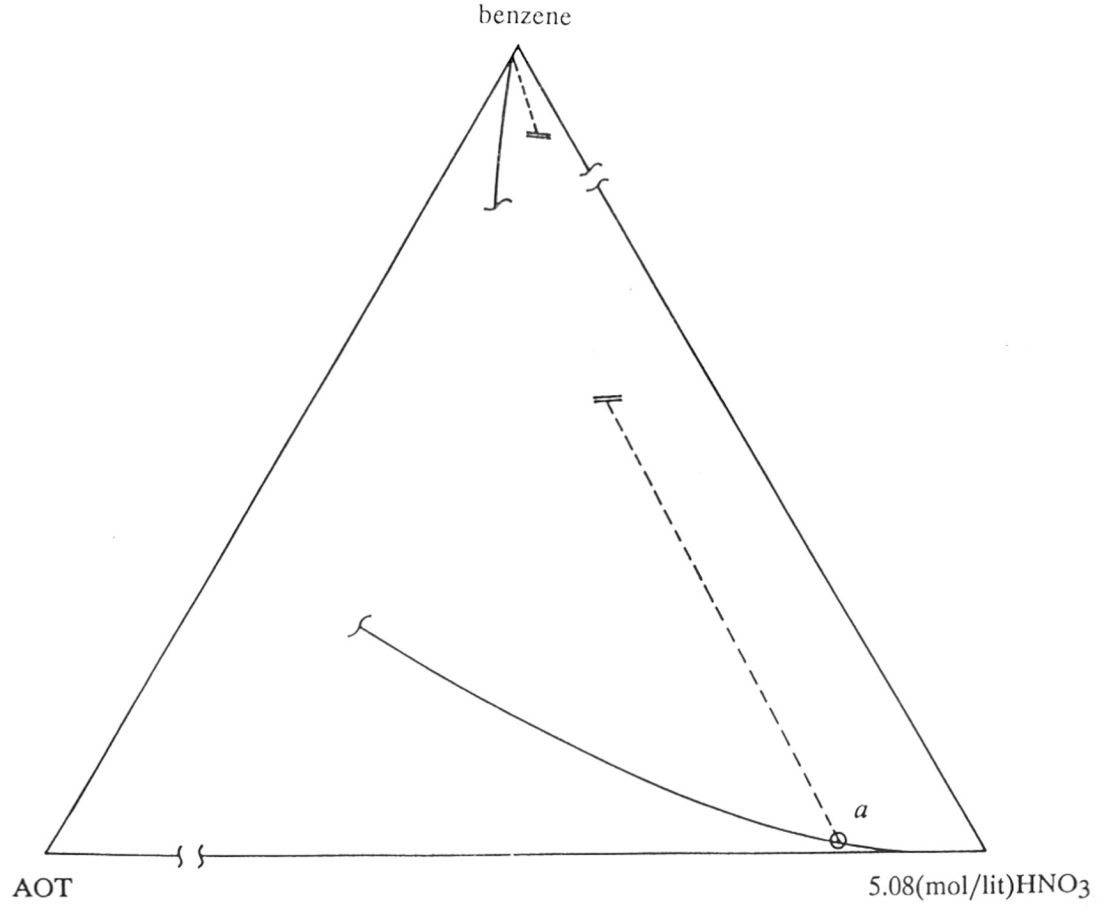

Fig. 5.1 **Partial phase diagrams of the pseudo-ternary system AOT/ 5.08 (mol/lit) HNO3/ benzene at 30°C:** *a* :- point representing overall composition of reaction system; (note break in scale)

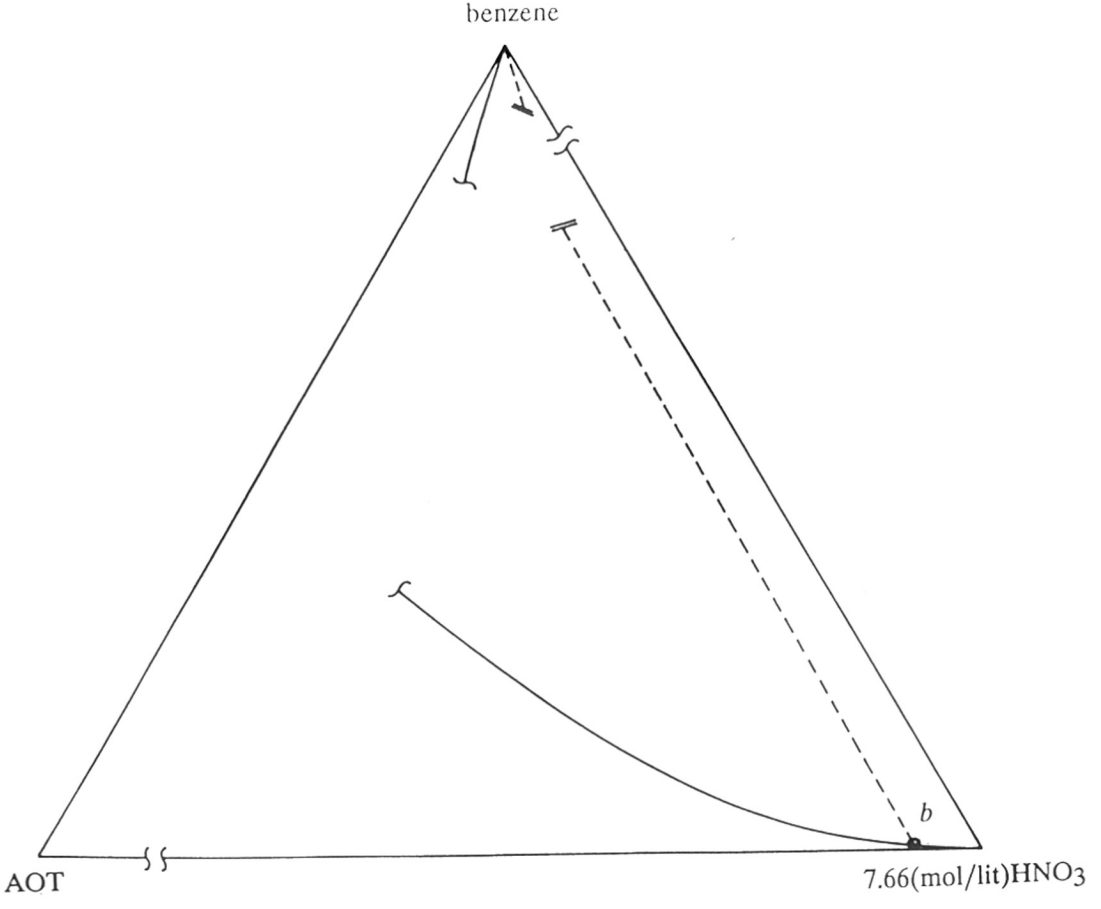

Fig. 5.2 **Partial phase diagrams of the pseudo-ternary system AOT / 7.66 (mol/lit) HNO3/ benzene at 30°C:** *b* :- point representing overall composition of reaction system; (note break in scale)

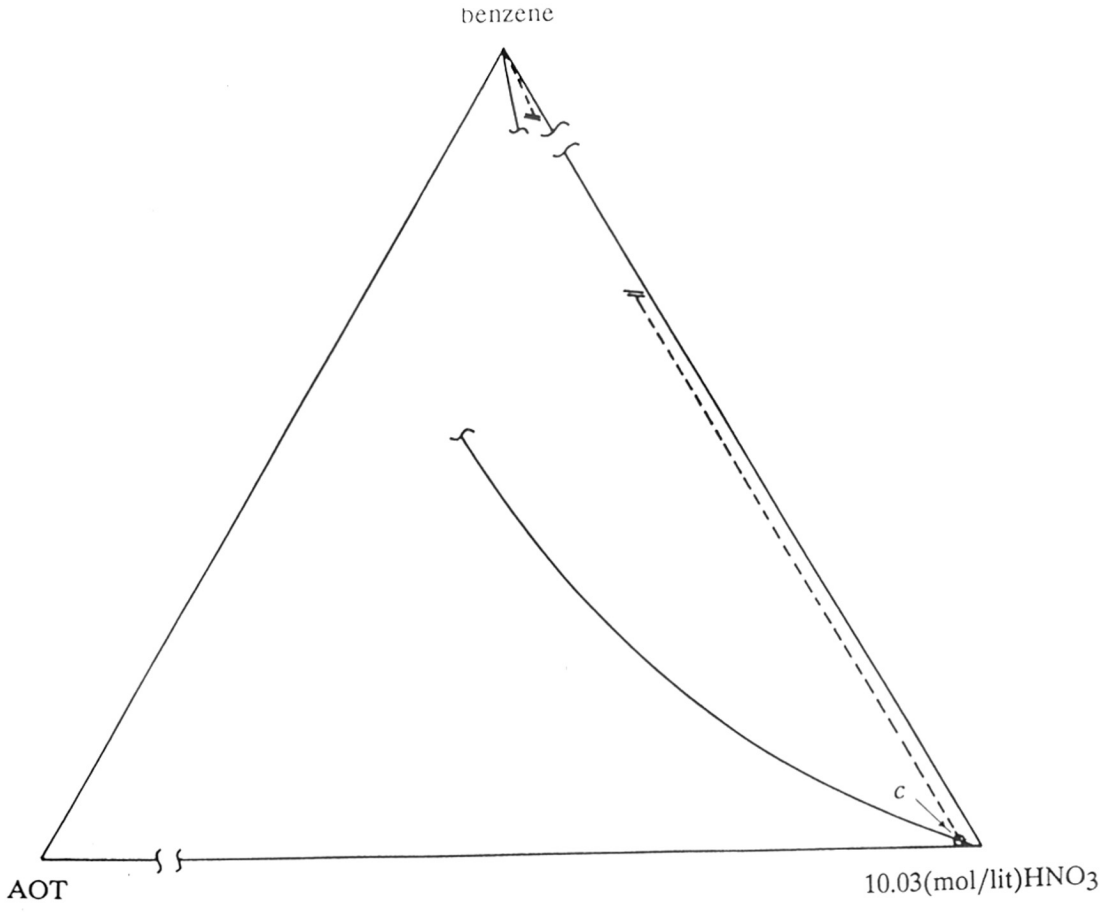

Fig. 5.3 **Partial phase diagrams of the pseudo-ternary system AOT/ 10.03 (mol/lit) HNO3/ benzene at 30°C:** *c* :- point representing overall composition of reaction system; (note break in scale)

Table 5.1 Composition of 400 ml of the aqueous phases used

Set no.	Run nos.	HNO_3 (mol/lit)	AOT (gm)	Benzene (ml)	% vol. holdup of organic phase
1	1-6	5.08	8.68	12.4	3.1
	7-12	7.66	10.66	8.7	2.2
	13-18	10.03	11.45	4.9	1.2
2	19-24	5.08	0.00	0.0	0.0
	25-30	7.66	0.00	0.0	0.0
	31-36	10.03	0.00	0.0	0.0

Table 5.2 Dependance of phenol conversion on stirrer speed

Set no.	Run no.	Stirrer speed (RPM)	[Phenol] initial mol/lit	[Phenol] final mol/lit	Conversion mol/lit	Percent conversion
	37	20	0.716	0.609	0.107	14.9
	38	30	0.716	0.599	0.117	16.3
	39	40	0.716	0.586	0.130	18.2
3	40	50	0.716	0.571	0.145	20.3
	41	60	0.716	0.554	0.162	22.6
	42	70	0.716	0.532	0.184	25.7

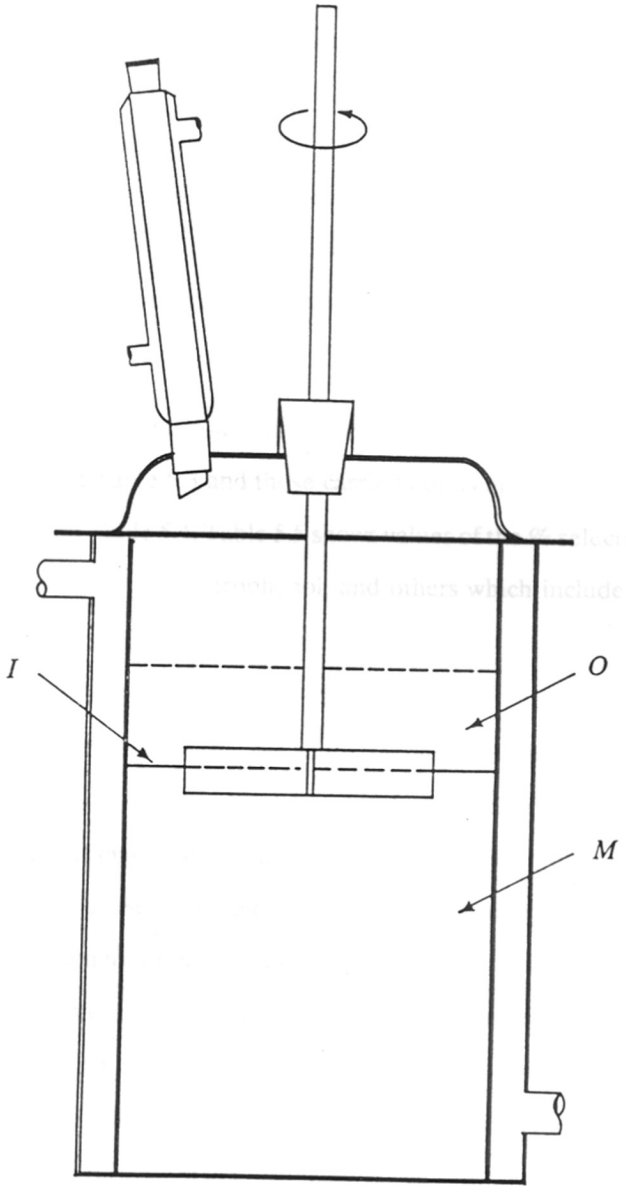

Fig. 5.4 **Jacketted reactor for phenol nitration:** *M* :- microemulsion phase; *O* :- excess organic phase; *I* :- interface.

rate has been maintained with an accuracy of about ± 1 rpm. The internal diameter of the reactor used was 6 cm. After 300 seconds of each reaction, the organic phase has been analyzed by GC. The aqueous phase which in case of runs 1-18 was a microemulsion, has been demulsified, repeatedly extracted with diethyl ether, and analyzed immediately on the GC for its composition. The aqueous phase was also analyzed by UV method for the total amount of the nitrated product in each run. The accuracy of the GC measurements has been estimated to be around 1%, and that of the UV measurements to be around 2%.

5.4 Results and discussions

The results of reactions carried out under *type I* microemulsion conditions are reported in Table 5.3 and those carried out using dilute acid (no surfactant) are reported in Table 5.4. Table 5.5 shows values of the % selectivity obtained for ortho nitrophenol, para nitrophenol, and others which include di- and trinitro-phenols.

It is evident from *fig.* 5.5 that % conversion of phenol is dependant on the stirrer speed. This means that the process is controlled by the diffusion of phenol through the organic phase. It is also seen from Table 5.4 that both the average specific rates of mass transfer and % conversion depend on initial concentration of the organic phase. The mechanism by which mass transfer from the organic phase to the aqueous phase takes place can be explained as follows. Phenol from the bulk organic phase is picked up by the benzene microdroplets present near the interface and reacts with the acid present in the bulk aqueous phase at the droplet surface. The intermediate formed at the surface decomposes into the acid phase, with the formation of nitrophenols. The concentration of the intermediate compound is quite low at any given time instant, and the overall heat effect in the system is negligible. Since the reaction is mass transfer controlled, the overall rate

Table 5.3 Reaction under microemulsion medium

Run no.	[HNO_3] mol/lit	[Phenol] initial mol/lit	[Phenol] final mol/lit	Conversion mol/lit	Percent conversion	Specific rate cm/sec ($\times 10^5$)
1	5.08	1.223	0.689	0.534	43.7	6.77
2	5.08	0.962	0.545	0.417	43.4	7.00
3	5.08	0.716	0.409	0.307	42.9	6.60
4	5.08	0.413	0.233	0.180	43.6	6.75
5	5.08	0.248	0.144	0.104	42.0	6.41
6	5.08	0.181	0.103	0.078	43.1	6.65
7	7.66	1.223	0.758	0.465	38.0	5.64
8	7.66	0.962	0.593	0.369	38.4	5.70
9	7.66	0.716	0.446	0.270	37.7	5.58
10	7.66	0.413	0.254	0.159	38.5	5.73
11	7.66	0.248	0.152	0.096	38.7	5.77
12	7.66	0.181	0.113	0.068	37.6	5.54
13	10.03	1.223	0.844	0.379	31.0	4.37
14	10.03	0.962	0.660	0.302	31.4	4.44
15	10.03	0.716	0.495	0.221	30.9	4.35
16	10.03	0.413	0.281	0.132	32.0	4.54
17	10.03	0.248	0.169	0.079	31.9	4.52
18	10.03	0.181	0.124	0.057	31.5	4.46

Table 5.4 Reaction with dilute nitric acid (no surfactant)

Run no.	$[HNO_3]$ mol/lit	[Phenol] initial mol/lit	[Phenol] final mol/lit	Conversion mol/lit	Percent conversion	Specific rate cm/sec ($X\ 10^5$)
19	5.08	1.223	0.975	0.248	20.3	2.67
20	5.08	0.962	0.766	0.196	20.4	2.69
21	5.08	0.716	0.567	0.149	20.8	2.75
22	5.08	0.413	0.330	0.083	20.1	2.65
23	5.08	0.248	0.196	0.052	21.0	2.77
24	5.08	0.181	0.144	0.037	20.4	2.70
25	7.66	1.223	0.968	0.255	20.9	2.76
26	7.66	0.962	0.770	0.192	20.0	2.63
27	7.66	0.716	0.571	0.145	20.3	2.67
28	7.66	0.413	0.326	0.087	21.1	2.79
29	7.66	0.248	0.206	0.042	17.0	2.19
30	7.66	0.181	0.147	0.034	18.8	2.45
31	10.03	1.223	0.971	0.252	20.6	2.72
32	10.03	0.962	0.758	0.204	21.2	2.81
33	10.03	0.716	0.566	0.150	21.0	2.77
34	10.03	0.413	0.333	0.080	19.4	2.54
35	10.03	0.248	0.199	0.049	19.8	2.60
36	10.03	0.181	0.148	0.033	18.2	2.37

Table 5.5 Selectivity achieved by using microemulsion

Run no.	Total conversion (mol/lit)	o-nitrophenol		p-nitrophenol		Others	
		mol/lit	%	mol/lit	%	mol/lit	%
1	0.534	0.466	87.2	0.044	8.2	0.024	4.6
2	0.417	0.366	87.7	0.035	8.4	0.016	3.9
3	0.307	0.272	88.5	0.021	6.9	0.014	4.6
4	0.180	0.156	86.9	0.015	8.1	0.009	5.0
5	0.104	0.085	81.9	0.008	7.9	0.011	10.2
6	0.078	0.059	75.0	0.007	8.6	0.013	16.4
7	0.465	0.355	76.4	0.033	7.2	0.076	16.4
8	0.369	0.283	76.7	0.024	6.4	0.062	16.9
9	0.270	0.198	73.2	0.019	7.2	0.053	19.6
10	0.159	0.124	78.2	0.010	6.6	0.024	15.2
11	0.096	0.070	72.5	0.007	7.8	0.019	19.7
12	0.068	0.051	75.7	0.005	7.4	0.011	16.9
13	0.379	0.262	69.1	0.058	15.4	0.059	15.5
14	0.302	0.209	69.3	0.047	15.4	0.046	15.3
15	0.221	0.161	72.8	0.033	15.0	0.027	12.2
16	0.132	0.087	65.8	0.022	17.0	0.023	17.2
17	0.079	0.054	68.9	0.012	15.3	0.012	15.8
18	0.057	0.040	70.3	0.009	15.0	0.008	14.7

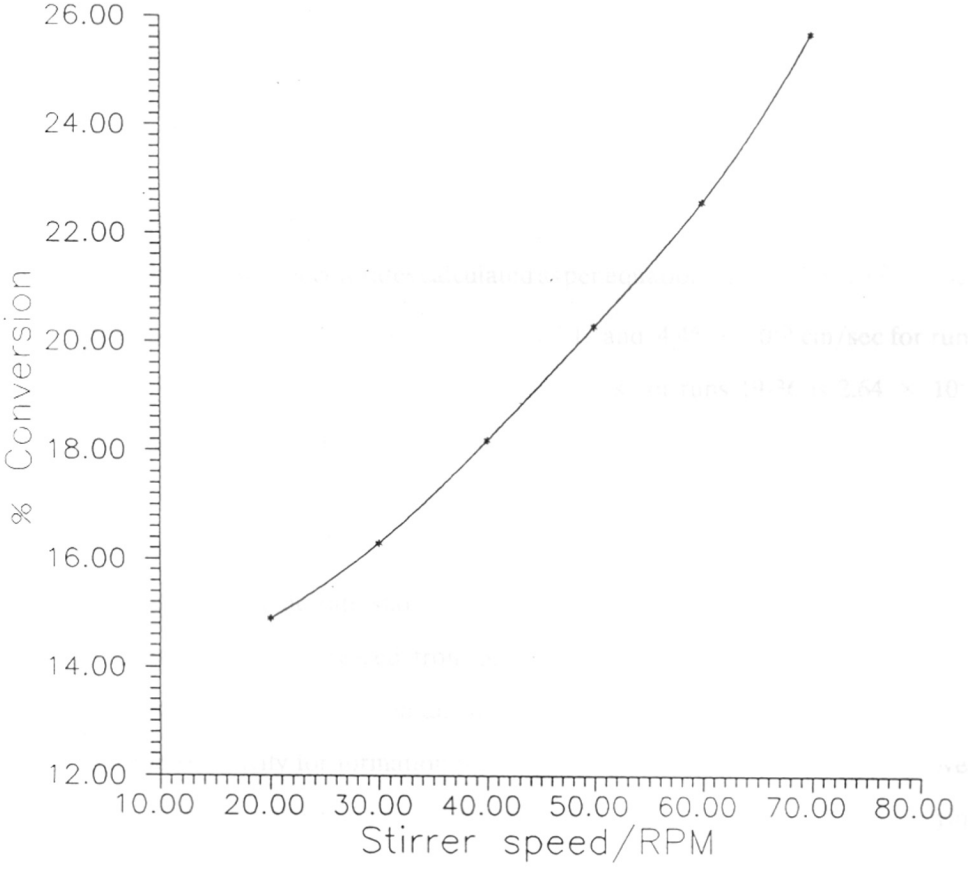

Fig. 5.5 **Percent conversion of phenol versus stirrer speed (RPM)**

of reaction is determined by the average flux across the aqueous-organic interface. The equation for specific rate of mass transfer or the molar flux across the aqueous-organic interface in the stirred cell reactor is given as

$$N = \{2.303 \log (Co/Ct)\} / st \qquad (1)$$

where s = specific area of the aqueous-organic interface, (cm^2/cm^3)

t = time of contact, (sec)

C_O = Initial concentration of the transferred substance in the transferring phase, (mol/lit)

C_t = Concentration of the transferred substance in the transferring phase at time t, (mol/lit)

The average specific rates calculated as per equation 1 are, 6.7×10^{-5} cm/sec for runs 1-6; 5.66×10^{-5} cm/sec for runs 7-12 and 4.45×10^{-5} cm/sec for runs 13-18. The average specific rate obtained in case of runs 19-36 is 2.64×10^{-5} cm/sec which is low as those obtained in the runs 1-18.

It is obvious that the overall specific rate is proportional to the net organic phase volumetric holdup of the microemulsion medium. As seen from table 5.3, the average specific rate shows a drop when the organic phase holdup of the microemulsion is decreased from 3.1% (runs 1-6) to 1.2% (runs 13-18). On comparing the selectivities obtained here with those found in literature[7] we find that the selectivity for formation of ortho nitrophenol is considerably improved on carrying out the reaction under microemulsion condition. The underlying mechanism for achieving such an improvement can be explained as follows. Phenol has a hydroxyl group which is more hydrophilic than its benzyl group. As a consequence, when phenol is subjected to interfacial conditions, it orients in such a way that the benzyl group remains extended towards the side of the organic phase whereas the hydroxyl group protrudes into the aqueous phase. This makes the attack of the nitronium ion more likely towards the ortho- carbon atom of phenol,

rather than the para- carbon atom which is relatively far from the interface. Nevertheless we do get a minor amount of para- and other nitrophenols which include di-nitrophenols.

5.5 Conclusions

The following conclusions have been drawn from the work reported in this chapter. Near selective nitration of phenol at ortho position has been carried out under microemulsion conditions using dilute nitric acid. The reaction rates have been reasonable and the heat released due to reaction can be controlled. The use of dilute acid as against concentrated nitric acid helps to avoid the process of resinification and formation of higher nitrates of phenol. Also the process of nitration as a whole becomes more economical and safer. Dilute nitric acid has been often used as an oxidizing agent and microemulsion offers a possibility to use it as a nitrating agent in organic reactions.

5.6 References

1 Ullmann's Encyclopedia of Industrial Chemistry, pages 411-455, 1991

2 P. D. I. Fletcher and J. Parrot, *J. Chem. Soc. Farad. Trans. I*, 1988, **84**, 1131

3 A. Mehra and M. M. Sharma, *Chem. Engng. Sci.*, **1985**, 40, 2382

4 M. Menger and A. R. Elrington, *J. Am. Chem. Soc.*, 1991, **113**, 9621

5 M. L. Moya, C. Izquierdo and J. Casado, *J. Phys. Chem.*, 1991, **95**, 6001

6 R. Schomacker, K. Stickdorn and W. Knoche, *J. Chem. Soc. Farad. Trans.*, 1991, **87(6)**, 847

7 K. Schofield, in *Aromatic nitration*, Cambridge University Press, 1980

8 V. M. Kaloshin, *Zh. Prikl. Khim.*, 1971, **44(3)**, 664

9 J. P. Alazard, H. B. Kagan and R. Setton, *Bull. Soc. Chim. Fr.*, 1977, 499

10 C. B. Thomas, M. J. Gregory and S. L. Walters, *J. Am. Chem. Soc.*, 1968, **90**, 1612

11 U. A. Spitzer and R. Stewart, *J. Org. Chem.*, 1974, **39**, 3936

12 M. Overtani, P. Girard and H. B. Kagan, *Tetrahedron Lett.*, 1982, **23**, 4315

13 D. Gaude, R. Le Goaller and J. L. Pierre, *Synth. Commun.*, 1986, **16(1)**, 63

List of Papers / Patents

Papers

1. "The Phase Behavior of Microemulsion Systems Containing Kerosene"

   A. S. Chhatre and B. D. Kulkarni, *J. Colloid Interface Sci.*, **150(2)**, 528-34, 1992

2. "Effects of Acid Concentration and Temperature on the Phase Behavior of a Microemulsion System Containing Kerosene"

   A. S. Chhatre and B. D. Kulkarni, *J. Chem. Res. (S), 1992, 209* and *J. Chem. Res. (M),* 1992, 1852-1870

3. "Microemulsions as a Media for Organic Synthesis: Selective Nitration of Phenol to o-nitrophenol using Dilute Nitric acid"

   A. S. Chhatre, R. A. Joshi and B. D. Kulkarni, *J. Colloid Interface Sci.*, (communicated)

4. "Enhanced Recovery of Nicotine from Tobacco waste Using Sulfuric Acid and Microemulsion medium"

   A. S. Chhatre, N. K. Yadav and B. D. Kulkarni, *Sep. Sci. Technol.* (communicated)

Patents filed

1. "An Improved process for preparation of Nicotine Sulfate"

   A. S. Chhatre, N. K. Yadav and B. D. Kulkarni (Indian patent)

2. "An Improved Process for the Preparation of the Ester of an Amino Acid using Microemulsion Medium"

   A. S. Chhatre, B. D. Kulkarni, R. A. Joshi, T. Ravindranathan and A. P. Pendse (Indian patent)

3. "A Process for the Selective Nitration of Phenol to o-nitrophenol Using Microemulsion and Dilute Nitric Acid"

   A. S. Chhatre R. A. Joshi and B. D. Kulkarni (Indian Patent)